TECHNISCHE UNIVERSITÄT WIEN
Vienna University of Technology

Diploma thesis

Synthesis of novel Si-based long wavelength photoinitiators for dental applications

Performed at the

Christian Doppler Laboratory for Photopolymers in digital and restorative dentistry

Institute of Applied Synthetic Chemistry
Vienna University of Technology

Under the supervision of

Ao. Univ. Prof. Dipl. Ing. Dr. techn. Robert Liska

by

Moritz Mitterbauer BSc
Spitalgasse 1/37, 1090 Vienna

Danksagung

Zuallererst möchte ich mich bei dir, Robert, bedanken, dass du mir ermöglicht hast, hier in deiner Gruppe im Bereich Macromolecular Chemistry am Institut für Angewandte Synthesechemie an meiner Diplomarbeit zu arbeiten. Danke für das interessante Thema und die richtungsweisenden Gespräche. Die Arbeit am Projekt mit der Firma Ivoclar Vivadent, bei der ich mich ebenfalls bedanken möchte, hat mein Interesse an der Photopolymerchemie zusätzlich vertieft und mir immer große Freude bereitet.

Zusätzlich möchte ich auch allen meinen Kollegen aus der Forschungsgruppe danken, speziell euch, Christoph und Johannes, da ihr die ganze Zeit über im selben Boot wie ich saßt und mir stets mit Rat und Tat zur Seite gestanden seid. Besonderer Dank gilt auch dir, Stephan, für deine fachkundige und moralische Unterstützung in jeder Situation. Seit dem ersten Tag in der Forschungsgruppe (damals im Rahmen der Bachelorarbeit) konnte ich sehr viel von dir lernen.

Riesiger Dank gebührt dir, Lisa, dass du mich während meines gesamten Studiums mit so viel Liebe unterstützt hast. Ich danke dir für die Kraft und die Motivation, die du mir jeden einzelnen Tag schenkst.

Ich danke auch meinen Eltern und dir, Nora, dass ihr mich mein ganzes Leben unterstützt habt, sowohl moralisch als auch und nicht zuletzt finanziell. Ich kann euch wirklich gar nicht genug dafür danken.

Auch meinen langjährigen Freunden Michael, Florian und Benjamin möchte ich danken. Besonders du, Michi, hast mich während meiner ganzen Studienzeit begleitet und ich weiß, dass ich mich stets auf dich verlassen kann.

Abstract

Visible light photopolymerization is widely used for modern applications, such as curing of dental filling materials. The currently used bimolecular photoinitiating system based on camphorquinone / dimethylamino benzoic acid ethyl ester (CQ/DMAB) shows quite limited reactivity. Other more efficient cleavable photoinitiators like bisacylphosphine oxides (BAPO) show an absorption band which does not overlap very well with the emission band of the applied dental LEDs. Also diacylgermane-based structures like Ivocerin with an absorption shifted to longer wavelengths revealed drawbacks relating to its high production costs.

Since Si-based photoinitators might have similar absorption properties as the Ge-based compounds, the synthesis and photochemical characterization of such a compound should be the target of this work. Due to the low stability of the existing acylsilane-based type I initiators novel concepts should show be explored. Furthermore, improved reactivity is desired, which should be achieved by repressing the photoinduced formation of a siloxycarbene, also known as Brook-rearrangement.

Therefore the synthesis of oxygen substituted acyl silanes was envisaged. Furthermore the strategy of multiple substitution at the silicon atom with aromatic acyl groups resulted in a successful synthesis of a tetraacylsilane, which showed good reactivity in photopolymerization of acrylates. Furthermore the absorption band overlaps very well with the emission band of dental LEDs. However its stability in aqueous media still leaves room for improvement.

Kurzfassung

Photopolymerisationen mittels sichtbaren Lichts finden ihre Anwendung heute in vielen modernen Einsatzgebieten, wie zum Beispiel beim Aushärten von Dentalfüllungen. Das derzeit für Photopolymerisationen von Acrylaten im sichtbaren Licht angewandte bimolekulare Photoinitiatorsystem Camphorchinon / Dimethylaminobenzoesäure-ethylester (CQ/DMAB) weist relativ limitierte Reaktivität auf. Andere effizientere spaltbare Photoinitiatoren, wie Bisacylphosphinoxide (BAPO) weisen hingegen eine Absorptionsbande auf, die nur in geringem Ausmaß mit der Emissionsbande von Dental-LEDs überlappt. Auch Diacylgerman-basierende Verbindungen wie Ivocerin mit einer zu längeren Wellenlängen verschobenen Absorption haben ihre Nachteile, wie die hohen Produktionskosten.

Da Photoinitiatoren auf Siliziumbasis ähnliche Absorptionseigenschaften wie Ge-basierte Verbindungen aufweisen könnten, sollte das Ziel dieser Arbeit die Synthese und Charakterisierung einer solchen Verbindung sein. Da die bekannten Acylsilan-Initiatoren vom Typ I oft geringe Stabilität aufweisen, sollten bezüglich dessen neue Konzepte getestet werden. Weiter wäre eine hohe Reaktivität wünschenswert, welche durch das Zurückdrängen der photoinduzierten Siloxycarben-Umlagerung (Brook-Umlagerung) erreicht werden soll.

Deshalb war die Synthese von Acylsilanen vorgesehen, bei welchen ein Sauerstoffatom direkt am Siliziumatom gebunden war. Zusätzlich resultierte die Strategie der Mehrfachsubstitution des Siliziumatoms mit aromatischen Acylgruppen in einer erfolgreichen Synthese eines Tetraacylsilans, das gute Reaktivität bei der Photopolymerisation von Acrylaten aufweisen konnte. Die Verbindung weist außerdem eine Absorptionsbande auf, die sehr gut mit der Emissionsbande von Dental-LEDs überlappt. Die Stabilität dieser Verbindung in wässrigen Lösungen ist jedoch verbesserungsbedürftig.

Index

	General	Experimental
INTRODUCTION	7	
OBJECTIVE	24	
STATE OF THE ART	26	
Photochemistry of acyl silanes	26	
Strategies for the synthesis of acyl silanes	30	
GENERAL AND EXPERIMENTAL SECTION	34	72
1. Synthesis	34	72
1.1 Oxygen- substituted acyl silanes	34	72
1.1.1 Bis(mesitoyl)tetramethyldisiloxane (7)	34	72
1.1.2 Hexakis(mesitoyl)cyclotrisiloxane (8)	37	
1.1.3 Diphenylmesitoyl(trimethylsilyl)disiloxane (9)	40	
1.2 Acyl silanes	42	73
1.2.1 Mesitoylsilanes	44	73
1.2.1.1 Tris(trimethylsilyl)mesitoylsilane (25)	44	73
1.2.1.2 Tetramesitoylsilane (19)	44	74
1.2.2 Toluoylsilanes	45	76
1.2.2.1 Tris(trimethylsilyl)o-toluoylsilane (26)	45	76
1.2.2.2 Tetra-o-toluoylsilane (20)	46	
1.2.3 Alternative Tetraacylsilanes	46	
1.2.3.1 Tetra(2,6-dimethoxybenzoyl) silane (21)	47	
1.2.3.2 Tetra(2,3,4,5,6-pentafluoro benzoyl)silane (22)	47	

1.2.3.3 Tetra[2,6-bis(trifluoromethyl) benzoyl]silane (23) 48

1.2.3.4 Tetra(2,4,6-triisopropyl benzoyl)silane (24) 49

2. Characterization 50 78

2.1 UV-Vis spectroscopy 50 78

2.2 Steady state photolysis (SSP) 54 78

2.3 Storage stability 58 79

2.4 Photo-DSC 60 79

SUMMARY 81

MATERIALS AND EQUIPMENT 84

ABBREVIATIONS 86

LITERATURE 87

Introduction

Until the end of the twentieth century mostly amalgam was used for dental fillings. Dental amalgam[1,2] is a mercury alloy containing 50% mercury and other metals like silver, tin or copper. It is a formable mass, which hardens within several minutes. The big advantages of amalgam are easy application to the cavity, its high stability and its low costs. However, with the technological progress in available analytical methods, the release of mercury to the body from amalgam fillings became evident. Since mercury shows high toxicity, but also for esthetic reasons, most patients nowadays prefer other dental filling materials over amalgam inlays for their teeth (Figure 1).

Figure 1: Amalgam filling compared to composite filling

To define the requirements for an ideal filling material, the natural structure of a tooth (Figure 2) needs to be considered.

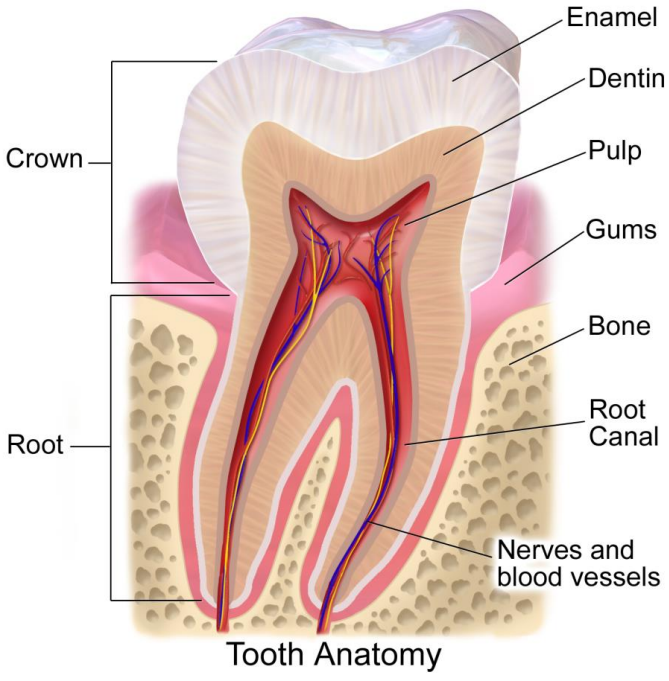

Figure 2: Natural build-up of a tooth[3]

Dental enamel[4] consists of almost 100% inorganic crystalline hydroxyl apatite $Ca_5(PO_4)_3(OH)$. The outstanding mechanical properties of this biogenic material come from the combination of those inorganic crystals with organic collagen fibers, which glue the inorganic crystals together. However, dental enamel shows relatively low stability against acidic conditions. Dentin consists of the same compounds as enamel, but the material is traversed by small channels, which are filled with a liquid and also the hydroxyl apatite content is lower for dentin.

To replace the natural tooth material with artificial materials the properties of the artificial material should be very similar to the ones in the natural tooth. Therefore the following properties are needed for a potential filling material:[4]

- Low solubility in acidic conditions
- Plasticity at room temperature with hardening in several minutes
- Outstanding mechanical properties regarding hardness and toughness
- Low abrasion
- Perfect covering of the cavity to hinder bacteria from getting into the tooth
- Appealing color (filling should not be distinguishable from the surrounding healthy tooth)
- Easy handling
- Low cost
- Biocompatibility

Research in the last years resulted in a lot of experimental inlays, fulfilling those properties.

Ormoceres:

The name ormocere comes from organically modified ceramic and ormoceres are polymer- based filling materials.[5] Ormoceres are similar to silicones, because after hydrolysis and condensation of silanes a Si-O network is formed containing organic groups on certain silicon atoms. Polymerizable functionalities like methacrylate groups in dental ormoceres can then be polymerized like a normal monomer. Ormoceres show low shrinkage, low abrasion and high biocompatibility due to the reduced solubility of residual monomer.

Glass ionomer cements:

Glass ionomer cements[4] are ionic networks, which are formed in a reaction of aqueous solutions of organic acids (e.g. polyacrylic acid) with fluoride- containing alumosilicate glasses, which release ions under acidic conditions. During this process the glass particles and also apatite crystals of the surrounding tooth are incorporated into to the network. Fluoride ions can embed into the tooth and therefore increase the resistance against tooth decay. Glass ionomer cements show disadvantages in terms of toughness and stability compared to other inlays.

Polymer- modified glass ionomer cements:

The sensitivity of glass ionomer cements against moisture can be reduced strongly by adding monomer to the cement, which can then be polymerized in a radical reaction[4]. The polymer network forms faster than the network of the glass ionomer and therefore the dentist can decide about the moment of hardening (e.g. via photocuring). The poor toughness of the material cannot be improved by this technique.

Compomeres:

Compomeres[4] are also modified glass ionomer cements except for the fact, that they do not contain any water anymore. Instead, after polymerization saliva diffuses into the compomer to start the glass ionomer reaction. This results in higher toughness and stability.

Composites:

Composites are the most widely used materials for dental fillings.[4] They consist of a liquid organic phase (methacrylate- matrix) and inorganic filler (grinded glass, micro-dispersed SiO_2 or hybrid materials). The organic phase usually consists of monomers (Scheme 1) like urethanedimethacrylate (UDMA), 1,10-decanedioldimethacrylate (D_3MA) and bisphenol A – diglycidylmethacrylate (bis-GMA).

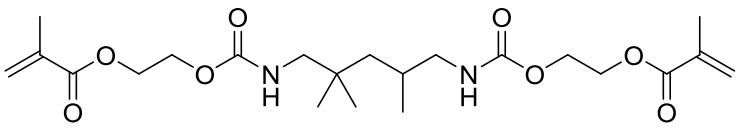

UDMA

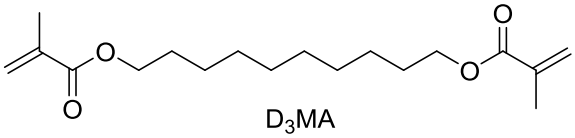

D_3MA

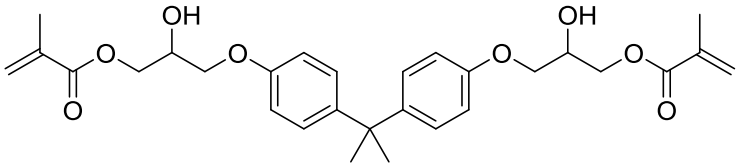

bis-GMA

Scheme 1: Methacrylates used in dental formulations

Radical polymerization of these methacrylates leads to a three- dimensional network. The choice of the monomer has a big influence on the reactivity, the viscosity and the shrinkage.[6] Additionally the used monomer influences the mechanical properties and the swelling due to water uptake.

To achieve a suitable adhesion of the hydrophobic composites onto the mainly inorganic hydrophilic tooth surface, many different adhesives were developed to connect the inlay to the tooth. In conventional systems, phosphoric acid was used to roughen the tooth surface and therefore cause better wetting. Afterwards a low viscosity primer (monomer mixture) was applied to the tooth surface, which can then intrude into the little surface irregularities. The primer polymerizes together with the composite and therefore the filling is connected to the tooth permanently.

Primer monomers usually contain two functional groups. A methacrylate group which reacts with the composite (connection to the hydrophobic matrix) and another functional group which reacts with the dentin (Figure 3). The dentin provides several functional groups as hydroxyl (-OH), carboxyl (-COOH), amine ($-NH_2$), amides ($-CONH_2$) and Ca^{2+} ions. For this reason, reactive groups in the primer monomers can be carboxylic acids, acid chlorides, carboxylic acid anhydrids, isocyanates, aldehydes and ketones.

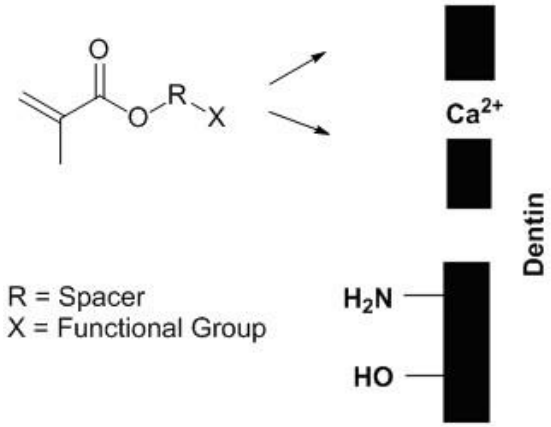

Figure 3: Structure of a primer molecule

Further research on this field led to the development of self- etching adhesives.[7, 8] These mixtures (Figure 4) combine the etching step and the primer adhesion step in one formulation. Additionally to the actual primer molecule, the formulation contains polymerizable phosphoric acid groups or phosphoric acid derivatives. The phosphoric acid group is embedded into the tooth substance via ionic interactions and the polymerizable methacrylate reacts then with the composite. To provide high compatibility concerning the tooth substance and to provide also high biocompatibility, the solvent of choice is water for such systems.

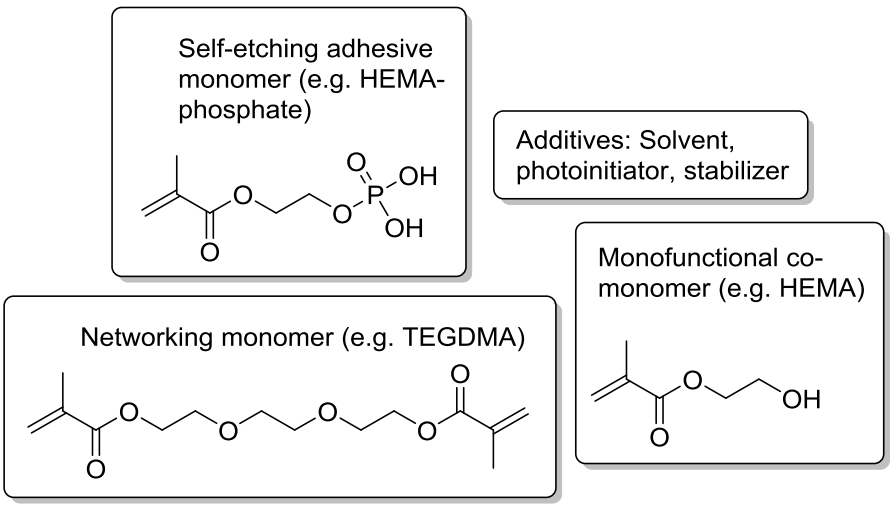

Figure 4: Composition of a self- etching enamel- dentin adhesive

The photoinitiator (PI) is the UV-Vis active component and therefore a key component in such formulations. These photosensitive molecules are able to convert the radiation energy into chemical energy by transferring the energy to their electronic structure.

Radiation leads to excitation processes in molecules. The photoinitiator can either absorb the radiation energy directly or it is transferred to the photoinitiator from a photosensitizer via triplet-triplet transfer. To absorb enough energy the main emission bands of the applied lamp have to overlap very well with the absorption bands of the photoinitiator (or photosensitizer). For the absorption of light the photoinitiator needs a chromophore, which means that is has to contain a functionality in its structure (Table 1), which is able to cause the transition to an excited state. These chromophores are mainly conjugated systems containing the carbonyl group making π-π* and n-π* transitions possible.[9]

Table 1: Different chromophores and absorption maxima of their transitions

Chromophore	**λ_{max} [nm] π-π***	**λ_{max} [nm] n-π***
C=C	170	-
C=O	166	280
C=N	190	300
N=N	-	350
C=S	-	500

At first, a photoinitiator molecule, which is in the ground state (S_0) is excited to the excited singlet state (S_1) upon radiation (Scheme 2).[10] This state has a very short lifetime (<10^{-8} s) and therefore it can hardly initiate photochemical reactions. From this state, the molecule can release its energy either by fluorescence or radiation-free deactivation to regain the ground state (Figure 5).

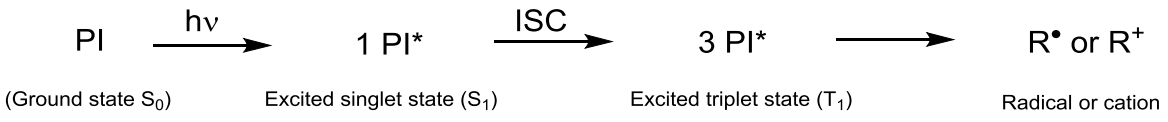

Scheme 2: Excitation, intersystem crossing and radical formation of a photoinitiator

Another possibility is the transfer to the excited triplet state (T_1) via intersystem crossing (ISC). This triplet state shows a much longer lifetime (10^{-6} s) and therefore radical formation is possible from this state, although the formation of radicals is in competition with phosphorescence, radiation- free deactivation and bimolecular quenching processes (e.g. caused by oxygen).

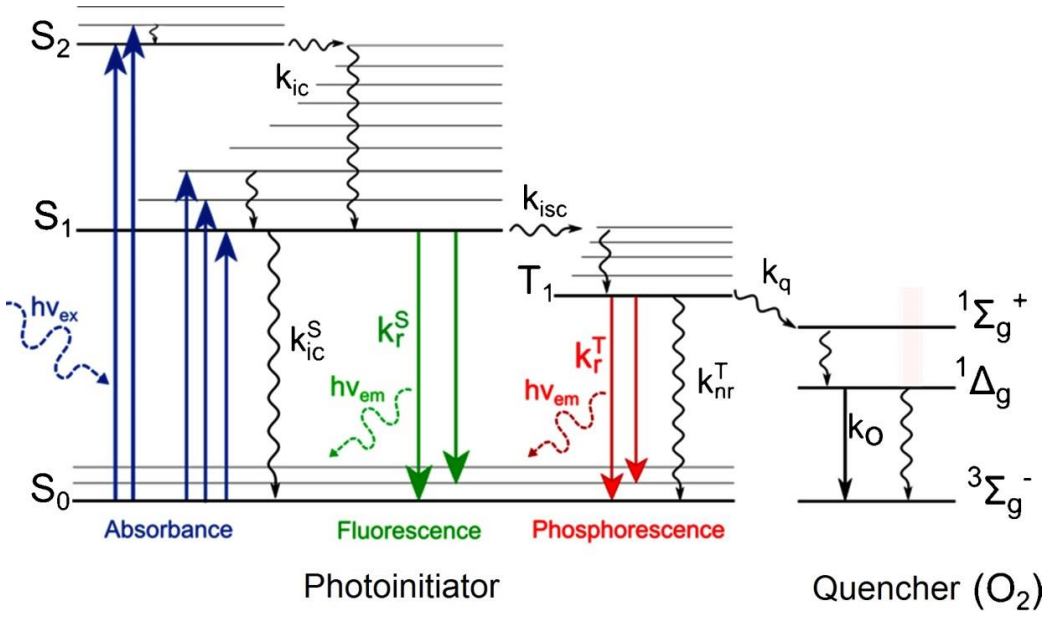

Figure 5: Jablonski diagram[11]

Generally, there are two different types of photoinitiators depending on the mechanism in which the radicals are formed from the photoinitiator molecule.[9] A compound, which undergoes an unimolecular reaction, called fragmentation, caused by irradiation is called Type I photoinitiator (Scheme 3).[12] However, if a photoinitiator molecule needs the presence of another species (coinitiator) to form radicals after irradiation, undergoing a bimolecular reaction, it is called Type II photoinitiator (Scheme 4).

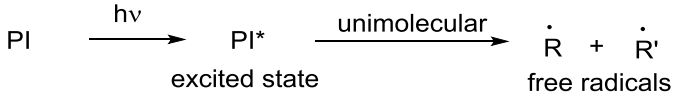

Scheme 3: Initiation process for type I photoinitiators

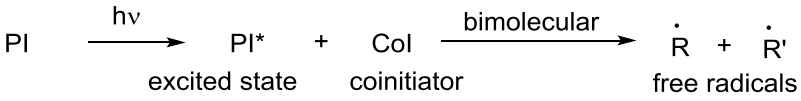

Scheme 4: Initiation process for type II photoinitiators

As already mentioned, Type II photoinitiators require a coinitiator to form radicals in a bimolecular reaction. There are mainly two kinds of reaction pathways possible for these compounds:

- Hydrogen abstraction
- Photoinduced electron transfer, followed by proton transfer

Diaryl ketones, excited to a triplet state, do not undergo α-cleavage, but in the presence of a suitable H- donor, they can abstract hydrogen from the coinitiator forming two radicals. In the example below (Scheme 5), photoinduced hydrogen abstraction (photoreduction) is shown for benzophenone and isopropanol.

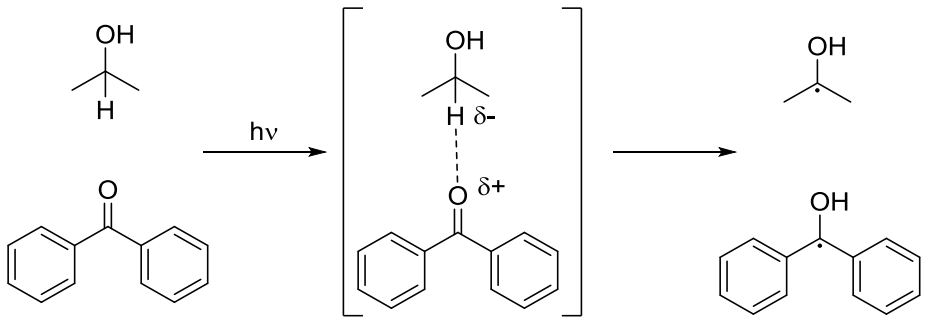

Scheme 5: Photoinduced H-abstraction in benzophenone/isopropanol system

Factors, which have high influence on H- abstraction are:

- Triplet state configuration and triplet state energy of the ketone
- Bond strength of the carbon-hydrogen bond, which has to be broken

The nπ* triplet configuration is more reactive than the ππ* triplet configuration, caused by the higher energy difference. The triplet energy has to exceed the bond dissociation energy of the C-H bond. The demerged hydrogen usually comes from an activated position, such as a carbon atom next to a heteroatom, e.g. hydroxyl or ether functions. The positive partial charge on the oxygen of the diaryl ketone is induced by the excitation of an electron from the n orbital of the oxygen atom to the π* orbital, which is delocalized over the aromatic π system. The δ^+ on the oxygen atom then interacts with the activated C-H bond of the alcohol. The ketyl radicals formed in by

H-abstraction are highly conjugated and therefore not very reactive towards carbon-carbon double bonds. In most cases the species initiating photopolymerization is the radical formed from the H-donor. Caused by electronic and energetic requirements, the hydrogen abstraction process in this case is limited to activation by UV light.

Electron transfer mainly occurs from the excited singlet state, because of the additional step of intersystem crossing required in excited triplet configurations. The most important properties for electron transfer processes are the redox potentials of the electron donor and the acceptor and of course the kinetics of the fragmentation reaction. In contrast to the hydrogen abstraction reaction, ketones possessing a ππ* configuration can be very efficient in combination with a coinitiator which acts via electron transfer (e.g. amine).

The photoinitiating system mainly used for dental applications is the camphorquinone/dimethylaminobenzoic acid ethyl ester (CQ/DMAB) system. Two species are necessary to form radicals (photoinitiator and coinitiator), therefore this system is a Type II photoinitiator. Radicals are formed through a bimolecular reaction after irradiation (Scheme 6).

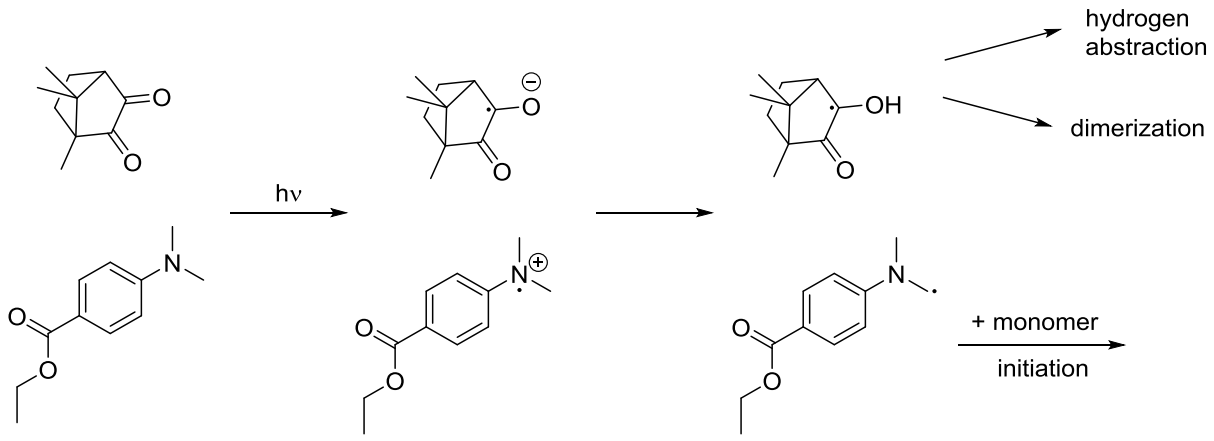

Scheme 6: Radical formation in CQ/DMAB system

Camphorquinone has its absorption maximum at 468 nm and has a very low extinction coefficient, caused by its nπ* transition, which is forbidden in terms of symmetry. The amine-based radical alone causes the initiation of the polymerization, not the one formed from CQ. Type II photoinitiators, such as CQ/DMAB are always

strongly influenced by the surrounding medium, which implies many disadvantages, especially in aqueous solutions.

As already mentioned, Type I photoinitiators form radicals in an unimolecular reaction. Most of the Type I photoinitiators are aromatic compounds containing a carbonyl group next to the aromatic ring.[9] This benzoyl chromophore is the most common moiety in such compounds. The prerequisite to react in the desired way is, that the photoinitiator has to have a bond with a dissociation energy lower than the excitation energy of the reactive excited state, but sufficiently high to provide at least a minimum of thermal stability. In the example below (Scheme 7), the bond next to the carbonyl carbon is cleaved homolyticly forming the benzoyl radical and another radical depending on the constitution of the rests R, R' and R''.

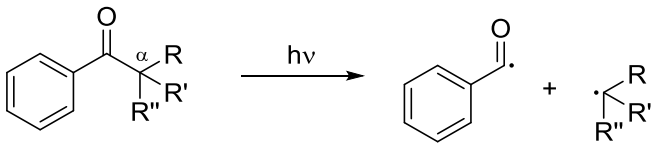

Scheme 7: Photoinduced α-cleavage

Mostly this α-cleavage of such arylalkyl ketones occurs from the $n\pi^*$ triplet state, caused by the higher reactivity related to the α-cleavage in comparison to the singlet state. After absorption of light, the photoinitiator exists in the excited singlet state. Through intersystem-crossing it changes to the triplet state from which it undergoes α-cleavage. Intersystem-crossing occurs quite fast in aromatic ketones, because the energy difference between the singlet and the triplet state is sufficiently small. This results in a very high quantum yield for these compounds, typically in the range of 0,5- 1,0. Competing deactivation processes like fluorescence usually have no relevance.

Quantum yield of radical formation is defined as number of initiating radicals formed per quantum of light absorbed:

$$\Phi_R = \frac{Initiating\ radicals\ formed}{Quanta\ of\ light\ absorbed}$$

The following two points have the biggest influence on the reaction rate of the α-cleavage:

The configuration of the excited state (transition):

The nπ* triplet state configuration is much more reactive in the described process than the ππ* triplet configuration. This means that changes in the molecular structure involving a change in configuration from nπ* triplet state to ππ* triplet configuration usually results in a loss of reactivity.

The substituent at the α- position:

Substituents, which are able to stabilize the positive charge on the carbonyl carbon atom increase the rate of cleavage massively. Because of the +M effect of heteroatoms like oxygen or nitrogen or the –M/+I effect regarding aromatic ring systems, they are very suitable in this case. The reaction Scheme 8 below (Scheme 8) shows the cleavage process in more detail and gives several suggestions for the substituents in highly reactive Type I photoinitiators.

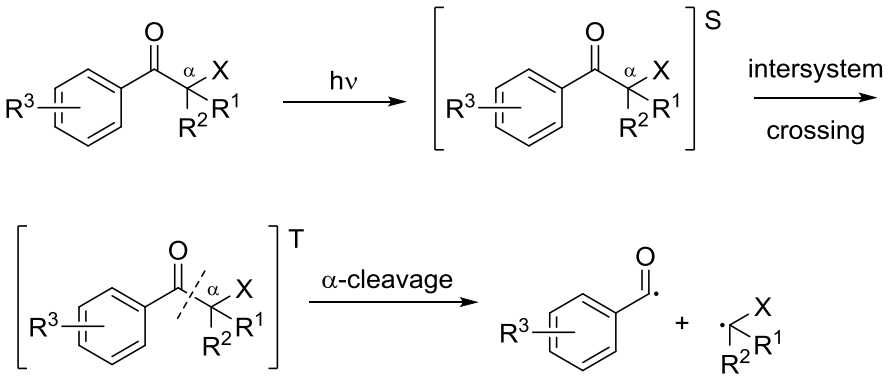

R^1, R^2 = aryl, alkyl
R^3 = alkyl, H
X = O, NR_2

S...singlet state
T...triplet state

Scheme 8: Cleavage process of arylalkyl ketones

Furthermore, the fact that makes these kind of compounds interesting for usage as photoinitiators, is the high reactivity of the benzoyl radicals towards C=C double

bonds. Its efficiency in initiating the polymerization reaction by adding to unsaturated compounds has been proven several times in literature.[13]

A typical example for type I photoinitiators are the alpha-hydroxy alkylphenones. Taking a look at the absorption spectra of these compounds (Figure 6) it is obvious, that the absorption maximum lies somewhere around 340 nm and therefore does not overlap with the emission spectrum of the dental LED (λ_{max} = 460 nm).

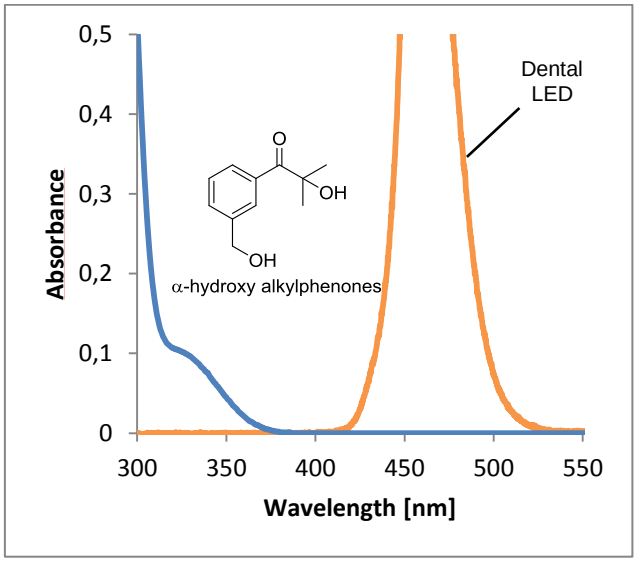

Figure 6: Absorption band of the nπ* transition in α-hydroxy alkylphenones compared to the emission band of the dental LED

The nπ* transition in bisacyl phosphine oxides (BAPOs) occurs at wavelengths coming up to the range of visible light. They possibly owe this to a conjugation between the phosphinoyl group and the carbonyl carbon atom as described by Berlin et al.[14] Another theory says, that the overlap of the π*-orbital of the carbonyl-C with the empty d- orbital of the phosphorus causes the redshift.[15] The formation of the radicals occurs through α- cleavage like described below (Scheme 9). Bisacylphosphine oxides have their absorption maxima around 365 nm tailing to about 420 nm[9].

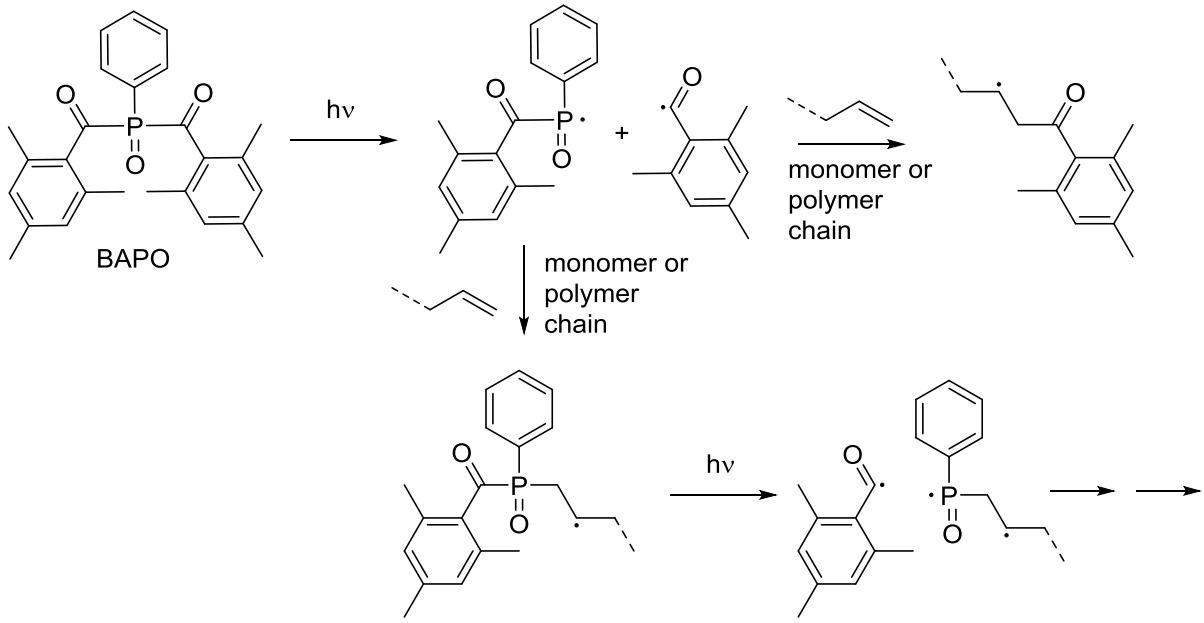

Scheme 9: Radical formation of BAPO and addition to the polymer chain

The big advantage of acylphosphine oxide compounds, such as bismesitoylphenylphosphine oxide (BAPO) is their excellent photobleaching property.[9] After cleavage, the carbonyl and the phosphonyl group do not interact anymore within the photoproducts. Therefore, the UV-Vis absorbing chromophore is destroyed during the photoreaction resulting in colorless compounds. Although there is a shift of the nπ* transition band to longer wavelengths observed for BAPO, there is still only poor overlap of the absorption band with the emission band of the commercially applied dental LED (Figure 7).

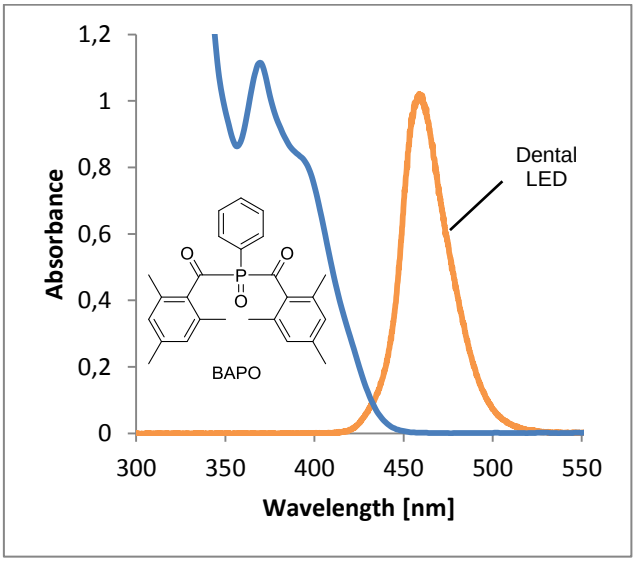

Figure 7: Absorption band of the nπ* transition in BAPO compared to the emission band of the dental LED

Bisacyl germanes like bis(4-methoxybenzoyl)diethyl germane[16] (Ivocerin, Ivoclar Vivadent) have excellent properties in terms of long-wavelength photoinitiators. The absorption maximum of the nπ* transition of Ivocerin is at 418 nm and besides a very high reactivity, this compound is sufficiently stable under normal conditions. Dibenzoyldiethyl germane (Ivocerin, Ivoclar Vivadent) undergoes an α-cleavage forming two benzoyl radicals (Scheme 10).

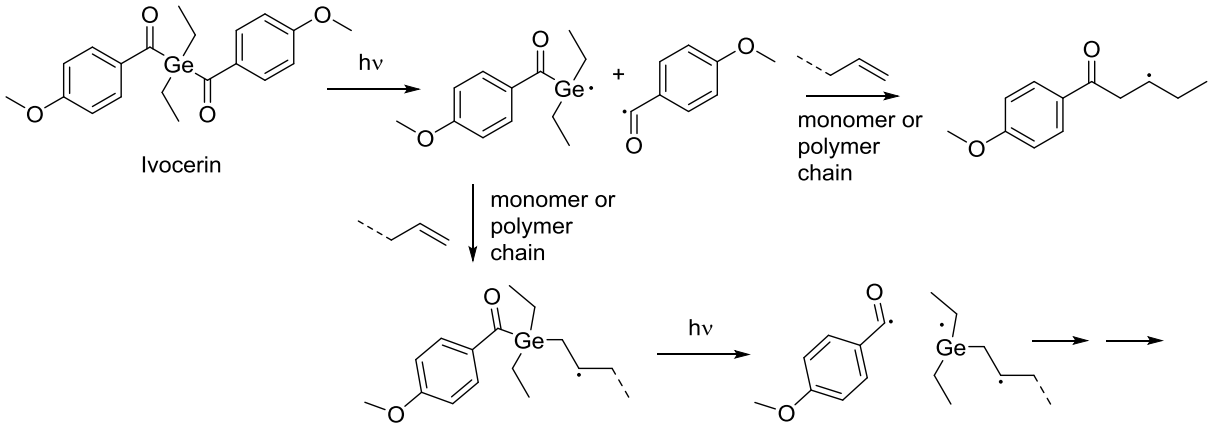

Scheme 10: Radical formation of Ivocerin

The shift of the absorption band in Ivocerin is caused by the overlap of the π*-orbital of the carbonyl-C with the d- orbitals of the germanium atom. With the acyl germanes and their absorption maxima above 400 nm the overlap of the absorption band of the nπ* transition and the emission band of the dental LED is much larger than for the bisacyl phosphine oxides (Figure 8). Furthermore, bisacyl germanes reveal good photobleaching properties as well.

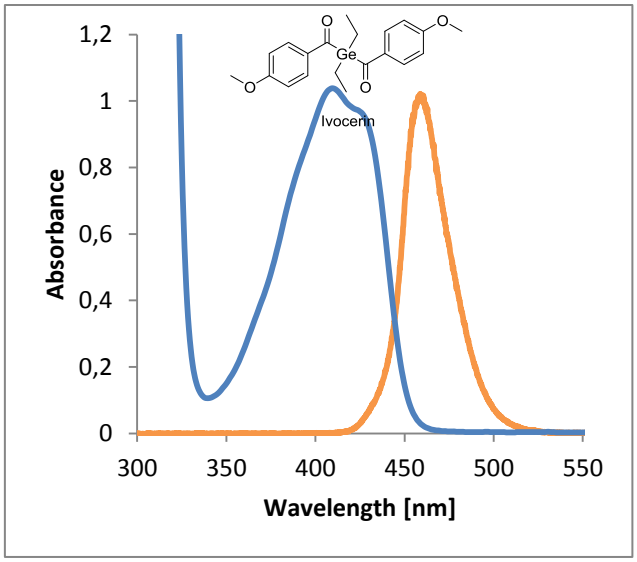

Figure 8: Absorption band of the nπ* transition in Ivocerin compared to the emission band of the dental LED

The biggest disadvantage of Ivocerin is definitely its expensive production, involving germanium organyls. Although usually only very little amounts of photoinitiators are needed in dental formulations (0,2 wt% or less), price is always an issue in industry. With production costs of about 10.000 € per kilogram Ivocerin is a very expensive compound compared to other photoinitiators.

Many alternative acyl metal/metalloid compounds have been successfully synthesized and described in literature, but have not yet been tested as type I photoinitiators for radical polymerization.

According to Peddle[17], an absorption maximum of 435 nm was detected for the nπ* transition in benzoyltriphenyl stannate. Generally, acyl stannanes (Scheme 11) are described as very sensitive to oxygen and moisture. Additionally, some of these compounds exhibit high thermal instability.[18]

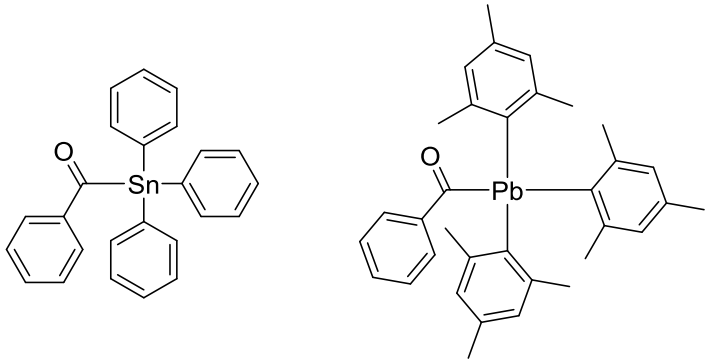

Scheme 11: Benzoyltriphenyl stannate and benzoyltrimesityl lead

Generally, organolead derivatives (Scheme 11) are also quite unstable, although the synthesis and successful characterization of benzoyltrimesityl lead led to a breakthrough[19]. This compound is stable under air and the nπ* transition shows an absorption maximum at 448 nm.

Photochemical studies on benzoylphenyl selenide and benzoylphenyl telluride showed, that these compounds (Scheme 12) formed radicals after irradiation (300 nm).[20] Bond cleavage occurred always between the carbonyl carbon atom and the selenium/tellurium atom leaving a benzoyl radical and a phenyl selenide/telluride radical behind.

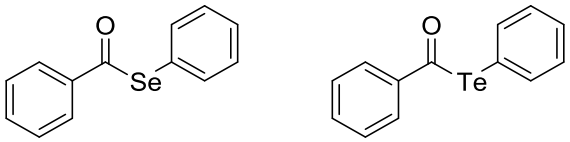

Scheme 12: Benzoylphenyl selenide and benzoylphenyl telluride

Additionally benzoylphenyl telluride could be discovered to be a highly reactive TERP- reagent for visible light induced (400- 500 nm) controlled radical polymerization[21].

The extraordinary absorption properties of acyl silanes were insistently discovered by Brook et al.[22] The absorption maximum referring to the nπ* transition is located above 400 nm. In competition to the α-cleavage reaction, a siloxycarbene can be formed reversibly (Brook- rearrangement). Generally acyl silanes are not very stable, because even air moisture causes hydrolysis of many of these compounds. Since the absorption behavior of acyl silanes is quite similar to that of acyl germanes this class of compounds always seemed to be very promising. The potential advantages concerning the production costs compared to the acyl germanes are quite obvious as well. For these reasons several compounds have been tested as type I photoinitiators[23] very recently. All of these three acyl silanes (Scheme 13) showed the ability to form radicals. Although the lability to hydrolysis in aqueous media was quite problematic, the assumed bathochromic shift of the nπ* absorption band as well as moderate reactivity in methacrylates could be shown. Furthermore the Brook-

rearrangement could be suppressed for the compounds containing an oxygen atom bound to the silicon.

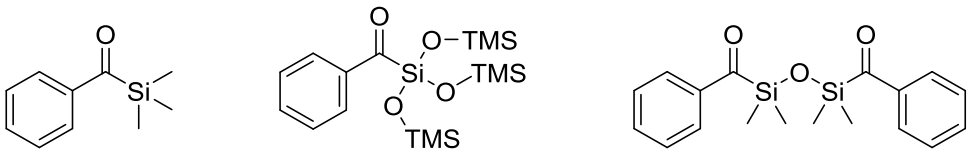

Scheme 13: Acyl silanes tested as photoinitiators

Objective

The currently used photoinitiator system for dental applications based on camphorquinone / dimethylaminobenzoic acid ethyl ester (CQ/DMAB) has some limitation concerning reactivity due to the bimolecular initiation system. The absorption spectrum of classical cleavable photoinitiators with high reactivities such as bisacyl phosphine oxides does not match with the emission spectrum of the dental LED. The existing Ge- based photoinitiators show absorption at longer wavelengths, however their very high production costs are quite problematic for commercial use. Therefore the objective of this thesis is the synthesis of novel Si-based long-wavelength photoinitiators. These compounds are expected to have similar absorption properties as the Ge- compounds but are by far cheaper than their analogues.

All in all there are several criteria that have to be met for efficient photoinitiators regarding dental applications:

- High reactivity towards double bonds
- Absorption around 450 nm
- Adequate solubility in the used monomer
- Stability against oxidation and hydrolysis at atmospheric conditions
- Thermal stability at room temperature
- Low toxicity
- Sufficient photobleaching

The bathochromic shift, caused by an overlap of the π and π* orbitals of the carbonyl group with the empty d orbitals of the silicon atom lets us expect the nπ*- transition in acyl silanes to occur above 400 nm. To achieve a repression of the Brook-rearrangement, two different main strategies should be pursued.

The first strategy is the synthesis of compounds, which have an oxygen atom bound to the silicon atom on which the benzoyl chromophore is bound. If there is one oxygen present already, the tendency to undergo a Brook- rearrangement could probably be reduced as well. Another strategy is the multiple substitution of the Si-atom with aromatic acyl groups. With four acyl groups present, the tendency of the formation of a siloxycarbene could probably be reduced.

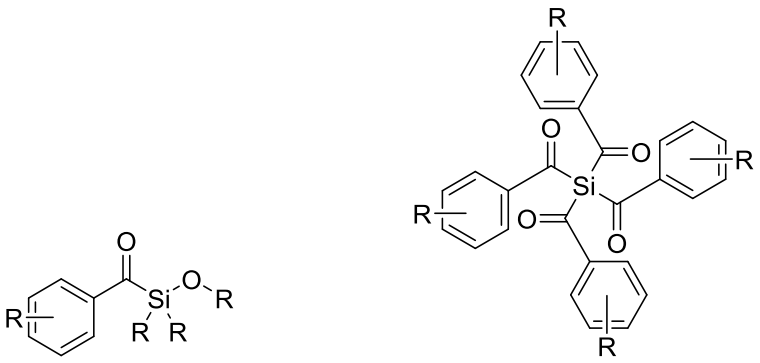

Scheme 14: Acyl-substituted siloxane and tetraacyl-substituted silicon compound

Since this type of compounds is known to be quite sensitive in terms of stability against aqueous hydrolysis, various aromatic acyl substituents should be introduced using the corresponding acyl halides (Scheme 15) to provide steric hindrance to the carbonyl group.

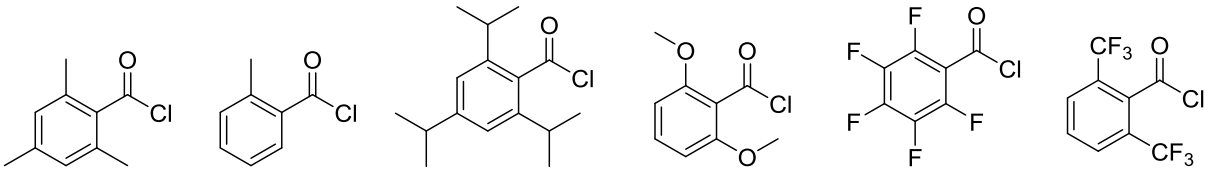

Scheme 15: Acid chlorides

The synthesized compounds should be tested relating to their photochemical properties. UV-Vis spectra should be acquired as well as the implementation of steady state photolysis experiments. The reactivity towards double bonds should then be investigated using photo-DSC. Additionally the stability in aqueous conditions of those compounds should be tested.

State of the art

Photochemistry of acyl silanes

Acyl silanes show similar absorption behavior to their germanium analogues. The introduction of the silicon atom next to the carbonyl group leads to a bathochromic shift of the absorption band of the nπ* transition compared to α-hydroxy alkylphenones as well as compared to bisacyl phosphine oxides. This shift can be explained by an overlap of the empty d- orbitals of the silicon atom with the π* orbital of the carbonyl group[24]. This leads to a lowering in energy and therefore to a longer wavelength needed to cause the n-π* transition.

The absorption maxima of acyl silanes such as **1-6** lie in the visible range at about 415 nm[22, 23, 25] (Scheme 16).

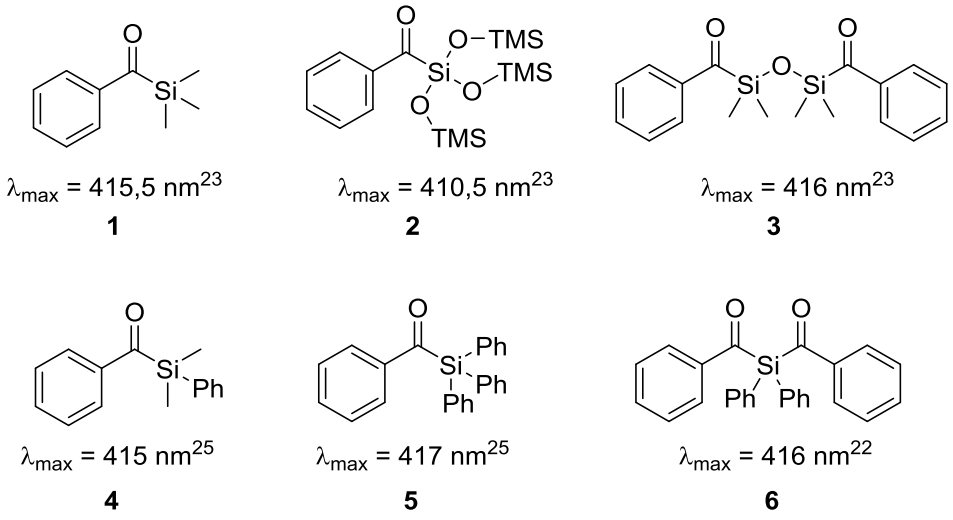

Scheme 16: Absorption maxima of 1-6

As one can see, the substituents at the silicon atom do not influence the absorption maximum strongly.

Although acyl silanes undergo photoinduced α- cleavage, there is another reaction occurring in competition to the α- cleavage, which is a photoinduced rearrangement of acyl silanes forming siloxycarbenes (Scheme 17), described by Brook et al.[26] This reaction is also known as Brook-rearrangement.

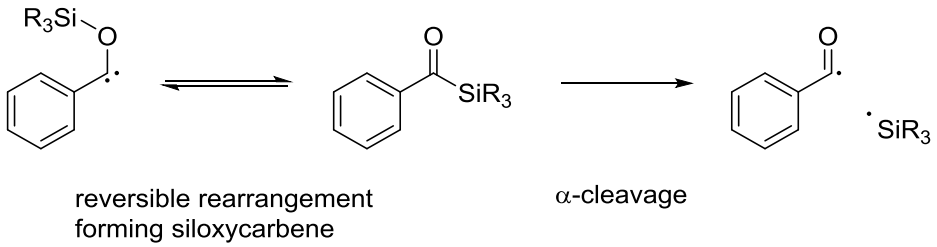

Scheme 17: Competition between α-cleavage and Brook-rearrangement[26]

If that rearrangement is preferred over the α-cleavage, no initiation of photopolymerization occurs, because no reactive radical is formed. It depends on the structure and the surrounding conditions, if α- cleavage or Brook- rearrangement or both processes occur at the same time

The appearance of the siloxycarbene gives an explanation for many different photolysis products[27] (Scheme 18) like the formation of acetals after photolysis of acyl silanes in alcohols.[28, 29] Furthermore, photolysis with compounds containing acidic protons give insertion products,[28] oxiranes are formed during a reaction with aldehydes and ketones,[30] esters are formed reacting with oxygen[31] and addition products can result from a reaction with aryl silanes.[32, 33]

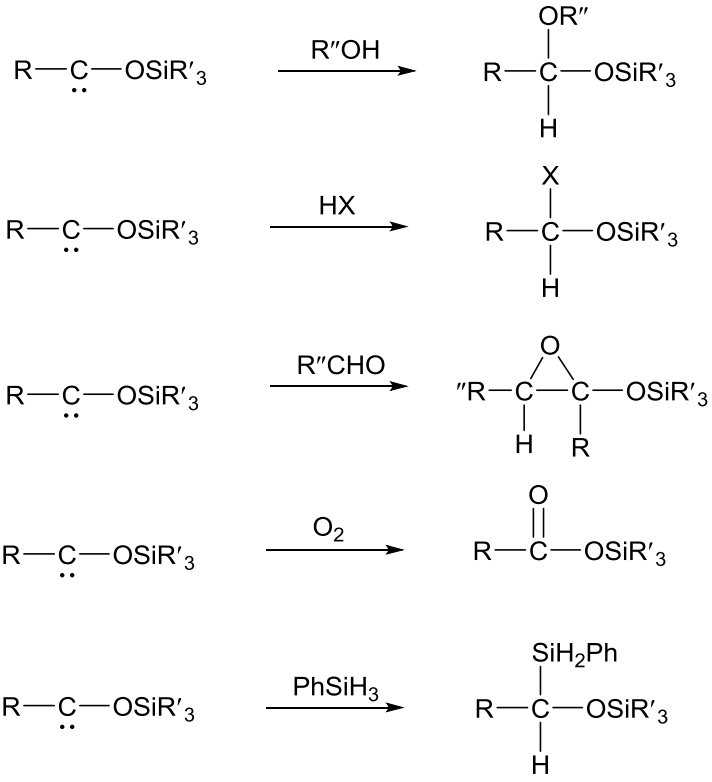

Scheme 18: Photolysis products from acyl silanes

The siloxycarbenes formed via Brook rearrangement are not very stable. If there is no “trapping agent” present they rearrange back forming the corresponding acyl silanes.[34, 35]

Under different reaction conditions, α- cleavage was observed. The photolysis products of different acyl silanes in tetrachlorocarbon indicated the formation of radicals like described for type I photoinitiators[36] (Scheme 19).

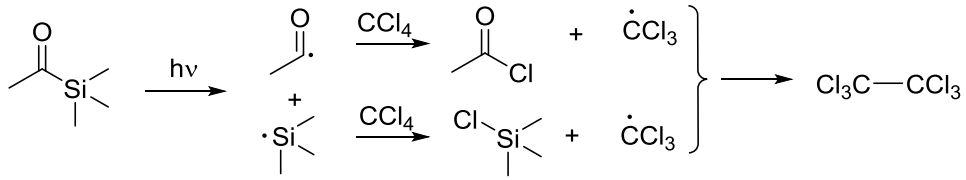

Scheme 19: Photolysis products of acetyltrimethyl silane in CCl_4

A variation of the substituents led to different photolysis products, which indicated a close relation between the exact structure of the acyl silane and the decision, whether Brook-rearrangement or α- cleavage is preferred.

Duff et al. also confirmed this dependency between the photolysis- mechanism and the structure.[28] In apolar solvents, the siloxycarbene was formed only from benzoyltrimethyl silane, however, only radicals were formed from phenylacetyltriphenyl silane. Another example of preferred radical formation was shown with the photolysis of pentafluorobenzoyltris(trimethylsilyl) silane in benzene.[37] Furthermore it was shown, that benzoyltriphenyl silane in tetrachlorocarbon[35] and benzoylphenyldimethyl silane in cyclohexane[38] did not show any photoinduced reaction at all.

Photo-DSC experiments of **1** and **3** showed the completely different reactivities of those two compounds in the dental formulation.[23] From compound **3** radicals were formed after irradiation and therefore photopolymerization was successful. In contrast to that, **1** did not show any reactivity at all. The big difference in reactivity indicates a different photolysis mechanism for the two compounds. It can be assumed, that for **3** α- cleavage is the preferred mechanism, where **1** probably shows a bigger tendency to undergo Brook- rearrangement. It is possible that the oxygen- atom in **3**, which is bound directly to the silicon atom lowers the tendency to undergo the rearrangement.

Generally acyl silanes are described as less stable than acyl germanes.[31, 39] They are quite sensitive at basic conditions and against aqueous hydrolysis.[22] Stability depends strongly on the structure. With the introduction of sterically hindered groups, stability could probably be increased. At the same time, the reactivity of the formed radicals could be decreased, if the radicals are stabilized to a large extent.

Strategies for the synthesis of acyl silanes

The most widely applied method for the synthesis of acyl silanes is the Corey-Seebach reaction (Scheme 20). An aldehyde is converted to its thioacetal derivative using 1,3-propanedithiol (Seebach- Umpolung). This compound can then be treated with organolithium compounds resulting in the formation of a formal acyl anion, which then undergoes a reaction with different electrophiles like chlorosilanes.[40,41]

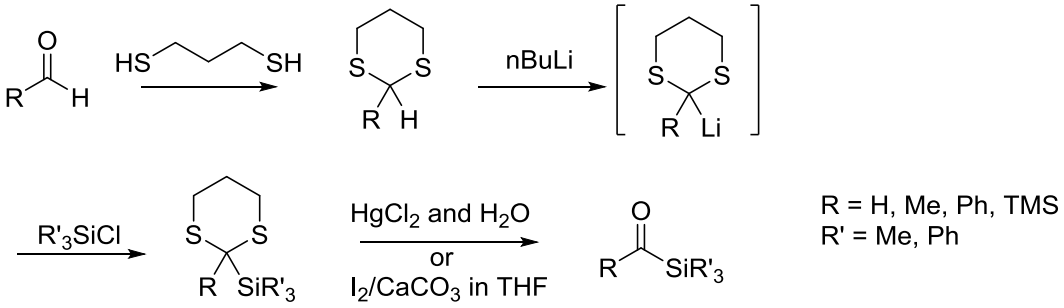

Scheme 20: Synthesis of acyl silanes via Corey-Seebach reaction

Another way to synthesize acyl silanes was described by Baines et al.[42]. In this case a silyllithium reagent is coupled with an appropriate acid chloride (Scheme 21). The silyllithium reagent is prepared using methyl lithium[43].

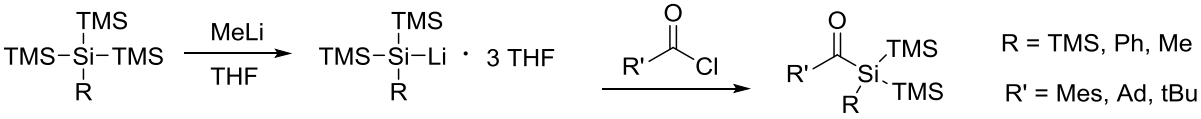

Scheme 21: Synthesis of monoacyl silanes via silyl-lithium species

This method could be adapted by Capperucci et al.[44], who use copper(I) salts like CuCN to get a silylcuprate intermediate, which then reacts with many different acid chlorides (Scheme 22).

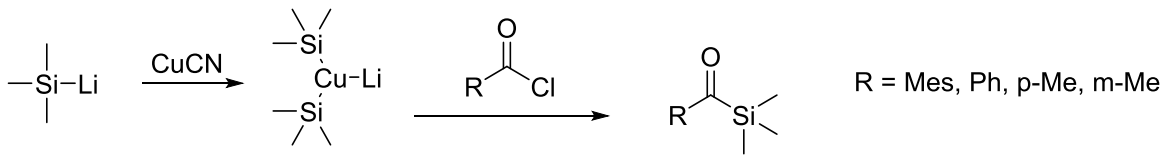

Scheme 22: Synthesis of monoacyl silanes via silylcuprate

Starting from a monoacyl compound, Oshita[45] described the synthesis of di- and tetraacyl silanes which are obtained after the formation of lithium silenolates and their reaction with the acid chlorides (Scheme 23).

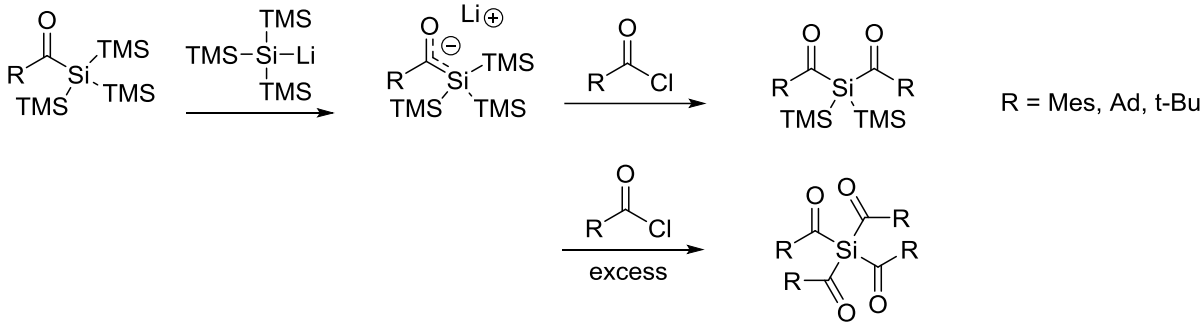

Scheme 23: Synthesis of di- and tetraacyl silanes via silyl-lithium species

Harloff et al.[46] describe the synthesis of silyllithium species containing OTMS groups. The scheme below (Scheme 24) shows the way, they were synthesized.

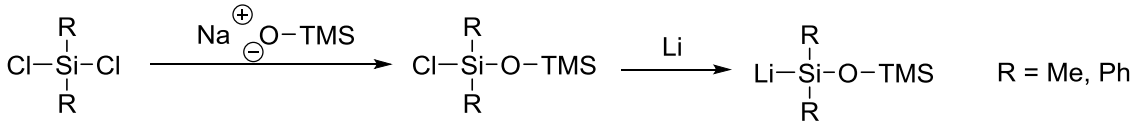

Scheme 24: Synthesis of siloxy-lithium species via sodium trimethylsilanolate

In another route, described by Marschner[47], potassium t-butoxide is used to form the potassium tris(trimethylsilyl)silanide species, which can then react with different electrophiles such as acid chlorides to form acyl silanes (Scheme 25).

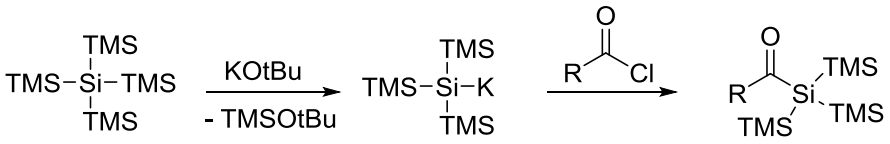

Scheme 25: Synthesis of monoacyl silanes via potassium-silyl species

Further it was reported[48], that also the dipotassium species can be synthesized from hexakis(trimethylsilyl)disilane and potassium t-butoxide (Scheme 26).

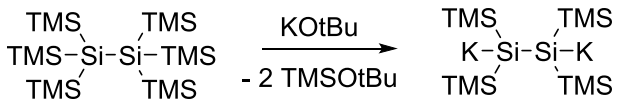

Scheme 26: Synthesis of a dipotassium-silyl species

Brook et al.[22] describe a synthesis, which starts from a chlorobenzylsilane (Scheme 27). Bromination with N-bromosuccinimide and oxidation using silver acetate at aqueous conditions gives acyl silanols like described below. The introduction of a methoxy group before carrying out bromination is also a possibility, to get the corresponding acyl silylether.

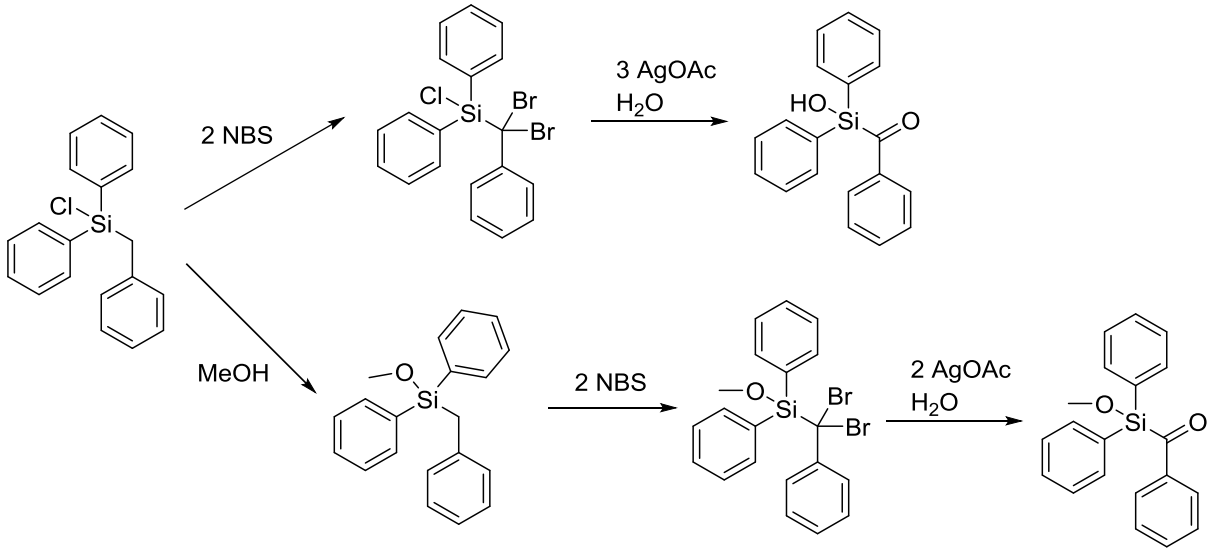

Scheme 27: Synthesis of acyl silanes via bromination followed by oxidation

With this approach the synthesis of diacyl silanes was successful as well (Scheme 28), however the stability of these compounds was described as not satisfying.

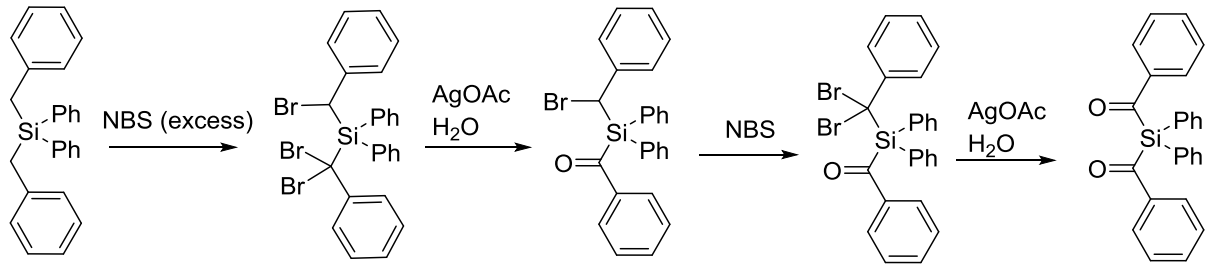

Scheme 28: Synthesis of diacyl silanes via bromination followed by oxidation

Another method is described by Yamamoto et al.[49], in which the acyl silanes are synthesized applying a palladium catalyst (Scheme 29). The aromatic acid chloride reacts with a disilane forming the desired products.

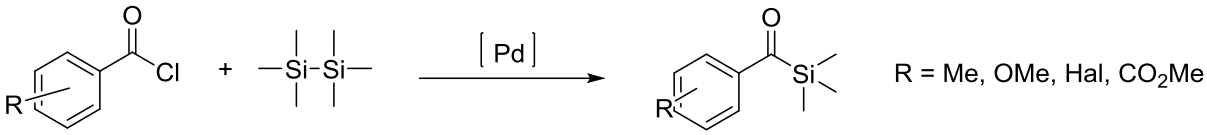

Scheme 29: Synthesis of acyl silanes via palladium-catalyzed coupling using acid chlorides

Wu et al.[50] also described the synthesis of these compounds, but starting from aryl iodides (Scheme 30). Applying CO atmosphere and a palladium catalyst as well, many different acyl silanes could be obtained.

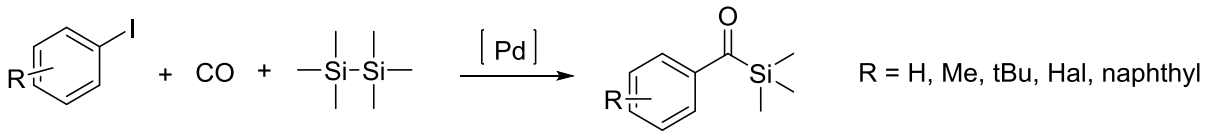

Scheme 30: Synthesis of acyl silanes via palladium-catalyzed coupling using aryl iodides and carbon monoxide

General section

1. Synthesis

1.1 Oxygen- substituted acyl silanes

As described previously, the synthesis of compounds with an oxygen- atom as well as an aroyl group bound to the Si- atom could lead to a repression of the Brook-rearrangement. Mesitoyl groups should be used as aroyl groups to provide a certain steric hindrance at the carbonyl group and therefore increase the stability. As first target compounds, structures **7**-**9** were chosen, because they all contain a Si-O bond next to the mesitoyl group (Scheme 31).

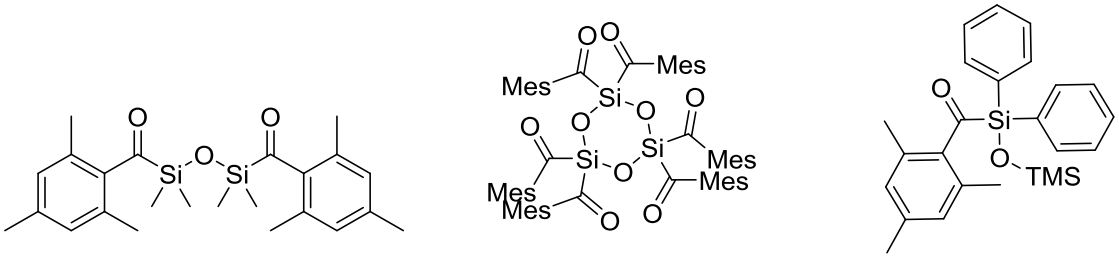

7 **8** **9**

Scheme 31: Target compounds for the synthesis of oxygen- substituted acyl silanes

1.1.1 Bis(mesitoyl)tetramethyldisiloxane (7)

For the synthesis of bis(mesitoyl)tetramethyldisiloxane (**7**) a method described by Corey and Seebach[41,40] should be applied (Scheme 32).

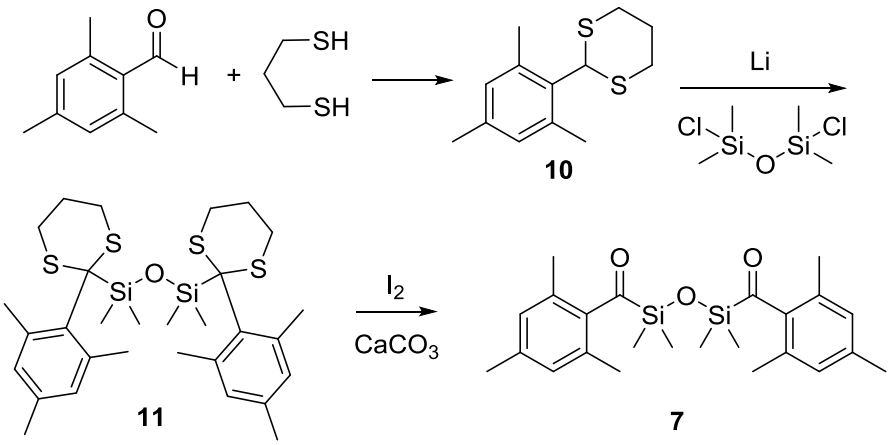

Scheme 32: Synthesis of bis(mesitoyl)tetramethydisiloxane (7)

In this 3- step synthesis the reaction of an aldehyde with a dithiol leads to the corresponding dithiane **10**. This reaction results in a reversion of polarity at the carbonyl- carbon and is known as Seebach- Umpolung. After lithiation the acyl anion is obtained, which can then react with different electrophilic partners (in this case dichlorotetramethylsiloxane) forming **11**. Afterwards the dithian groups are cleaved off using iodine and calcium carbonate to get the carbonyl groups back for **7**.

The Seebach- reagent **10**, formed from mesitaldehyde is not commercially available, thus it was synthesized like described by Kazahaya et al.[51] (Scheme 33).

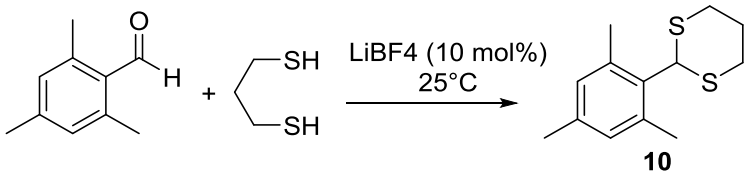

Scheme 33: Synthesis of 2-mesityl-1,3-dithian (9)

For the preparation of **10**, 1,3 eq. of mesitaldehyde and 0,1 eq. of lithium tetrafluoroborate were weighed into a schlenk tube and 1 eq. of dithiane was added over 10min at RT. The formation of the product (white solid) occurred spontaneously. After stirring for 3h the reaction mixture was distilled using a Kugelrohr apparatus, giving the pure product mesityldithiane as a white solid in quantitative (99%) yield.

In the next step mesityldithiane (**10**) should be reacted with n- butyl lithium to form the lithiated intermediate **12**, which is then reacted directly with dichlorotetramethyldisiloxane[52] (Scheme 34).

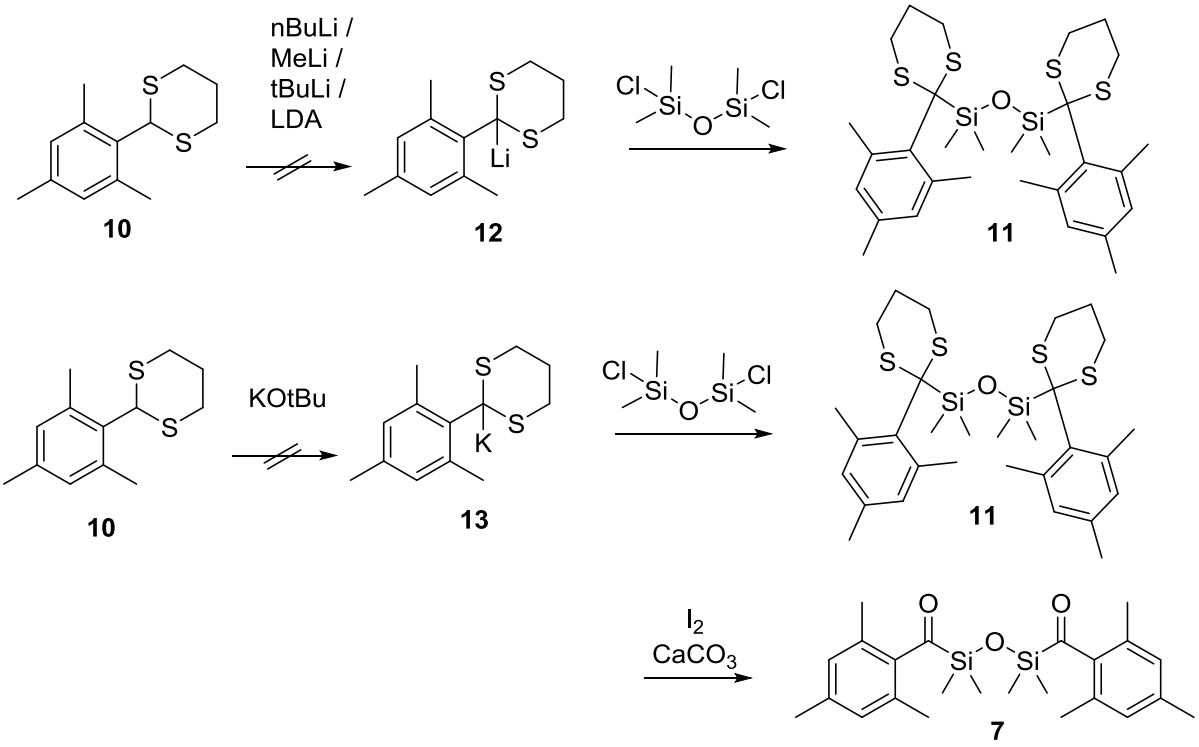

Scheme 34: Synthesis of bis(mesitoyl)tetramethyldisiloxane (7)

Therefore, 2,4 eq. mesityldithiane in dry THF were reacted with 2,4 eq. n-butyl lithium in hexane for 3h at 0°C. Afterwards 1 eq. dichlorotetramethyldisiloxane in dry THF was added slowly, stirred for further 3h and another separately prepared solution of mesityllithiodithiane (0,7 eq.) was added. After stirring for further 3h the reaction vessel was kept in the fridge at 6°C overnight. The next day the solution was quenched with water and extracted with diethylether.

NMR and GC-MS measurements showed that this attempt did not lead to the desired product, assuming that the lithiation of mesityldithiane did not work out. The lithiation step was then repeated with different lithium organyls (MeLi, t-BuLi and LDA[53]), which did not lead to a satisfying result either. The addition of the potential lithium organyl followed by quenching with acetone further showed (Scheme 35), that alkylation under opening of the thioacetal is obviously preferred compared to the desired lithiation. As confirmed by GC-MS, compound **14** was obtained during these experiments. A decrease of the reaction temperature to -78°C to favor the kinetic product, which could eventually be the desired **12** could also not counter that.

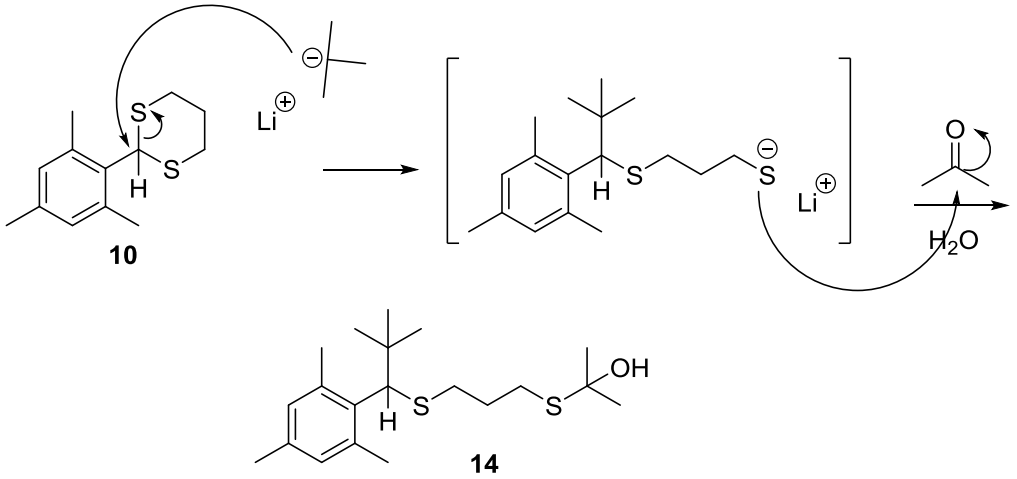

Scheme 35: Potential mechanism for the alkylation under opening of the thioacetal ring

Since potassium tert.- butoxide should also act like a sterically hindered base[54], it could possibly deprotonate compound **10** as desired and therefore work as an alternative reactant to n-butyl lithium. For this reason, another attempt using KOtBu instead of lithium organyls for the synthesis of **11** was carried out. This experiment was carried out exactly like the one using n- butyl lithium, but NMR measurements showed, that KOtBu did not react with the dithiane, but reacted directly with the chlorosiloxane. Therefore the usage of potassium tert.- butoxide did also not lead to the desired product.

Since both lithium organyls and potassium organyls did not react with mesityldithiane (**10**) in the desired way, the compound bis(mesitoyl)tetramethyldisiloxane (**7**) could not be achieved.

1.1.2 Hexakis(mesitoyl)cyclotrisiloxane (8)

Another interesting compound for further photochemical studies is hexakis(mesitoyl)cyclotrisiloxane (**8**). This compound might be synthesized from the analogue hexakis(trimethylsilyl)- compound **15**. Brook et al.[55] describe the synthesis of this compound starting from dichlorodi(trimethylsilyl)silane (**16**) (Scheme 36), which can be synthesized in a 2- step synthesis starting from dichlorodiphenylsilane[56,57] (Scheme 37).

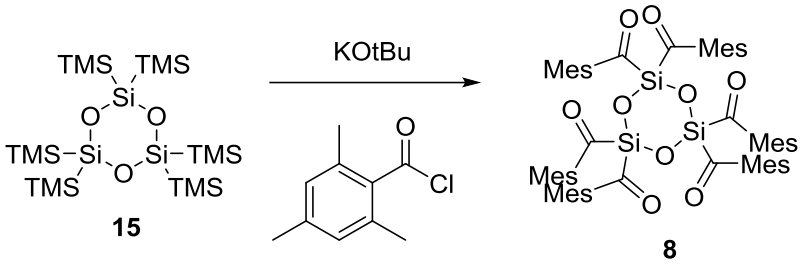

Scheme 36: Synthesis of hexakis(mesitoyl)cyclotrisiloxane (8)

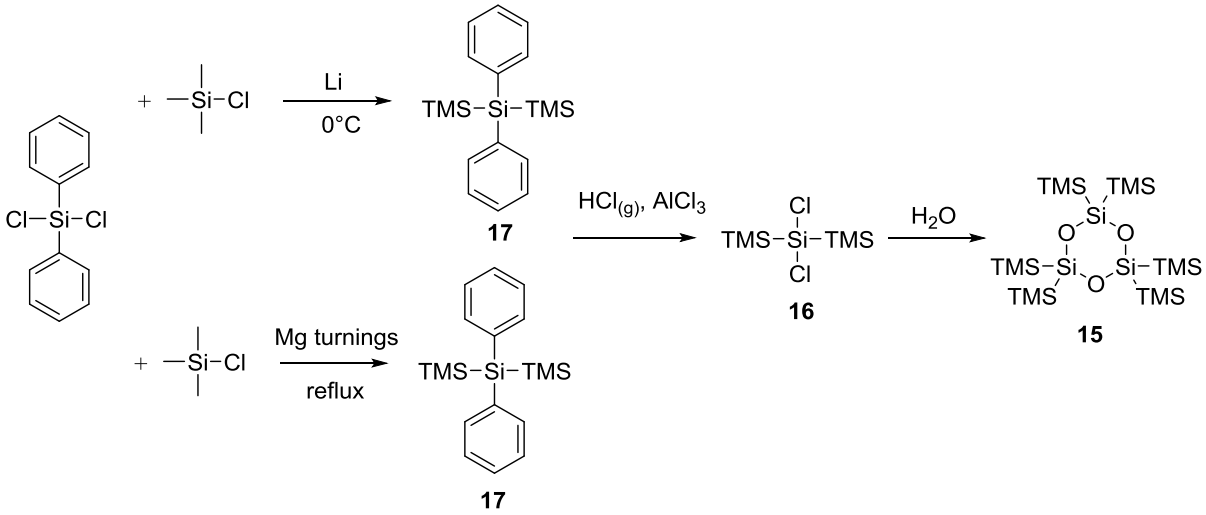

Scheme 37: Synthesis of dichlorodi(trimethylsilyl)silane (16) and hexakis(trimethylsilyl)cyclotrisiloxane (15)

For the synthesis of the first intermediate diphenyldi(trimethylsilyl)silane[56] (**17**), a mixture of 1 eq. dichlorodiphenylsilane and 20 eq. trimethylsilylchloride was added to 6 eq. lithium wire in dry THF at RT. After stirring for 48h at RT no reaction occurred, indicated by the remaining amount of lithium wire. Either the lithium wire was fully passivated from the beginning or the surface of the wire was simply too small. Moreover the solvent and the reaction temperature could be the reason for the absence of a reaction.

In another attempt (Scheme 38) trimethylsilyl bromide (1,5 eq.) in diethylether was used instead of trimethylsilyl chloride (Scheme 38). 1,5 eq. lithium wire in diethylether were weighed into a schlenk tube and the mixture was then cooled down to -78°C. Trimethylsilyl bromide was added before stirring the reaction mixture for 2h. The cooling was removed and the mixture was stirred overnight at RT. As it was the case already in the first attempt, there was no formation of the lithiated TMSBr (again

indicated by the remaining amount of lithium wire in the reaction vessel) and therefore no successful synthesis of diphenyldi(trimethylsilyl)silane (**17**).

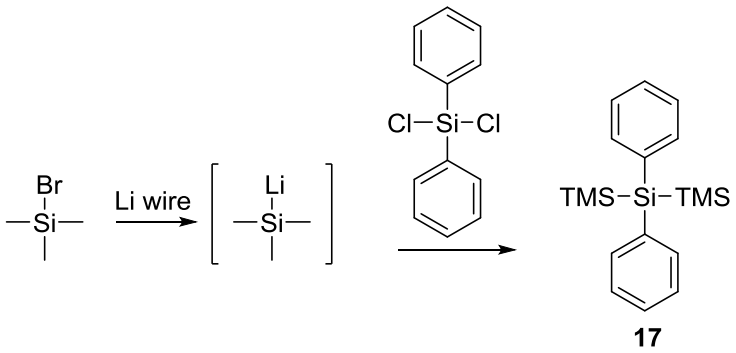

Scheme 38: Synthesis using trimethylsilyl bromide for the synthesis of 17

The next attempt[56] was carried out using a 25 wt% lithium dispersion (6 eq.) instead of the wire. With the much bigger surface of the lithium suspension compared to the wire the reaction could potentially work out as desired. Apart from that, the first attempt was repeated like described. After stirring for a few hours, the suspension changed its color to brownish and after stirring overnight at RT, a large amount of white precipitate had formed. The mixture was filtrated and the solvent evaporated. LiCl is soluble in THF, so the product was dissolved in dichloromethane, filtered and the solvent was evaporated again giving a beige sticky substance. The desired product could be confirmed using GC- MS, but the chromatogram showed also a large amount of educts and many different side products (Scheme 39) in the mixture. Kugelrohr- distillation was applied, but with this method the pure product could not be achieved either. Especially the different oxidation products could not be separated from the target compound. Probably those products formed mainly during Kugelrohr distillation at high temperatures.

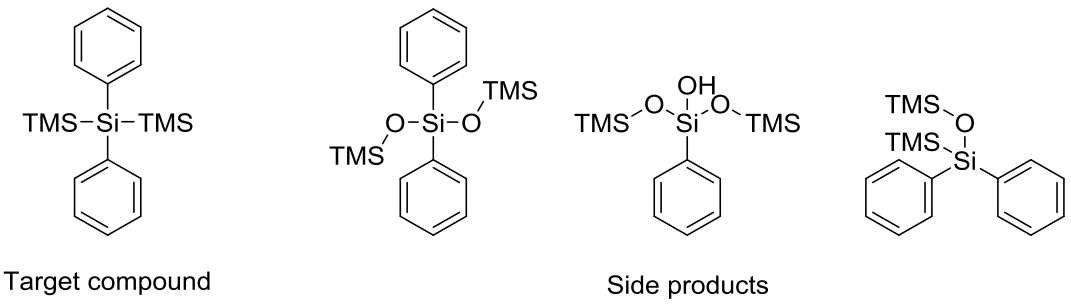

Scheme 39: Some of the achieved side products, which could not be separated using Kugelrohr distillation

Since the described methods did not lead to success so far, an alternative synthesis[58] describing the preparation of the exact same compound **17** was carried out using magnesium cuttings instead of lithium. Therefore 2,2 eq. magnesium cuttings were weighed into a schlenk tube together with THF and then a mixture of 1 eq. dichlorodiphenylsilane and 2,2 eq. trimethylsilyl chloride was added at RT. The mixture was heated to 60-70°C and one small piece of iodine was added to start the Grignard- reaction. The mixture was then refluxed overnight and stirred for further 24h at RT. Formation of a white precipitate occurred during that time. The reaction mixture was quenched with saturated aqueous ammonium chloride solution, filtrated and extracted with diethylether, giving again a beige sticky substance after solvent evaporation. GC- MS confirmed the target compound, but the large amount of side products made further purification impossible.

Diphenyldi(trimethylsilyl)silane, which was the first intermediate in the sequence of synthesis for hexakis(mesitoyl)cyclotrisiloxane (**8**) could not be achieved during several different attempts. Obviously, diphenyldi(trimethylsilyl)silane (**17**) forms various oxidation products after very short exposition to air or/and moisture. Therefore, the promising compound hexakis(mesitoyl)cyclotrisiloxane (**8**) could not be achieved with the applied syntheses.

1.1.3 Diphenylmesitoyl(trimethylsilyl)disiloxane (9)

Another interesting compound with an oxygen- atom next to the Si- atom is diphenylmesitoyl(trimethyl)disiloxane (**9**). Harloff et al.[46] described both the synthesis of the siloxychlorosilane **18** and the following formation of a Li- intermediate, which can then react with different electrophiles (Scheme 40). Mesitoylchloride could work as an electrophile, but additionally there is the possibility of a Cu- catalysis of this reaction relating to Capperucci.[44]

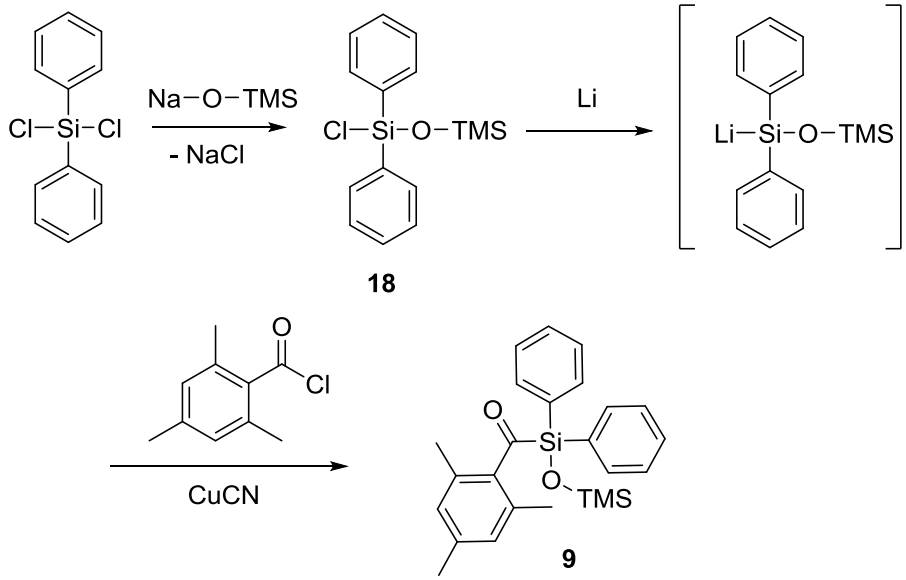

Scheme 40: Synthesis of diphenylmesitoyl(trimethyl)disiloxane 6

For the synthesis of **18**, 1 eq. of sodium trimethylsilanolate in a mixture of dry n-pentane and dry diethylether (ratio 3:2) was reacted with 1,1 eq. of dichlorodiphenylsilane at -78°C for 15min. The mixture was allowed to reach RT, which caused the formation of a white precipitate. The mixture was then filtrated under inert conditions and the resulting solid was washed twice with a small amount of dry diethylether. The filtrate was concentrated by evaporating the solvent carefully and the crude product **18** was then purified applying Kugelrohr- distillation.

NMR spectra of the product fraction indicated a successful synthesis of the target compound **18** nevertheless the used purification method could not give the pure product. The amount of side products in the product fraction was huge.

Maybe compound **18** rearranges forming other compounds at temperatures, which are required for Kugelrohr- distillation, although oxygen and moisture were excluded during the whole synthesis. The actual target molecule **9** could therefore not be synthesized with the applied syntheses.

1.2 Acyl silanes

Since the strategy of synthesizing oxygen- substituted acyl silanes did not lead to success due to the elaborate syntheses required for this type of compounds, another strategy was needed to achieve a suitable long-wavelength photoinitiator. Oshita et al.[45] described the synthesis of acyl silanes via an intermediary formed Li- silenolate starting from a monosubstituted acyl silane. From this silenolate the tetrasubstituted compound can be achieved directly using an excess of acid chloride. As this synthesis path did not lead to success as described, an alternative synthesis according to Marschner[47] was applied. This synthesis should in theory lead to several different tetraacylsilanes (**19**-**24**) depending on the used acid chlorides (Scheme 41).

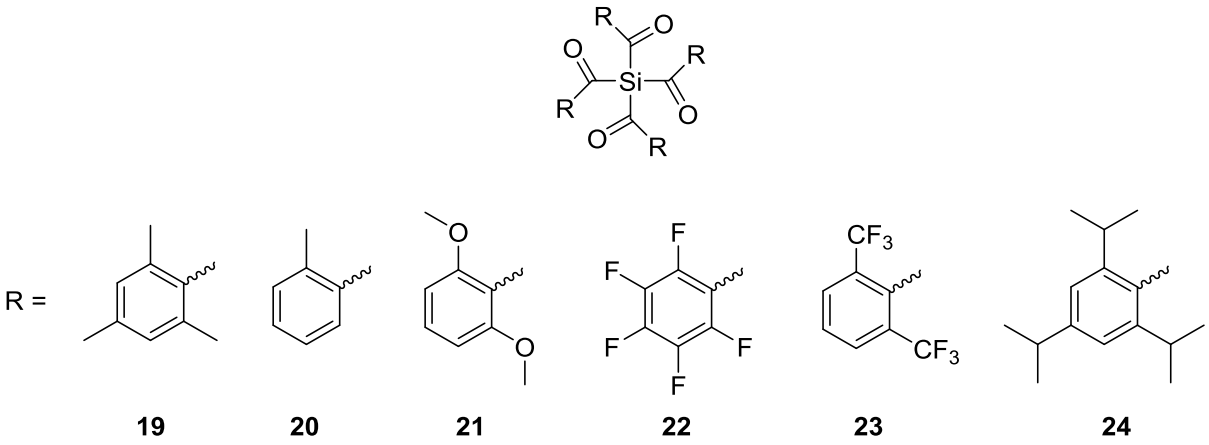

Scheme 41: Tetraacylsilanes: target compounds

In this route, tetrakis(trimethylsilyl)silane reacts with potassium tert- butoxide forming a potassium silanide, which reacts then together with the acid chloride forming the desired product. The distinction between the formation of the monosubstituted or the tetrasubstituted product mainly depends on the rate of addition and the used amount of acid chloride. Slow addition and a small excess of acid chloride gives mainly the monosubstituted, fast addition and a shortfall of acid chloride gives the tetrasubstituted silane. The following Scheme 42 shows the proposed mechanism for the formation of tetramesitoylsilane (**19**).

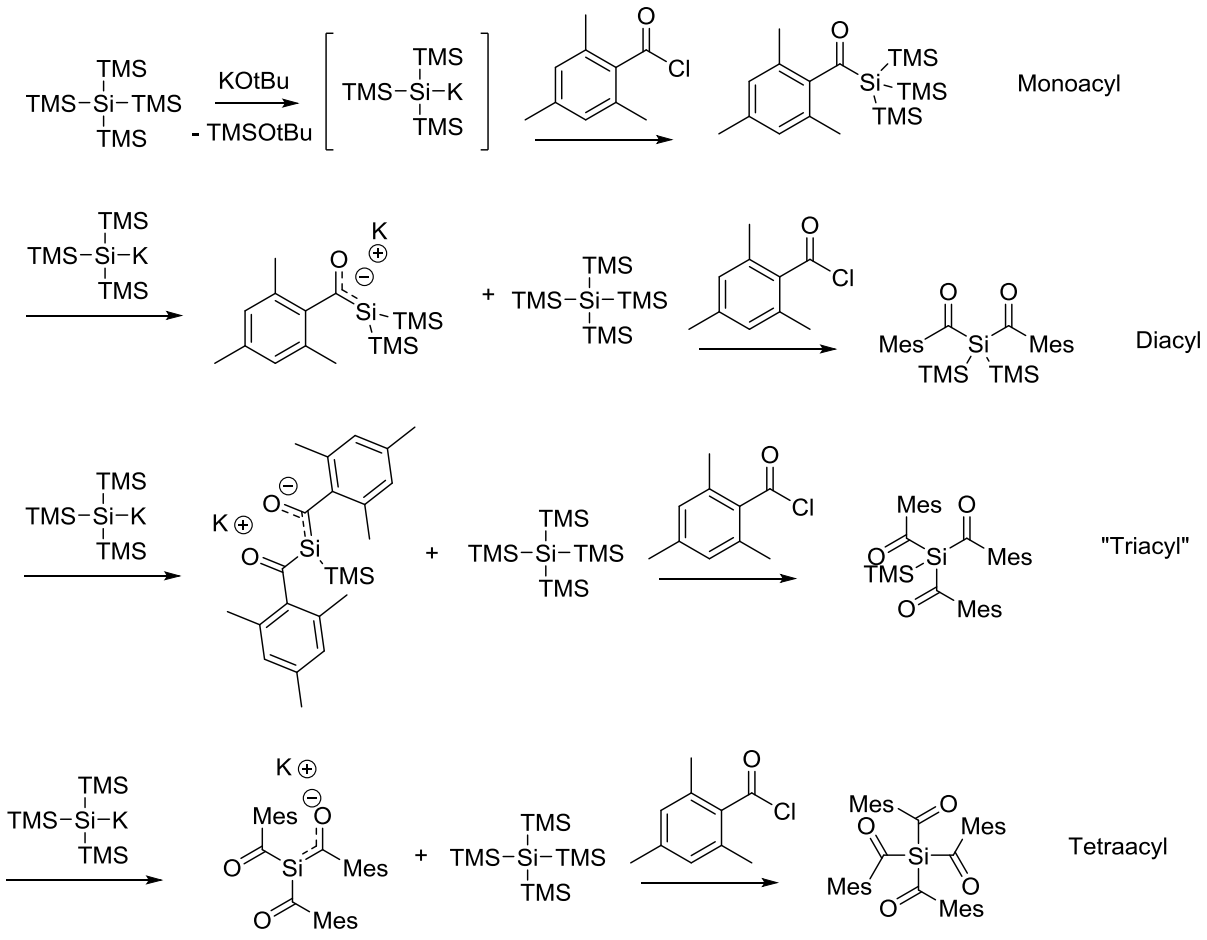

Scheme 42: Proposed mechanism for the formation of tetramesitoylsilane (19)

Potassium silanide, which is formed in the first step, reacts at first with one equivalent of acid chloride forming monoacyl silane. This species reacts then with another potassium silanide molecule forming one equivalent potassium silenolate and one equivalent tetrakis(trimethylsilyl)silane. Then, the silenolate reacts with the acid chloride forming the diacyl compound. This compound was detected, but could not be isolated. These last two steps are repeated two times, giving the tetrasubstituted product in the end. The trisubstituted product probably reacts very fast, thus it could not even be detected. The formation of the silenolate is probably the rate-determining step, which is the reason for the used shortfall of acid chloride. The Usage of a small excess of potassium silanide probably accelerates the formation of the acyl silanes. To synthesize the target compounds, the used acid chlorides were chosen to provide steric hindrance at the carbonyl group and to make the silanes more stable against nucleophilic attacks on that carbonyl carbon, such as hydrolysis or oxidative decomposition.

1.2.1 Mesitoylsilanes

1.2.1.1 Tris(trimethylsilyl)mesitoylsilane (25)

At first the tetrasubstituted compound **19** was not considered to be synthesizable directly, so the monosubstituted mesitoylsilane **25** was prepared (Scheme 43). This compound should then react to form the tetrasubstituted one. The mesitoyl group should provide enough steric hindrance at the carbonyl carbon to increase the stability to an acceptable level.

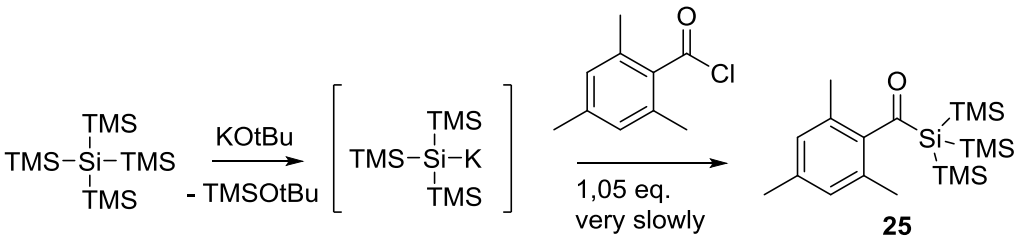

Scheme 43: Synthesis of tris(trimethylsilyl)mesitoylsilane (25)

For the synthesis of **25** one equivalent of tetrakis(trimethylsilyl)silane and 1,05 eq. of potassium tert- butoxide were reacted together with dry 1,2-dimethoxyethane. During stirring for 2h the potassium silanide species was formed, which was then added to 1,05 equivalents of 2,4,6-trimethylbenzoylchloride very slowly at -40°C. After that, cooling was removed and the mixture was stirred for 2h before being quenched with a mixture of 3% H_2SO_4 (pH 5) and ice. The crude product was obtained after liquid-liquid extraction and purification was carried out using recrystallization and a silicagel column giving the pure product as a light yellow solid in 11% yield.

1.2.1.2 Tetramesitoylsilane (19)

As mentioned previously, tetramesitoylsilane (**19**) could be synthesized directly from tetrakis(trimethylsilyl)silane by adopting the rate of addition and the used amount of acid chloride (Scheme 44).

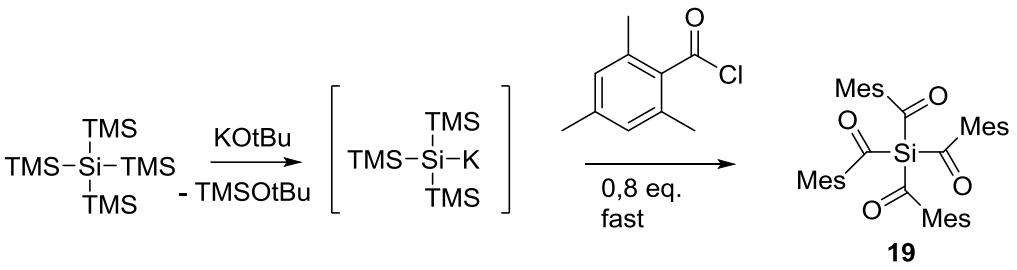

Scheme 44: Synthesis of tetramesitoylsilane (19)

For the synthesis of **19** the same general synthesis as for the monofunctional mesitoylsilane was carried out. The things, which had been changed to achieve the tetrasubstituted compound **19** were the rate of addition of the potassium silanide solution to the acid chloride and the amount of used acid chloride. For **19** the potassium silanide solution was added quite fast to only 0,8 equivalents of the acid chloride. Furthermore no silicagel column was needed for the isolation of tetramesitoylsilane (**19**) in 8% yield as a deep yellow solid.

1.2.2 Toluoylsilanes

o-Toluoyl substituents provide less steric hindrance against nucleophilic attacks towards the carbonyl group, but compared to the mesitoyl group, they can rotate more freely and therefore might shift the absorption to higher wavelengths. Hence the mono- and the tetrasubstituted o-toluoylsilane should be synthesized. Especially for the tetrasubstituted silane the increased rotational freedom of the substituents could make a difference.

1.2.2.1 Tris(trimethylsilyl)-o-toluoylsilane (26)

At first the tetrasubstituted compound **20** was not considered to be synthesizable directly, so the monosubstituted toluoylsilane **26** was prepared (Scheme 45).

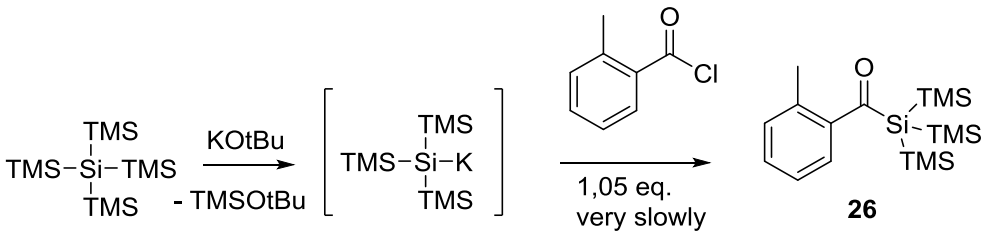

Scheme 45: Synthesis of tris(trimethylsilyl)-o-toluoylsilane (26)

For the synthesis of tris(trimethylsilyl)-o-toluoylsilane (**26**) the exact same synthesis as for tris(trimethylsilyl)mesitoylsilane (**25**) was carried out. Compound **26** could be isolated using recrystallization from n-pentane in 20% yield as dark yellow liquid.

1.2.2.2 Tetra-o-toluoylsilane (20)

As mentioned already, the increased rotational freedom of the o-toluoyl substituents might shift the absorption to higher wavelengths. Therefore tetra-o-toluoylsilane **20** should be synthesized (Scheme 46).

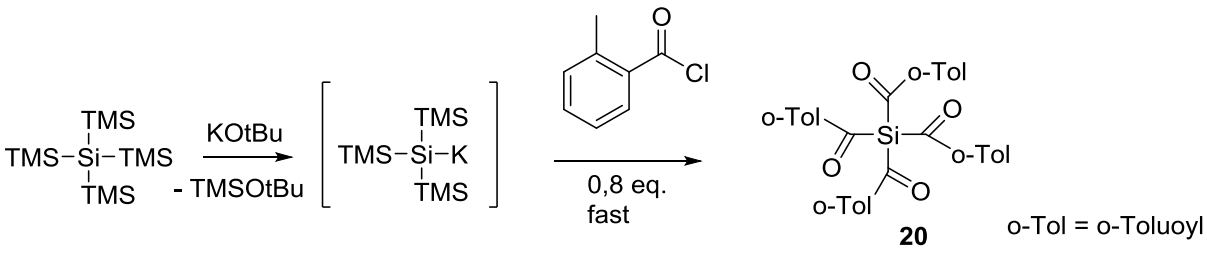

Scheme 46: Synthesis of tetra-o-toluoylsilane (20)

To achieve compound **20** the exact same synthesis as for tetramesitoylsilane (**19**) was carried out. After the given reaction time a NMR- sample was taken from the reaction solution, which indicated no formation of the product at all. Obviously the synthesis used for tetramesitoylsilane (**19**) could not be applied for the product with the sterically less hindered substituent. Additionally the synthesis path described by Oshita et al.[45] in which the tetrasubstituted compound is achieved from the monosubstituted one was tried for this compound, but did not lead to the desired product **20** as well.

1.2.3 Alternative tetraacyl silanes

To further vary the rotational freedom of the substituents, the stability and the solubility properties of **19**, the tetrasubstituted compounds with other substituents at the benzoyl group should be synthesized.

1.2.3.1 Tetra(2,6-dimethoxybenzoyl)silane (21)

The two methoxy groups should provide strong steric hindrance at the carbonyl group. Additionally the electronic properties of target molecule **21** should be changed significantly compared to compound **19** by introducing those groups (Scheme 47).

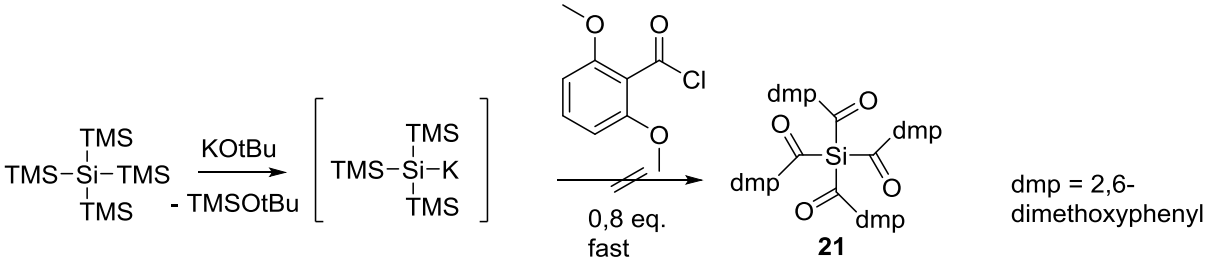

Scheme 47: Synthesis of tetra(2,6-dimethoxybenzoyl)silane (21)

To achieve compound **21** the exact same synthesis as for tetramesitoylsilane (**19**) was carried out. The crude product, a white solid was identified as a mixture of tetrakis(trimethylsilyl)silane and hexakis(trimethylsilyl)disilane (**27**) by GC-MS and NMR spectroscopy. This indicated, that 2,6-dimethoxybenzoylchloride was too unreactive to react with the potassium silanide. Thus the potassium silanide preferably reacted with itself forming hexakis(trimethylsilyl)disilane (**27**) (Scheme 48).

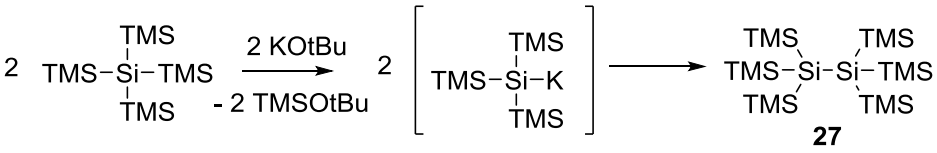

Scheme 48: Formation of hexakis(trimethylsilyl)disilane 27

1.2.3.2 Tetra(2,3,4,5,6-pentafluorobenzoyl)silane (22)

The five fluorine atoms at the benzoyl structure (Scheme 49) should provide different stability and solubility in target molecule **22** compared to compound **19**. Although the fluorine atoms are very small and therefore not very useful for steric reasons, they can act via hydrophobic shielding to protect the carbonyl group.

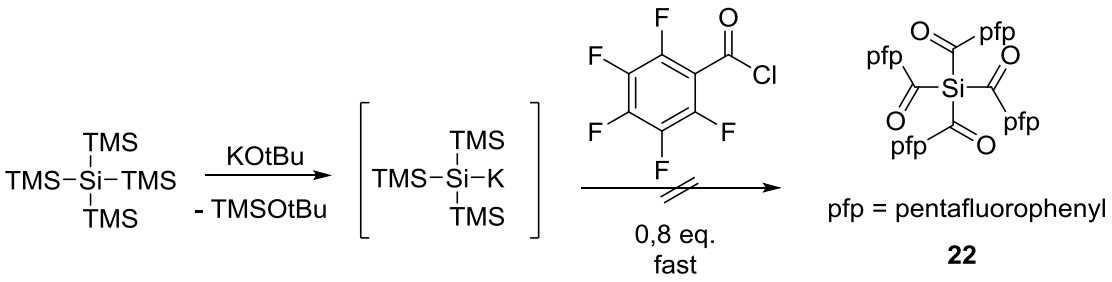

Scheme 49: Synthesis of tetra(2,3,4,5,6-pentafluorobenzoyl)silane (22)

To achieve compound **22** the exact same synthesis as for tetramesitoylsilane (**19**) was carried out. For the crude product, a yellow, sticky substance, NMR and ATR-IR experiments were carried out, but these experiments could not confirm, that the obtained yellow substance contained tetra(2,3,4,5,6-pentafluorobenzoyl)silane (**22**). HPLC analysis was not possible due to solubility issues. Probably the effect of the hydrophobic shielding is too strong and the acid chloride does not react in the desired way with the potassium silanide.

1.2.2.3 Tetra[2,6-bis(trifluoromethyl)benzoyl]silane (23)

The trifluoromethyl group and the methyl group have very similar properties regarding the steric dimensions. Therefore tetra[2,6-bis(trifluoromethyl)benzoyl]silane (**23**) should be synthesized as well to investigate its stability, reactivity and solubility (Scheme 50).

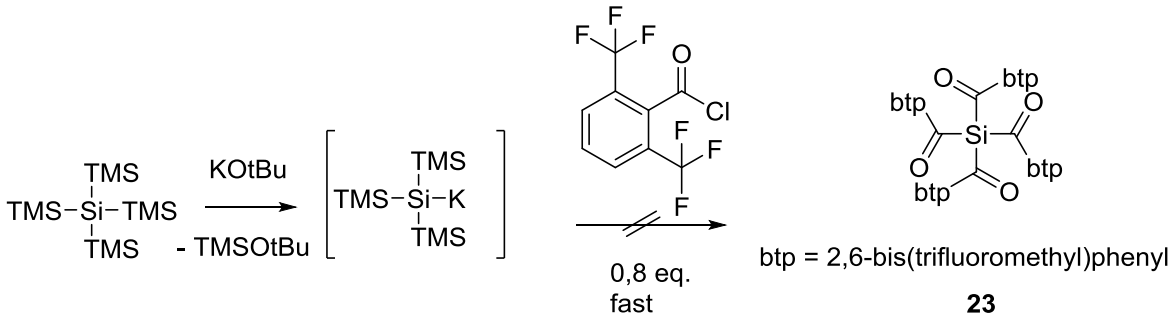

Scheme 50: Synthesis of tetra[2,6-bis(trifluoromethyl)benzoyl]silane (23)

To achieve compound **23** the exact same synthesis as for tetramesitoylsilane (**19**) was carried out. For the crude product, a sticky red substance, NMR and ATR-IR measurements were carried out, which did not indicate the desired product **23** at all. Obviously, the trifluoromethyl groups change the electronic properties of the acid

chloride to a large extent compared to the methyl groups in compound **19** and therefore the reaction did not work out in the desired way.

1.2.2.4 Tetra(2,4,6-triisopropylbenzoyl)silane (24)

Since the isopropyl group is quite similar to the methyl group regarding their electronic properties, the triisopropylbenzoyl acid chloride should be used to synthesize tetra(2,4,6-triisopropylbenzoyl)silane (**24**) (Scheme 51). Furthermore the isopropyl groups provide strong steric hindrance at the carbonyl group.

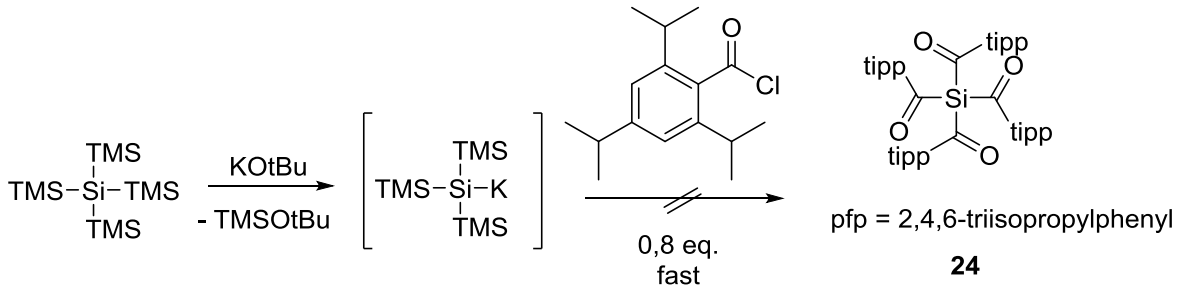

Scheme 51: Synthesis of tetra(2,4,6-triisopropylbenzoyl)silane (24)

To achieve compound **24** the exact same synthesis as for tetramesitoylsilane (**19**) was carried out. For the crude product, a white solid, NMR and GC-MS measurements were carried out, which indicated no formation of target compound **24**.

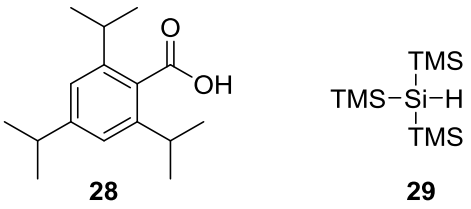

Scheme 52: 2,4,6-Triisopropylbenzoic acid (28) and tris(trimethylsilyl)silane (29) formed during aqueous workup

Large amounts of 2,4,6-triisopropylbenzoic acid (**28**) indicated, that the acid chloride did not react with the potassium silanide, but was hydrolyzed during the aqueous workup (Scheme 52). The appearing of tris(trimethylsilyl)silane (**29**) supports this assumption as well. Probably the steric hindrance at the carbonyl group, caused by the introduction of the isopropyl groups was too large.

2. Characterization

The successfully synthesized compounds **25**, **19** and **26** (Scheme 53) were tested regarding to their photochemical properties.

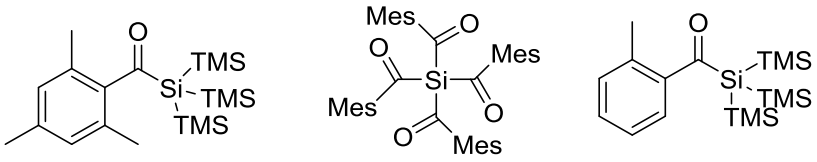

25 **19** **26**

Scheme 53: Synthesized acyl silanes

Photo-DSC experiments were carried out for **25**, **19** and **26** to determine the reactivity towards double bonds. As only compound **19** showed high reactivity in those preliminary experiments UV-Vis spectroscopy should be carried out for compound **19** to investigate the absorption of the nπ* transition. Additionally, steady-state photolysis experiments using a LED should give information about the photobleaching behavior of **19**. The storage stability was also investigated, especially the stability of **19** and **25** in aqueous solutions.

2.1 UV-Vis spectroscopy

UV-Vis spectra of tetramesitoylsilane (**19**) were recorded and then compared to the spectra of the reference photoinitiators camphorquinone, BAPO and Ivocerin. This should confirm the absorption of **19** between 400 and 500 nm, caused by the nπ* transition. Solutions in dichloromethane were prepared (c = 1x 10^{-3} mol L^{-1} for tetramesitoylsilane (**19**), BAPO and Ivocerin; c = 1 x 10^{-2} mol L^{-1} for camphorquinone), which were then transferred to quarz cuvettes.

The figure below (Figure 9) shows the assembled spectra of **19**, CQ, BAPO and Ivocerin and also the emission band of the currently applied dental LED.

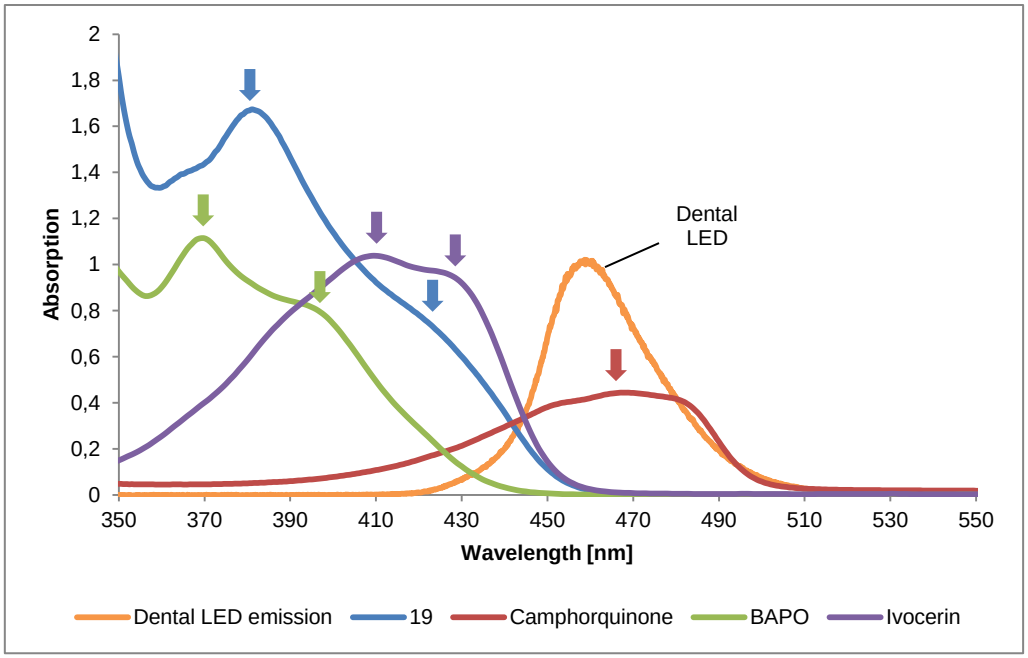

Figure 9: UV-Vis spectra of tetramesitoylsilane (19) compared to the reference initiators

The nπ* absorption band of tetramesitoylsilane (**19**, blue curve) reaches into the area above 450 nm, thus fulfilling one criterion of the objective. It also overlaps well with the emission band of the dental LED.

The absorption maxima were determined via mathematical peak deconvolution. For the determination of the molar extinction coefficients at the absorption maxima, Lambert-Beer law was applied.

$$a = \varepsilon \cdot c \cdot d$$

a…absorbance

c…concentration [mol L^{-1}]

d…path length [cm]

As the absorption bands of BAPO and Ivocerin also do, the band of **19** shows a shoulder, which indicates a second absorption maximum (422 nm) overlaid by the main band with an absorption maximum at 382 nm. This could be the result of the restricted rotational freedom of the mesitoyl substituents in **19**.

The results for tetramesitoylsilane (**19**) and the reference initiators are shown below (Scheme 54).

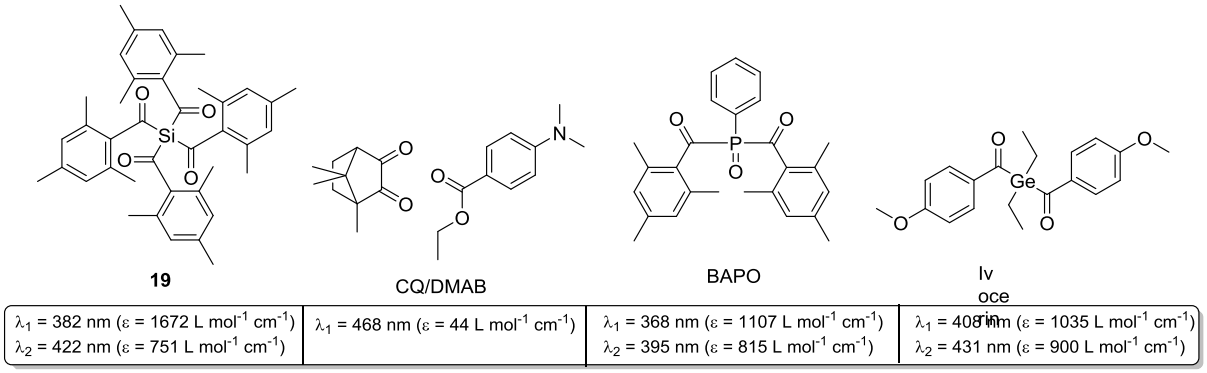

Scheme 54: Results of the UV-Vis measurements for tetramesitoylsilane (19) and the reference photoinitiators

Comparing the λ_1 values of **19** (382 nm), BAPO (368 nm) and Ivocerin (408 nm) the the silicon atom next to the mesitoyl chromophore seems to cause a significant bathochromic shift compared to the phosphorus atom in BAPO, although the germanium in Ivocerin shifts the band even further to longer wavelengths. The same goes for the λ_2 values of **19** (422 nm), BAPO (395 nm) and Ivocerin (431 nm).

Tetramesitoylsilane (**19**) showed very high extinction coefficients (ε_1 = 1672 L mol^{-1} cm^{-1} and ε_2 = 751 L mol^{-1} cm^{-1}) compared to camphorquinone. They also exceeded those of BAPO and Ivocerin.

Additionally, the influence of a Si-Si bond next to the mesitoyl chromophore on the nπ* absorption band should be investigated in greater detail. For this reason, an UV-Vis spectrum of tris(trimethylsilyl)mesitoylsilane (**25**) was recorded (Figure 10) and then compared to the absorption spectrum of benzoyltrimethylsilane[59] (**30**) (Scheme 55). The question was, if the Si-Si bond could lead to a further bathochromic shift as it is known for polysilanes.[60]

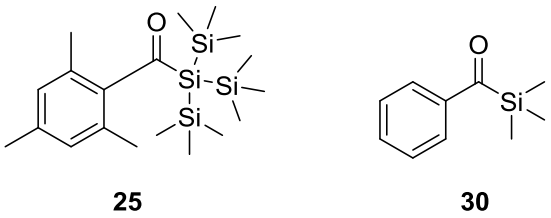

25 **30**

Scheme 55: Tris(trimethylsilyl)mesitoylsilane (25) with Si-Si bond and the reference compound benzoyltrimethylsilane[23] (30)

For both compounds, the same solvent (acetonitrile) and the same concentration (c = 5 x 10^{-3} mol L^{-1}) were used.

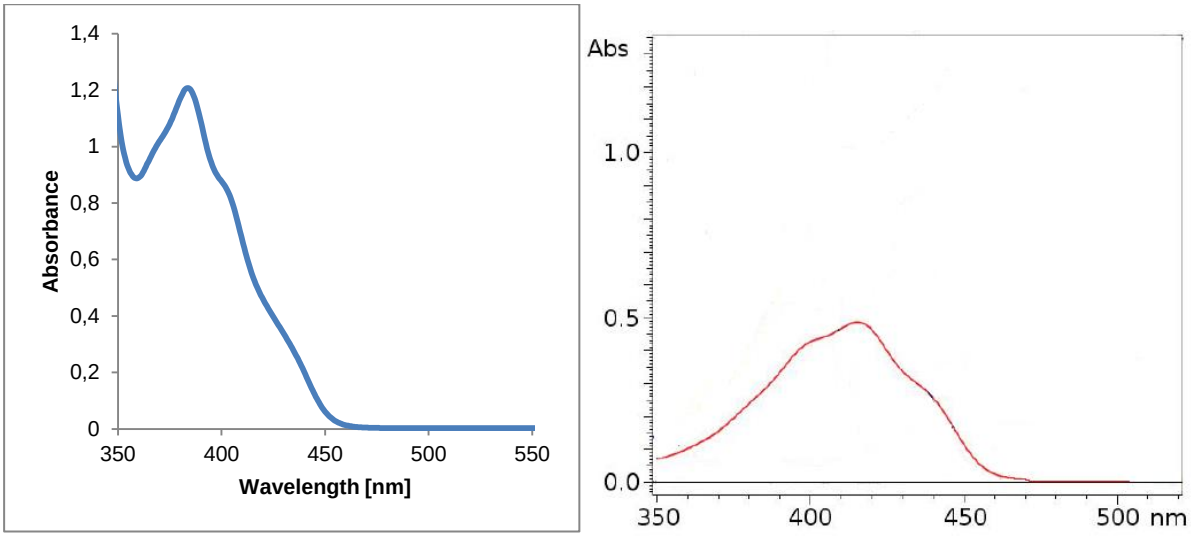

Figure 10: UV-Vis absorption spectra of tris(trimethylsilyl)mesitoylsilane (25) and benzoyltrimethylsilane[23] (30)

The absorption maxima were determined via mathematical peak deconvolution and the extinction coefficients were calculated as described above. The results are shown below (Scheme 56).

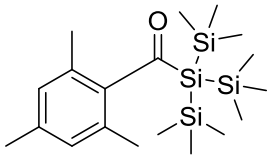

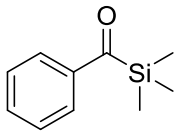

25	**30**
λ_1 = 383 nm (ε = 241 L mol^{-1} cm^{-1})	λ_1 = 398 nm (ε = 86 L mol^{-1} cm^{-1})
λ_2 = 400 nm (ε = 175 L mol^{-1} cm^{-1})	λ_2 = 416 nm (ε = 97 L mol^{-1} cm^{-1})
λ_3 = 422 nm (ε = 87 L mol^{-1} cm^{-1})	λ_3 = 440 nm (ε = 54 L mol^{-1} cm^{-1})

Scheme 56: Comparison of the absorption maxima of 25 and 30

The scheme above shows, that the Si-Si bond in **25** did not cause a further redshift of the nπ* absorption band. The absorption maxima of benzoyltrimethylsilane (**30**) did show up at longer wavelengths instead. Therefore it can be told, that a Si-Si bond right next to the chromophore does not cause a bothochromic shift in the absorption spectrum.

2.2 Steady state photolysis (SSP)

To use a photoinitiator in dental formulations, its chromophore should be fully or at least partly destroyed during polymerization to achieve a photopolymer, which is not colored. This process is called photobleaching. Photopolymers from polymerization using the camphorquinone/amine system often show a slight yellowness. In steady state photolysis, a photoinitiator solution is irradiated and samples are taken at defined intervals to investigate irradiation time dependent properties such as photobleaching.

To investigate the photobleaching effect of tetramesitoylsilane (**19**), such steady-state photolysis experiments were carried out. A two-necked photoreactor was equipped with a quickfit, which had been closed with a quarz window. One end of an optical waveguide was then placed on this quarz window inside the quickfit, the other end was connected to a LED (400 nm) and an Omnicure unit. The intensity of the LED was adjusted to be 1 W/cm^2 right after the quarz window. The figure below (Figure 11) shows the used apparatus for the SSP experiments.

For the steady- state photolysis experiments it is necessary to apply certain experimental conditions, in which the same amount of photons is absorbed over the whole time. It is quite difficult to find such conditions, because there is always some scattering and it is impossible to keep the height of the solution constant, if samples are taken out of it, but the amount of photons absorbed should at least stay almost constant. To check, whether this is the case, the extinction coefficients at 400 nm were calculated from the UV- Vis experiments via Lambert-Beer law. With these extinction coefficients and the initial height of the solution (d_1) and the height of the solution at the end of the experiment (d_2) the initial absorbance and the absorbance at the end of the experiment were calculated. From these values the corresponding values for the transmittance were calculated and compared to each other.

$$a = \log\left(\frac{1}{\tau}\right) = \varepsilon \cdot c \cdot d$$

τ…transmittance

For all three initiators the absorbance at the beginning is very high and additionally the change in the absorbance during the experiments is only marginal. Therefore, the amount of transmitted light lies far below 0,01% providing a reasonable optical thickness during the whole photolysis. The concentration was assumed to stay constant for these calculations.

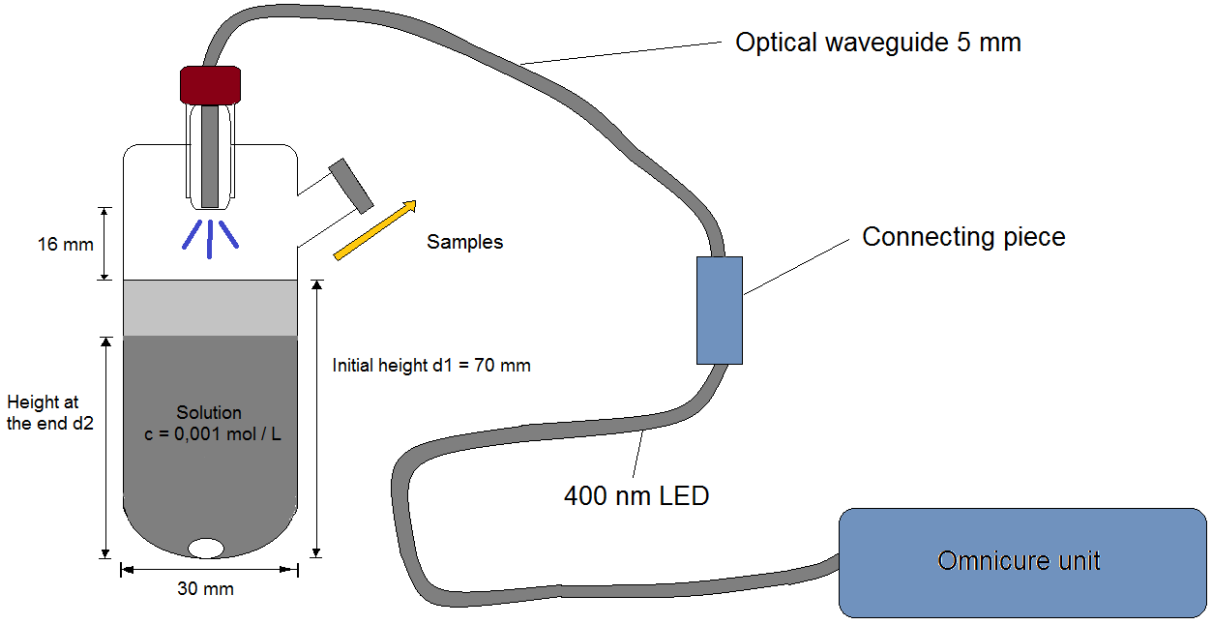

Figure 11: Apparatus for steady state photolysis (SSP) experiments

Another important fact about the experiments is the overlap of the absorption band with the emission band of the applied LED. In the figure below (Figure 12), the absorption spectra of all photoinitiators are displayed together with the emission band of the 400 nm LED. As one can see, the nπ* bands of **19**, BAPO and Ivocerin overlap very well with the emission band of the used LED and therefore this LED can be used in these experiments. However, the absorption band of the CQ/DMAB system does not overlap very well with the emission band of the 400 nm LED.

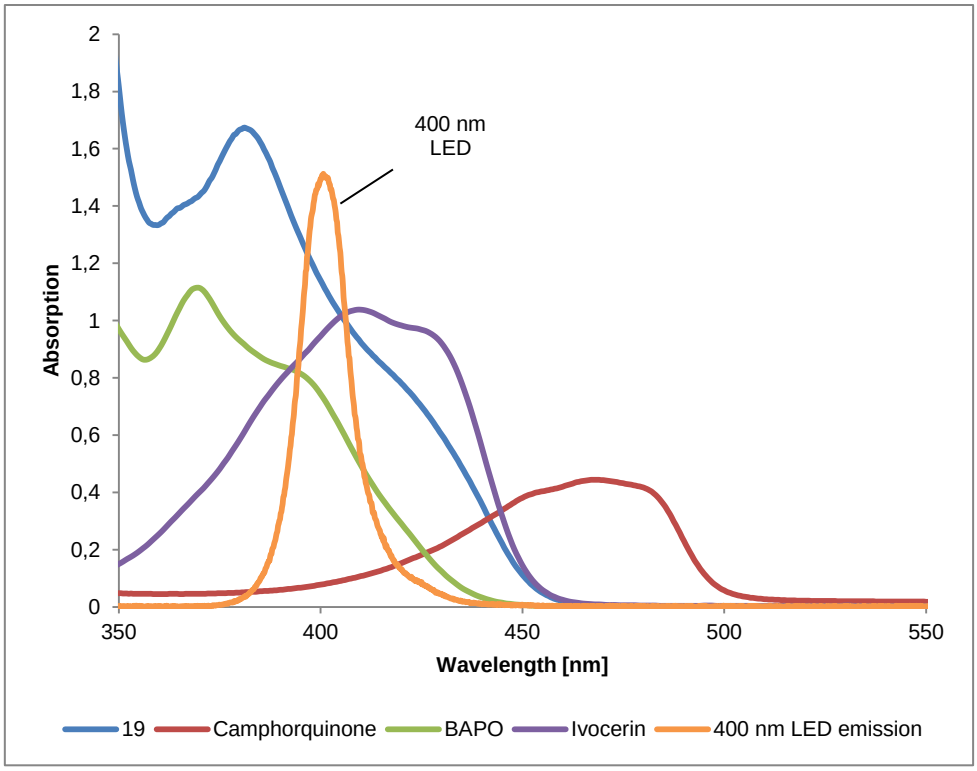

Figure 12: Absorption bands of the photoinitiators compared to the 400 nm LED emission band

To carry out the experiments, tetramesitoylsilane (**19**) as well as the reference initiators BAPO and Ivocerin were dissolved in dichloromethane (c_0 = 1x10^{-3} mol L^{-1}). For each experiment the solutions were then transferred to the photoreactor. The reaction solution was then irradiated and samples were taken in a certain interval. For each sample an UV-Vis spectrum was acquired. The figures below (Figure 13) show the achieved results for tetramesitoylsilane (**19**), BAPO and Ivocerin.

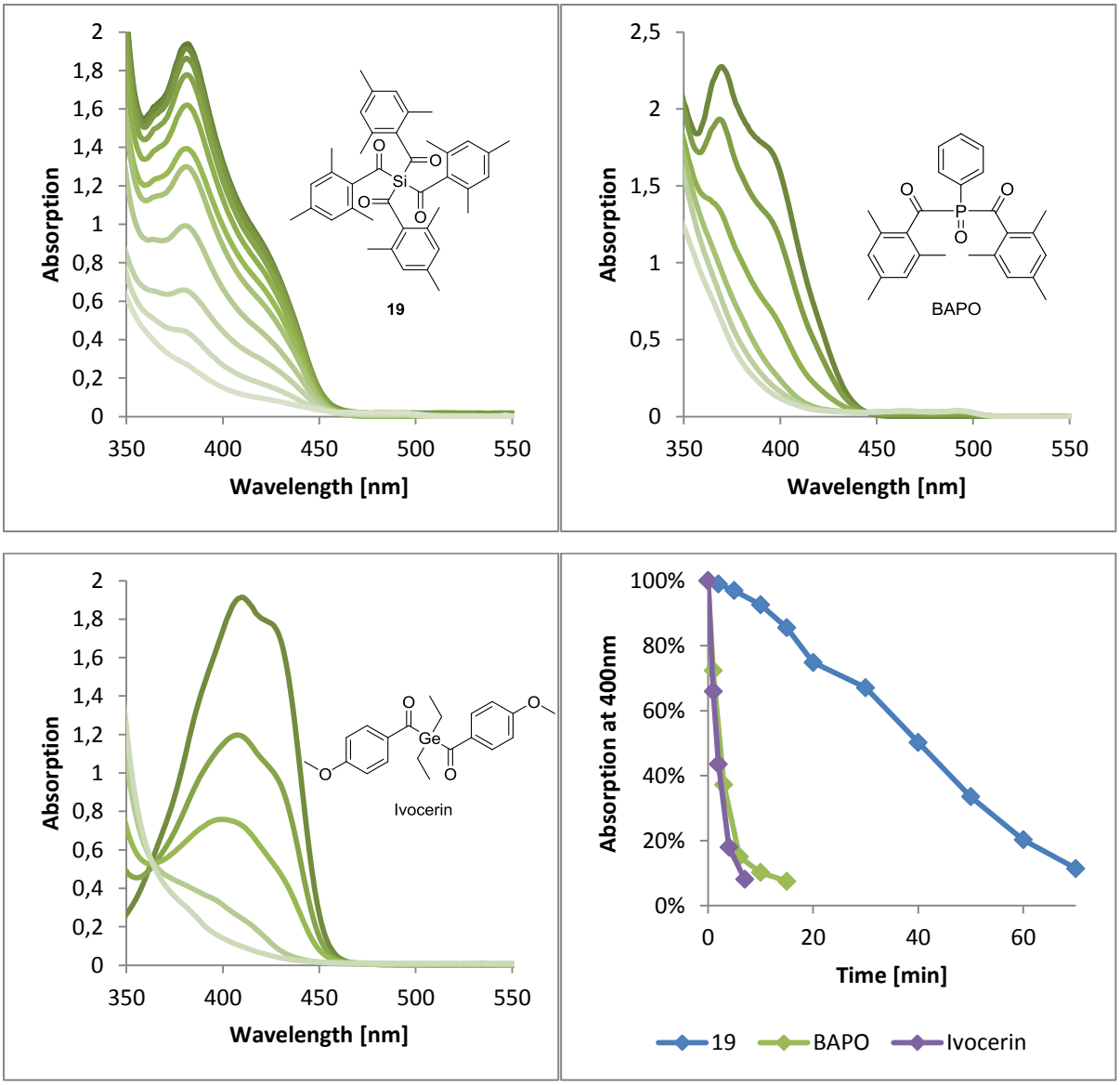

Figure 13: UV-Vis spectra achieved from the steady- state photolysis of 19, BAPO and Ivocerin and decrease of the absorption at 400 nm over time

For all three photoinitiators the absorption at long wavelengths decreases strongly with increasing irradiation time (photobleaching). This is shown additionally in the tables next to the figures. For tetramesitoylsilane (**19**), 70 min of irradiation were required to fully destroy the chromophore. This seems to be quite long compared to BAPO (15 min) and Ivocerin (7 min), but compared to other systems like CQ/DMAB, these results are quite pleasant.

For CQ/DMAB the SSP experiment should be carried out with a 460 nm LED for a better overlap of the absorption band with the LED emission band, but was abandoned after observing no decrease of absorption after 15 minutes irradiation at

all. Maybe this experimental approach did simply not work for type II systems like CQ/DMAB.

2.3 Storage stability

All monomer mixtures used for dental applications contain a certain amount of water. This is the reason for the importance of novel photoinitiators to be stable in aqueous media. To investigate the stability of the synthesized compounds in aqueous media, the new photoinitiators tris(trimethylsilyl)mesitoylsilane (**25**) and tetramesitoylsilane (**19**) were dissolved in acetone:water, ratio 9:1 (c_0 = 1x10^{-3} mol/L). It has to be mentioned, that **19** was not soluble in mixtures of acetonitrile:water or DMSO:water. The absorption of those solutions was then measured via UV-Vis spectroscopy after defined time intervals (0 min, 30 min, 120 min, 300 min). Between these measurements the solutions were stored at RT in the dark.

The figures below (Figure 14, Figure 15) show the decomposition of tetramesitoylsilane (**19**) and tris(trimethylsilyl)mesitoylsilane (**25**) starting already after 30 min. After 120 min it has become difficult to identify the absorption maxima and finally after 300 min the absorption had reached a minimum.

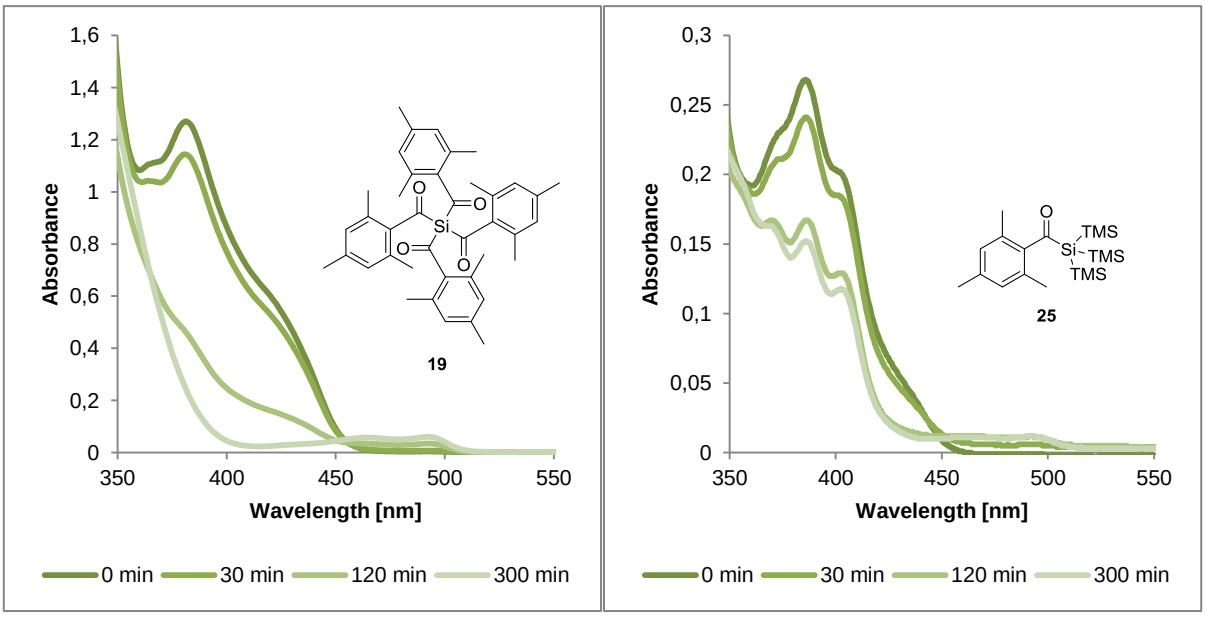

Figure 14: UV-Vis spectra achieved from the storage stability study of 19 and 25

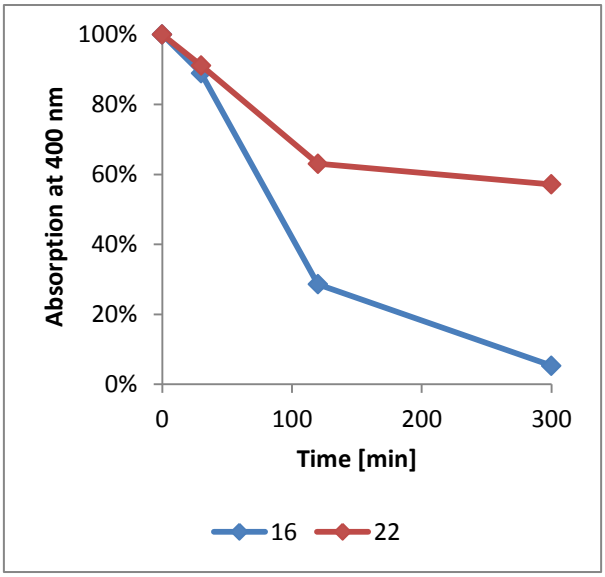

Figure 15: Decrease of the absorption of 16 and 22 at 400 nm over time

In aqueous media, **25** and **19** decompose forming a diketone- compound, mesitil[61] (**31**). This compound shows absorption up to above 500 nm (Figure 16).

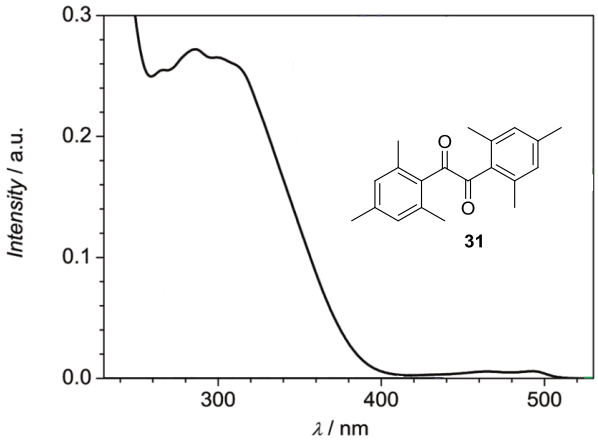

Figure 16: UV-Vis spectrum of mesitil[61] (31)

With the extinction coefficient of **31** at 480 nm from literature[61] the amount of formed mesitil (**31**) during the stability experiments could be calculated via Lambert- Beer law. For tetramesitoylsilane (**19**) the formation of **31** occurred quantitatively within 300min. For compound **25**, almost half of the used amount of **25** reacted forming mesitil (**31**) within 300min.

The storage stability of tetramesitoylsilane (**19**) was also tested concerning the pH. For this reason three solutions of **19** were prepared in acetone:water, ratio 9:1. Then

one of the solutions was acidified with conc. H_3PO_4 (pH 2). To another one, sat. NaOH solution was added (pH 11) and the third solution was kept neutral. UV-Vis spectra were recorded directly after the preparation of these solutions, which were then stored at 40°C and in the dark for 25 days. After this time, another spectrum was acquired. In all three cases, **19** decomposed fully. In alkaline conditions decomposition occurred instantly, indicated by a bright precipitate. In acidic conditions decomposition was resulting in the formation of mesitil (**31**), as already discussed for the neutral study.

2.4 Photo-DSC

Photo-DSC experiments were carried out to explore the photochemical reactivity of the products and thus test the compounds for their suitability as long-wavelength photoinitiators. For this purpose, tetramesitoylsilane (**19**), tris(trimethylsilyl)mesitoylsilane (**25**) and tris(trimethylsilyl)-o-toluoylsilane (**26**) (Scheme 57) should be dissolved in a three-component monomer mixture (UDMA, D_3MA, bis-GMA with the molar ration of 1:1:1), which is used for dental formulations.

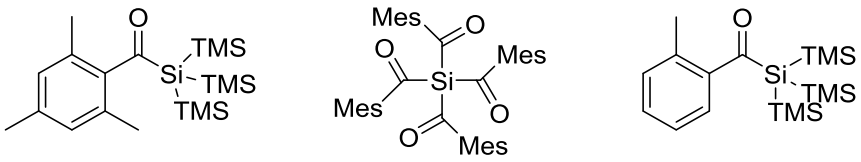

25 **19** **26**

Scheme 57: Compounds for which photo-DSC experiments were carried out

However, tetramesitoylsilane (**19**) did not dissolve in this monomer at all and the solubility of the other two compounds was not satisfying as well. For this reason an acrylate 1,6-hexanediol diacrylate (**32**, HDDA) was used as monomer for all photo-DSC studies (Scheme 58).

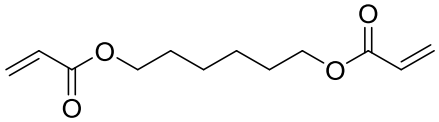

32

Scheme 58: 1,6-Hexanediol diacrylate (32) used as monomer in photo-DSC experiments

Photo-DSC can be used to determine the double bond conversion (DBC [%]), the time until heat flow maximum is reached (t_{max} [s]), the time until 95 percent of total heat flow is reached (t_{95} [s]) as well as the total heat of polymerization, which is related to the peak area. Additionally, the rate of polymerization R_p can be calculated. These values provide quite good information on photoreactivity of the analyzed compound. For curing, a medium pressure mercury lamp with filter (400 – 500 nm) was used with an intensity of 1 W/cm^2 at the tip of the light guide.

Double bond conversion can be calculated as shown below:

$$DBC\ [\%] = \frac{\Delta H}{\Delta H_T} \cdot 100$$

ΔH…peak area [J mol^{-1}]

ΔH_T…theoretical polymerization heat of the monomer [J mol^{-1}]

ΔH_T (HDDA) = 167119,09 J mol^{-1} (Berdzinski et al.[62])

The rate of polymerization can be determined using:

$$R_p\ [mol\ L^{-1}\ s^{-1}] = \frac{h \cdot \rho_{monomer}}{\Delta H_T}$$

h…peak height [mW mg^{-1}]

$\rho_{monomer}$…density of the monomer

ρ_{HDDA} = 1010 g L^{-1}

The figures below (Figure 17, Figure 18) show the achieved results for the synthesized compounds.

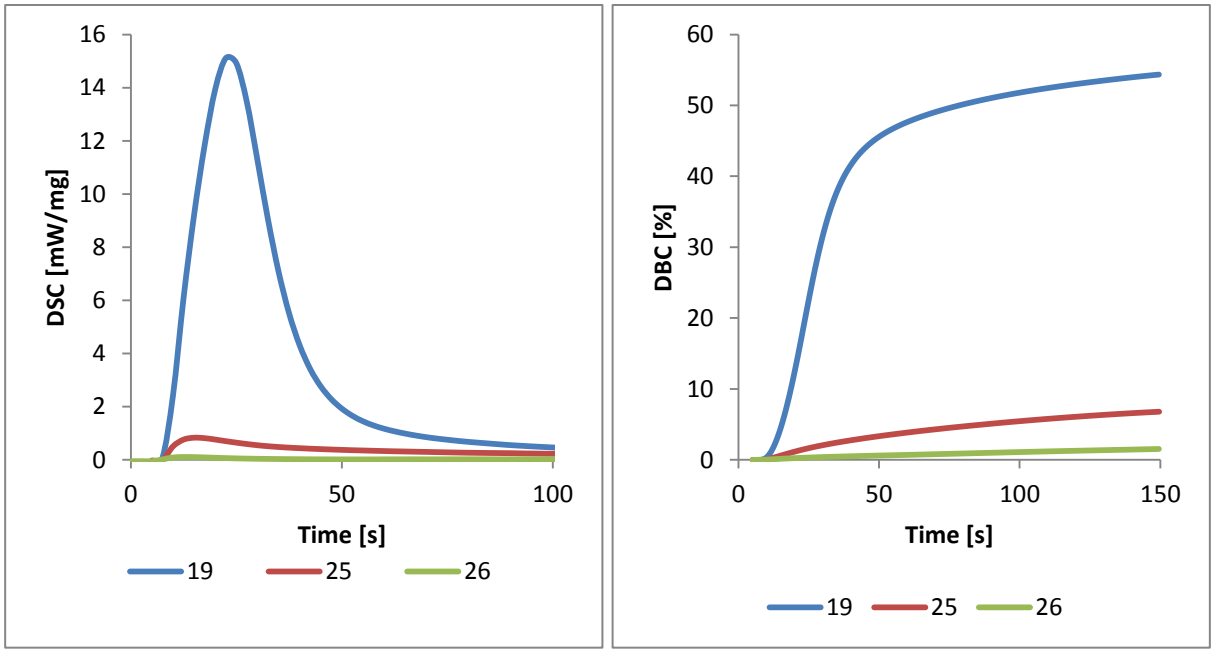

Figure 17: Achieved DSC-curves and conversion curves for 19 (blue), 25 (red) and 26 (green)

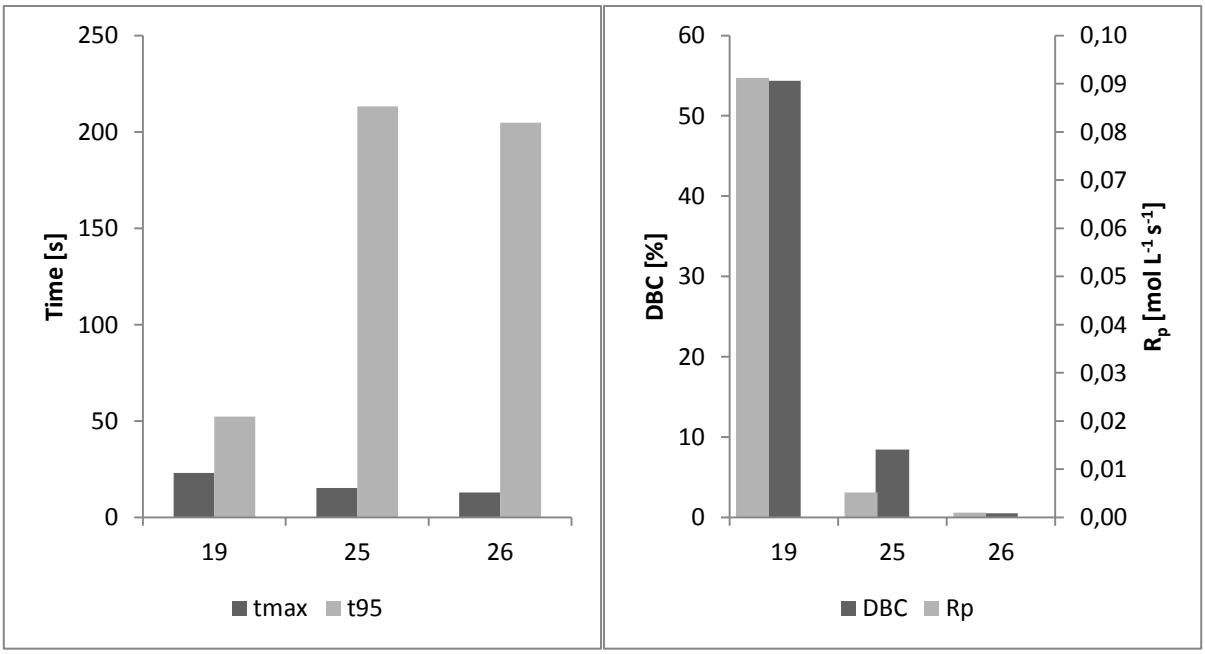

Figure 18: Achieved photo-DSC results for 19, 25 and 26

Tetramesitoylsilane (**19**) showed remarkable reactivity. With a double bond conversion of 44% and t_{max} = 23 s and t_{95} = 52 s α-cleavage was probably preferred over the Brook-rearrangement for tetramesitoylsilane (**19**). The other two compounds tris(trimethylsilyl)mesitoylsilane (**25**) and tris(trimethylsilyl)-o-toluoylsilane (**26**) showed very low to even no reactivity at all. For **25** at least a double bond conversion of 8% could be calculated, but for **26** no considerable conversion could be calculated.

For compounds **25** and **26** the Brook-rearrangement is probably preferred, which results in this bad reactivity towards double bonds.

Since tetramesitoylsilane (**19**) showed good reactivity in the first measurements, further experiments should be carried out to compare **19** to other photoinitiators known from literature (Scheme 59). As reference initiators, a bisacylphosphine oxide (BAPO) and a diacylgermane-based photoinitiator (Ivocerin) were chosen. Additionally, tetramesitoylsilane (**19**) should also be compared to the camphorquinone / dimethylaminobenzoic acid ethyl ester (CQ/DMAB) system, which is a Type II system.

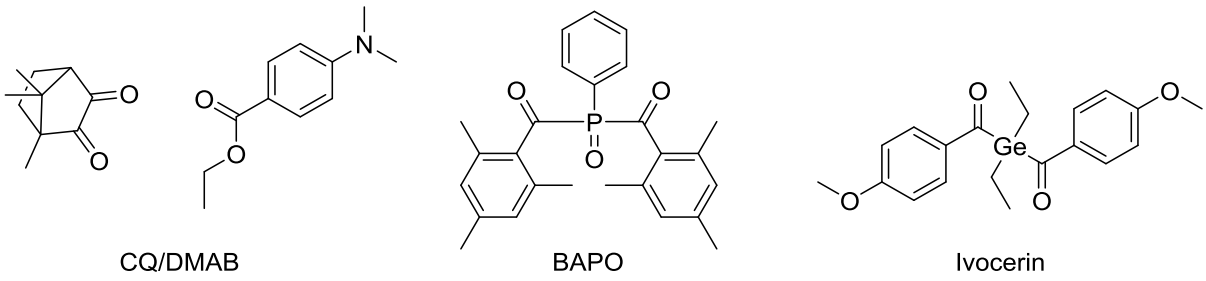

CQ/DMAB BAPO Ivocerin

Scheme 59: Reference photoinititators

For tetramesitoylsilane (**19**) four solutions with concentrations of 0,1 wt%, 0,2 wt%, 0,4 wt% and 0,8 wt% in HDDA were prepared to investigate the influence of the initiator concentration as well. Then, for each reference photoinitiator four equimolar solutions related to those of tetramesitoylsilane (**19**) were prepared. To discuss the influence of the initiator concentration on the photopolymerization the results for all four photoinitiators are shown below (Figure 19, Figure 20, Figure 21, Figure 22).

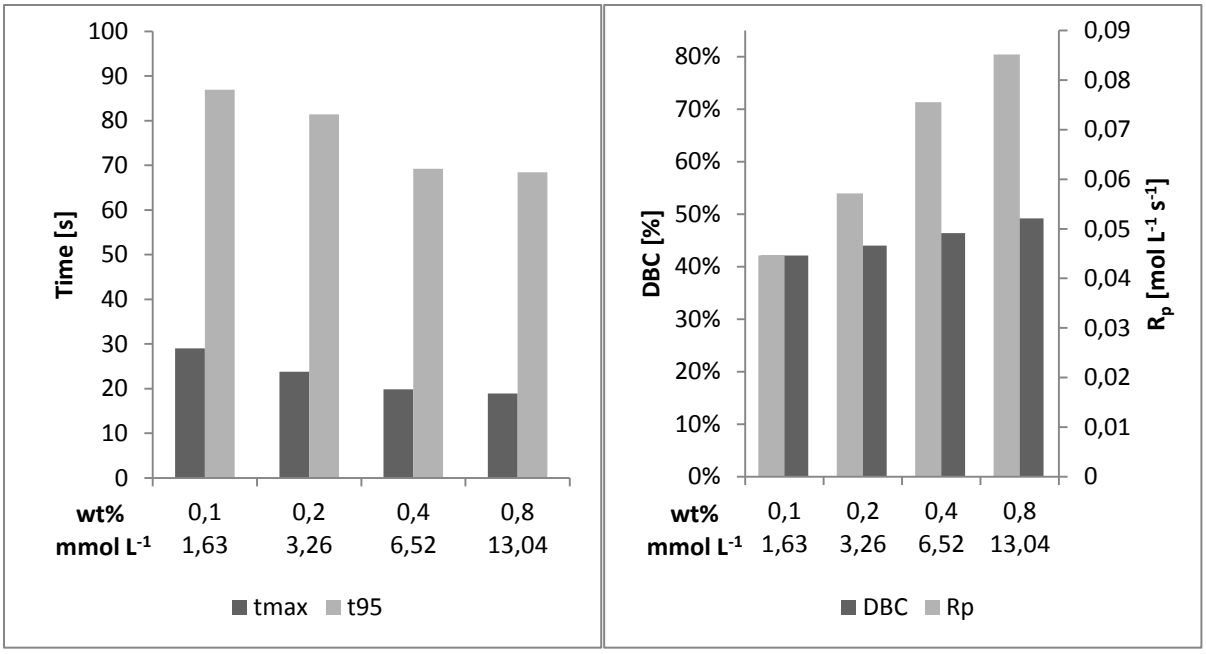

Figure 19: Results for tetramesitoylsilane (19) at four different concentrations

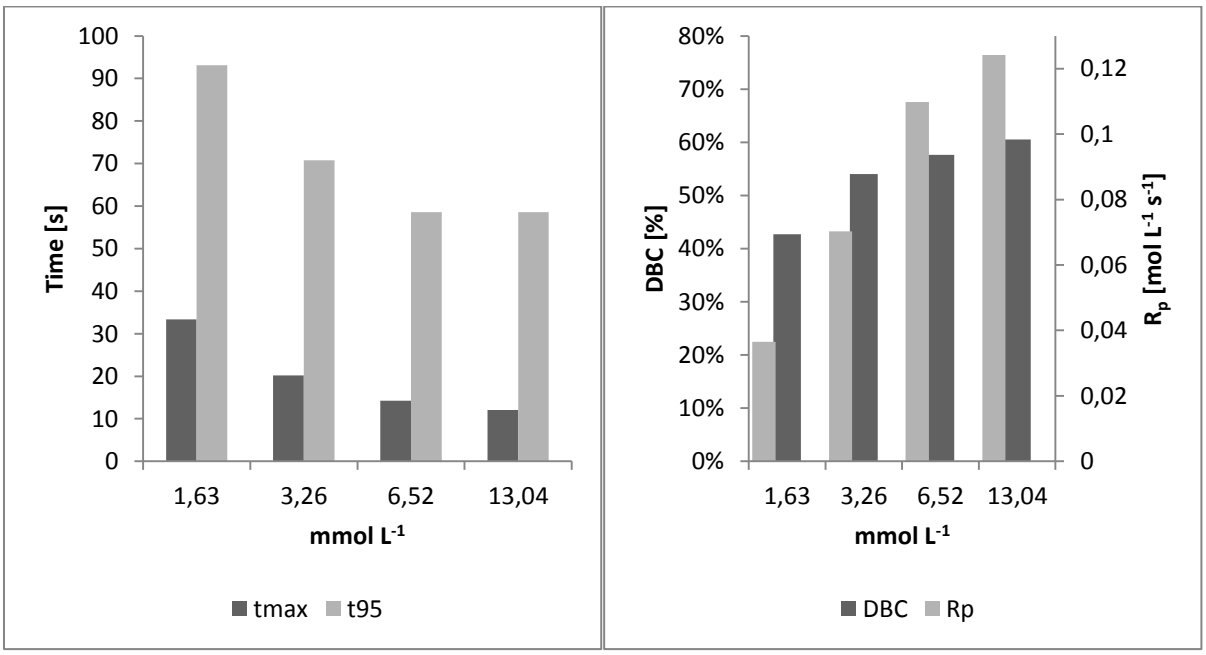

Figure 20: Results for the equivalent amounts of CQ/DMAB

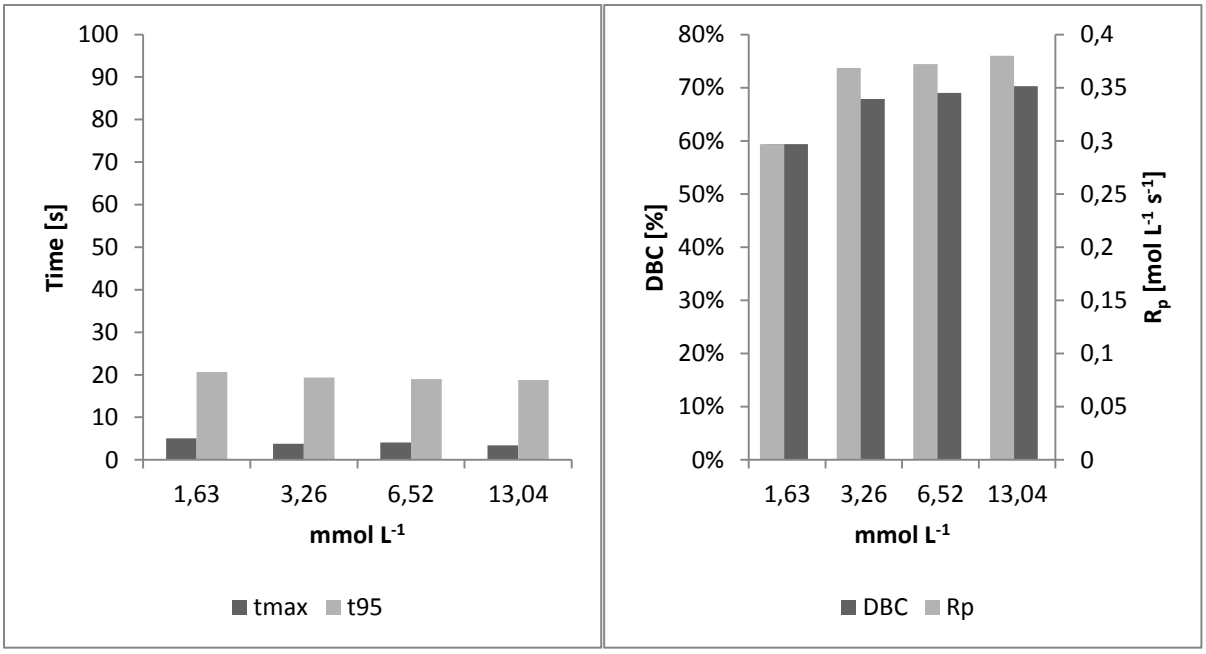

Figure 21: Results for the equivalent amounts of BAPO

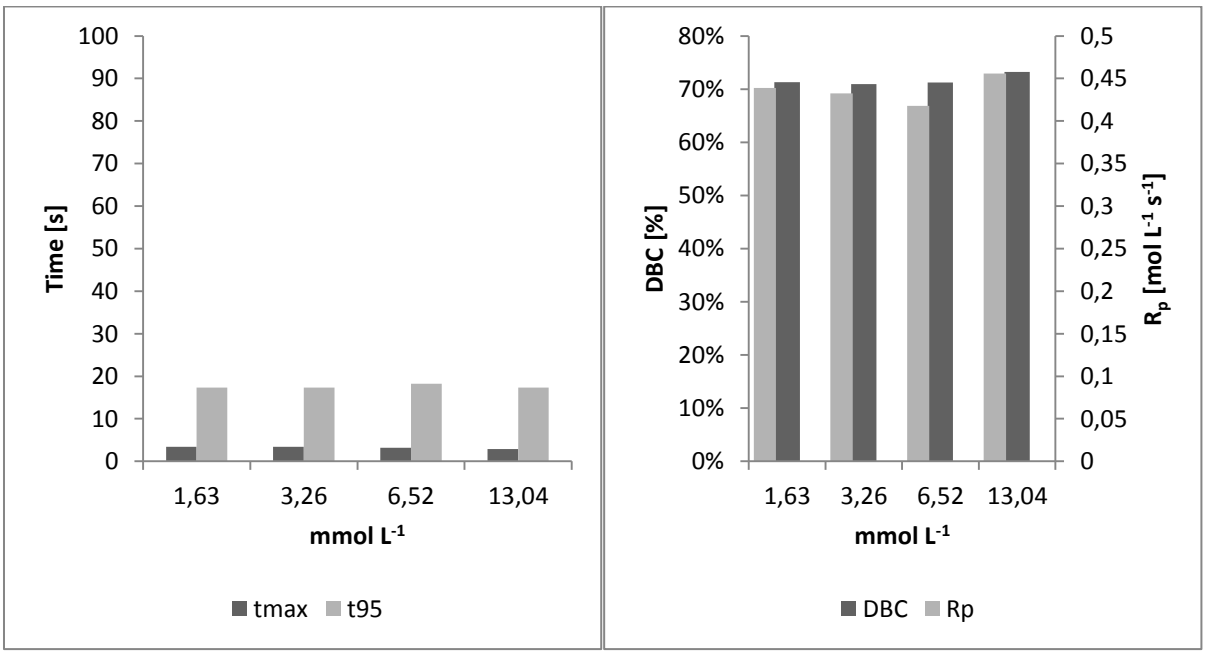

Figure 22: Results for the equivalent amounts of Ivocerin

As one can see, the DBC as well as t_{max} and t_{95} strongly depend on the applied initiator concentration for tetramesitoylsilane (**19**) and CQ/DMAB. The DBC increased with higher concentrations, while t_{max} and t_{95} decreased. For tetramesitoylsilane (**19**) t_{max} could be lowered by one third by using the eightfold concentration. For BAPO and Ivocerin this phenomenon could not be observed in that way. Though DBC

increases as well for this compounds, t_{max} and t_{95} stayed constant. Very little amounts of BAPO and especially Ivocerin are already enough to cause fast photopolymerization with high conversion values. To illustrate these results in greater detail, conversion-time curves for all four initiators were created (Figure 23, Figure 24).

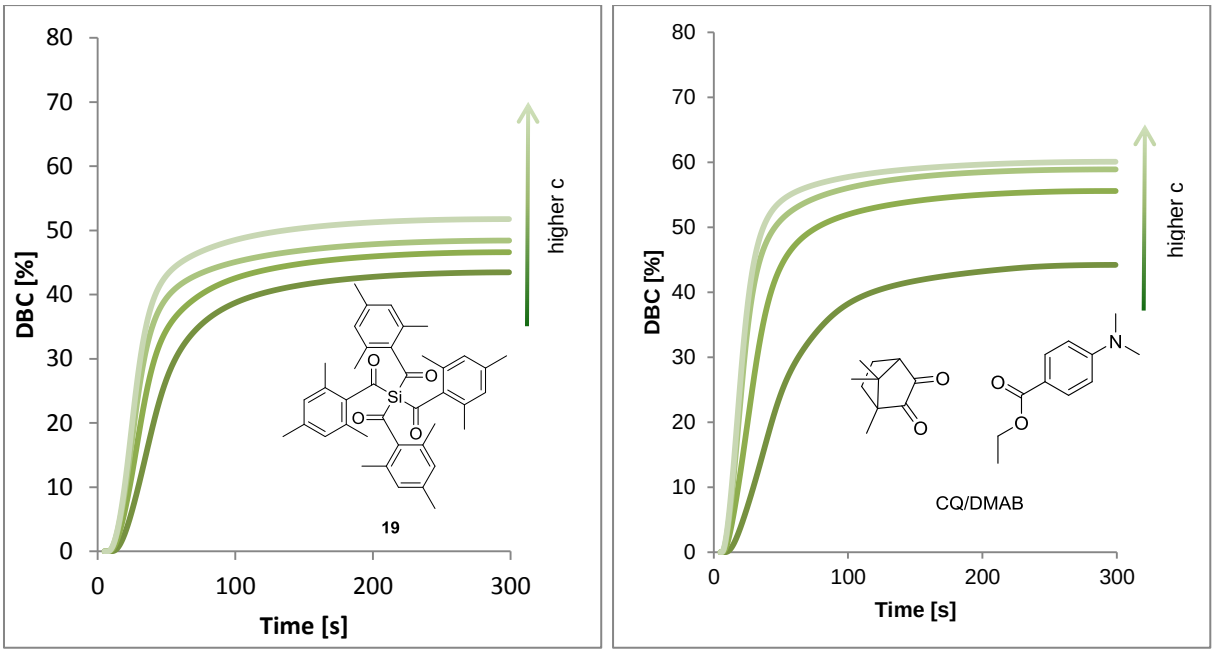

Figure 23: Conversion-time curves for four different concentrations of tetramesitoylsilane (19) and CQ/DMAB

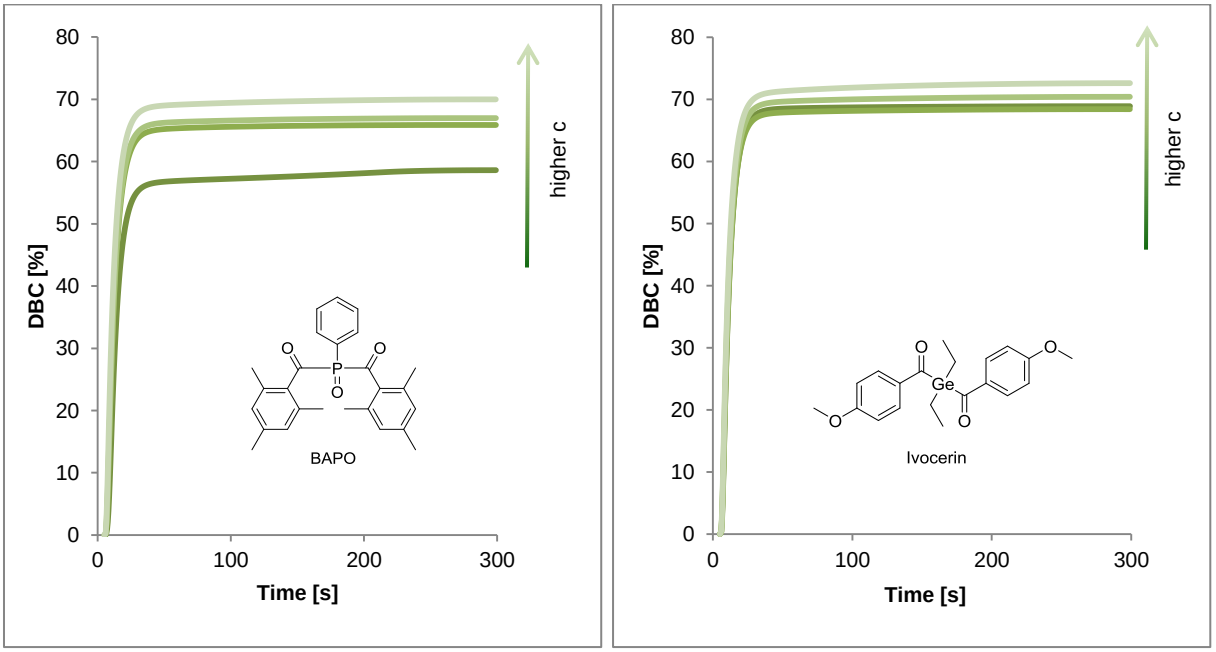

Figure 24: Conversion-time curves for four different concentrations of BAPO and Ivocerin

Additionally, the concentration dependency of t_{max}, t_{95}, DBC and R_p for all initiators is shown as well (Figure 25, Figure 26).

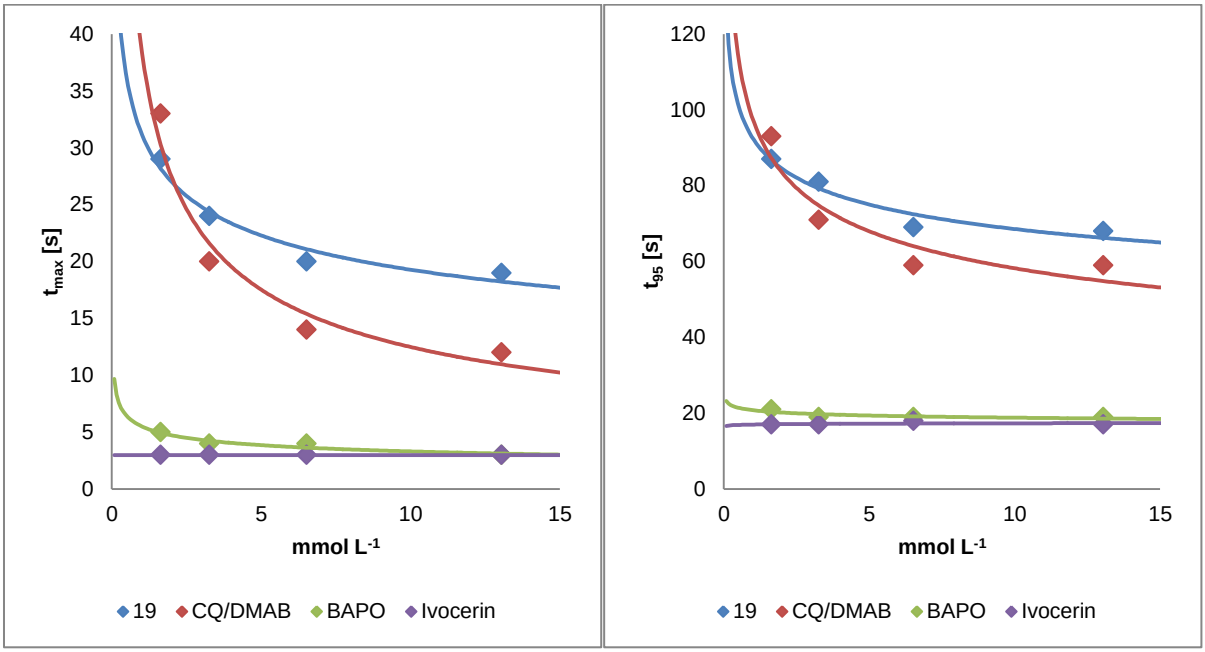

Figure 25: Concentration dependency of t_{max} and t_{95}

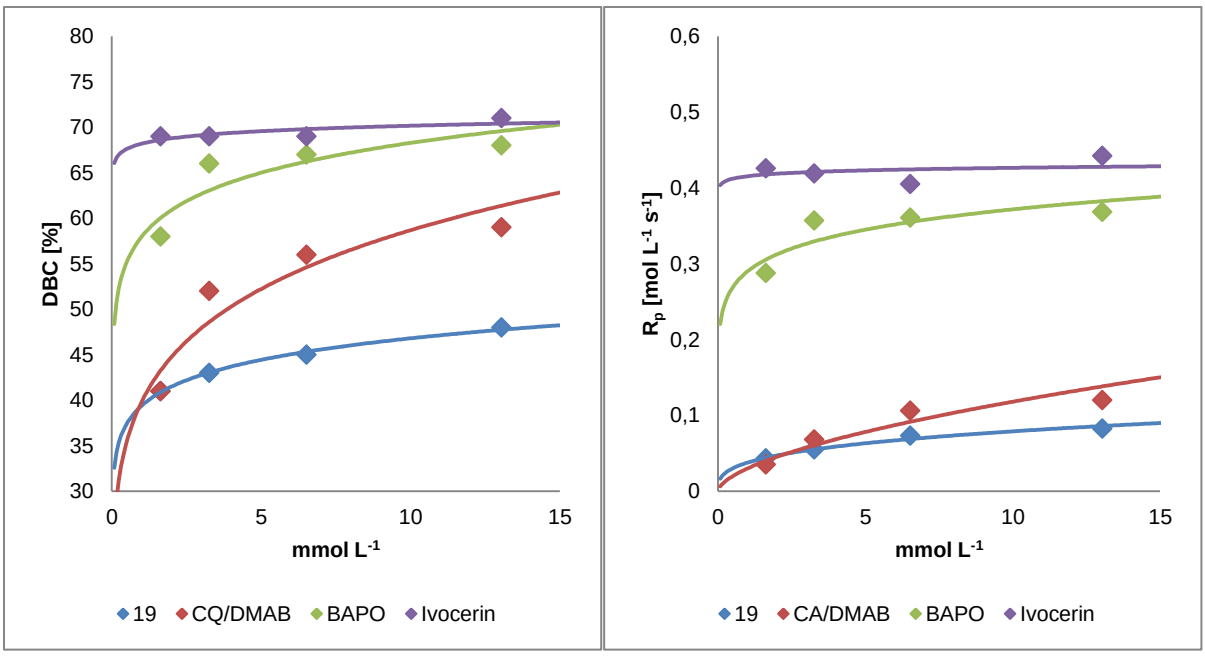

Figure 26: Concentration dependency of DBC and R_p

The four initiators should then be compared to each other at different concentrations. For this reason, the achieved results are assembled in the following figures (Figure 27, Figure 28, Figure 29, Figure 30).

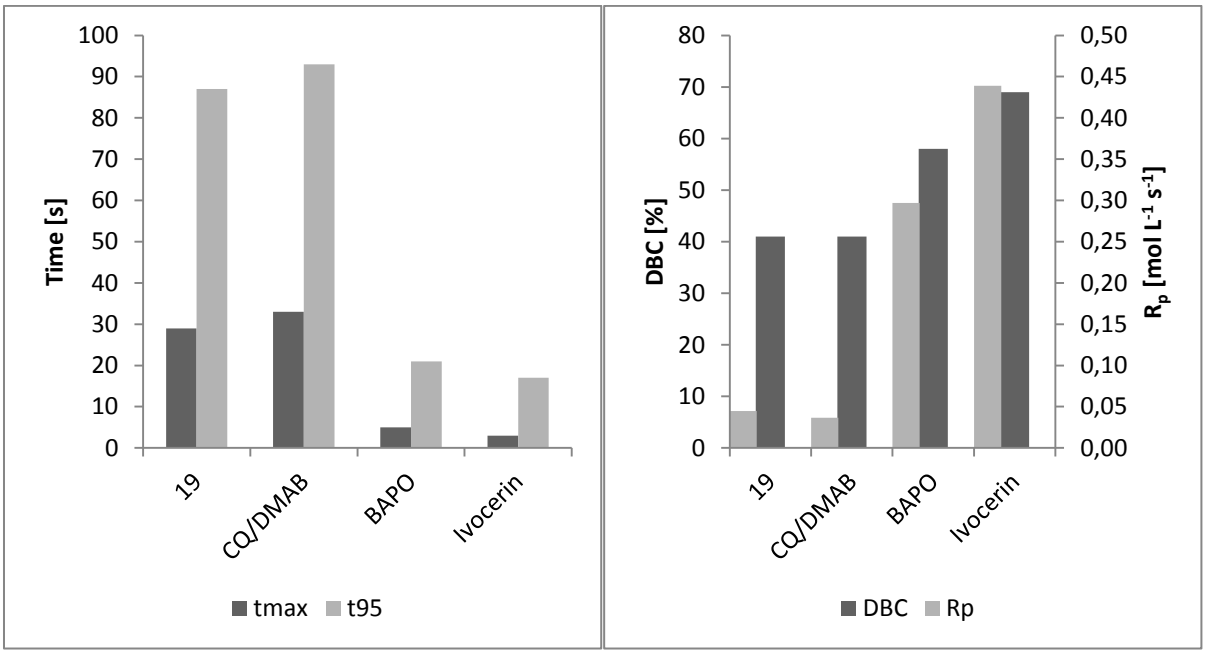

Figure 27: Results for all four photoinitiators at a molar concentration related to 0,1 wt% of tetramesitoylsilane (19)

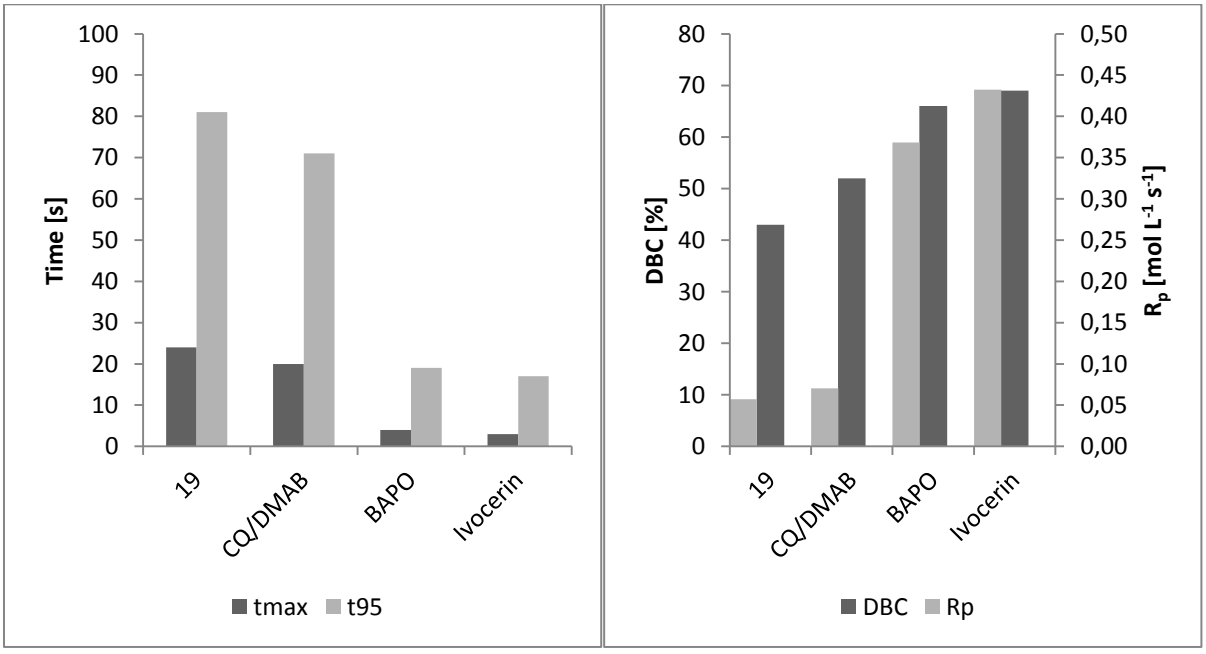

Figure 28: Results for all four photoinitiators at a molar concentration related to 0,2 wt% of tetramesitoylsilane (19)

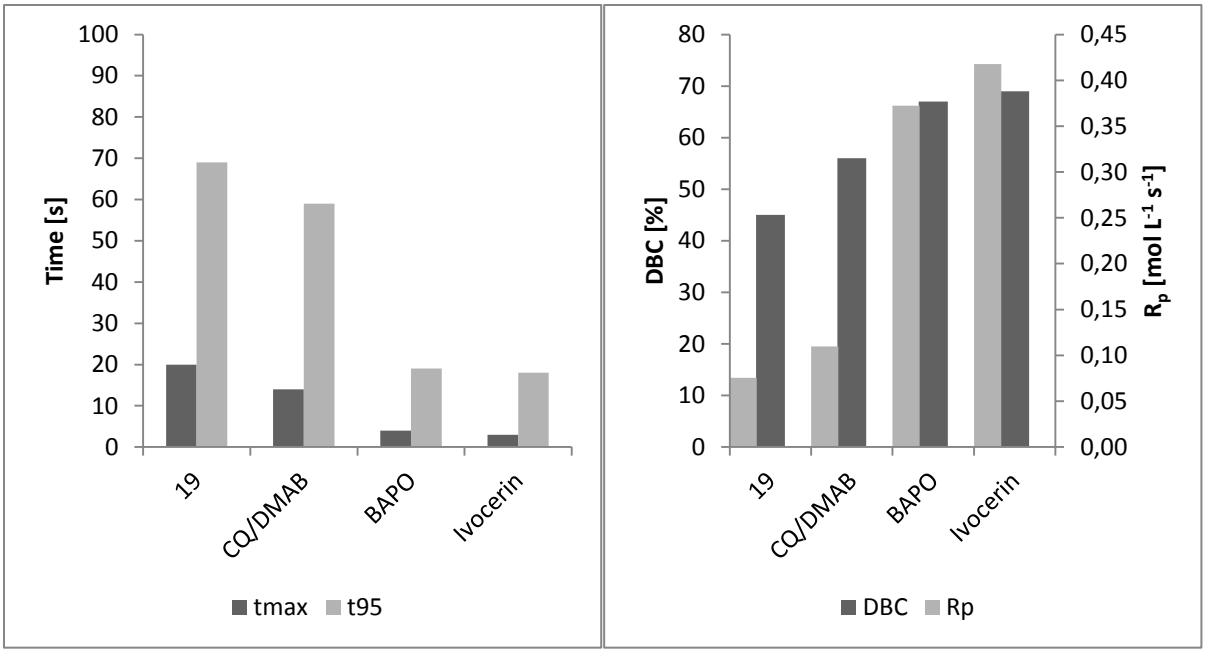

Figure 29: Results for all four photoinitiators at a molar concentration related to 0,4 wt% of tetramesitoylsilane (19)

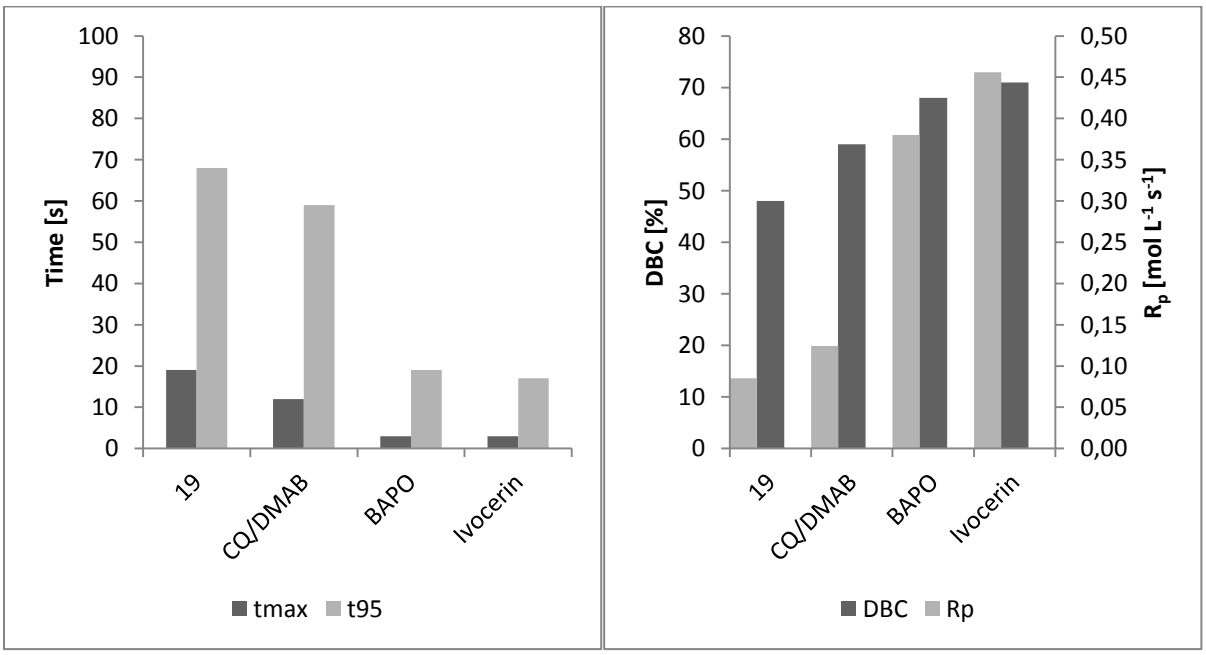

Figure 30: Results for all four photoinitiators at a molar concentration related to 0,8 wt% of tetramesitoylsilane (19)

The achieved conversion-time curves for all four photoinitiators were also assembled together to compare them (Figure 31, Figure 32).

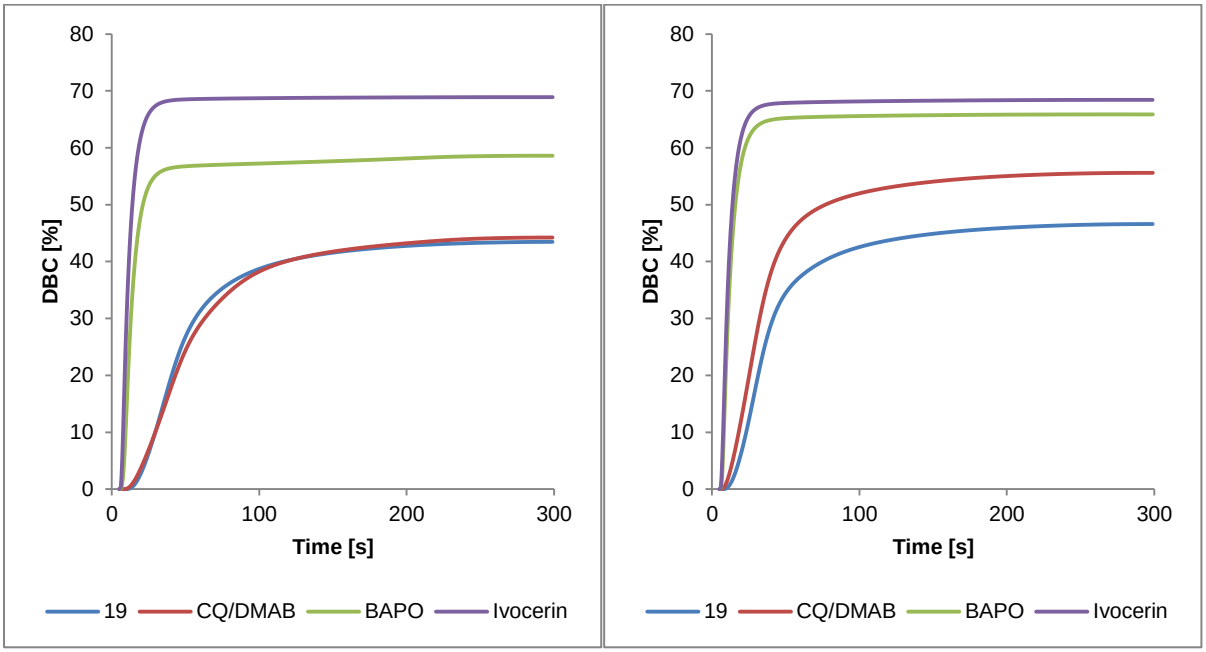

Figure 31: Compared Conversion-time curves for all four photoinitiators (19 blue, CQ/DMAB red, BAPO green, Ivocerin purple) at a molar concentration related to 0,1 wt% and 0,2 wt% tetramesitoylsilane (19)

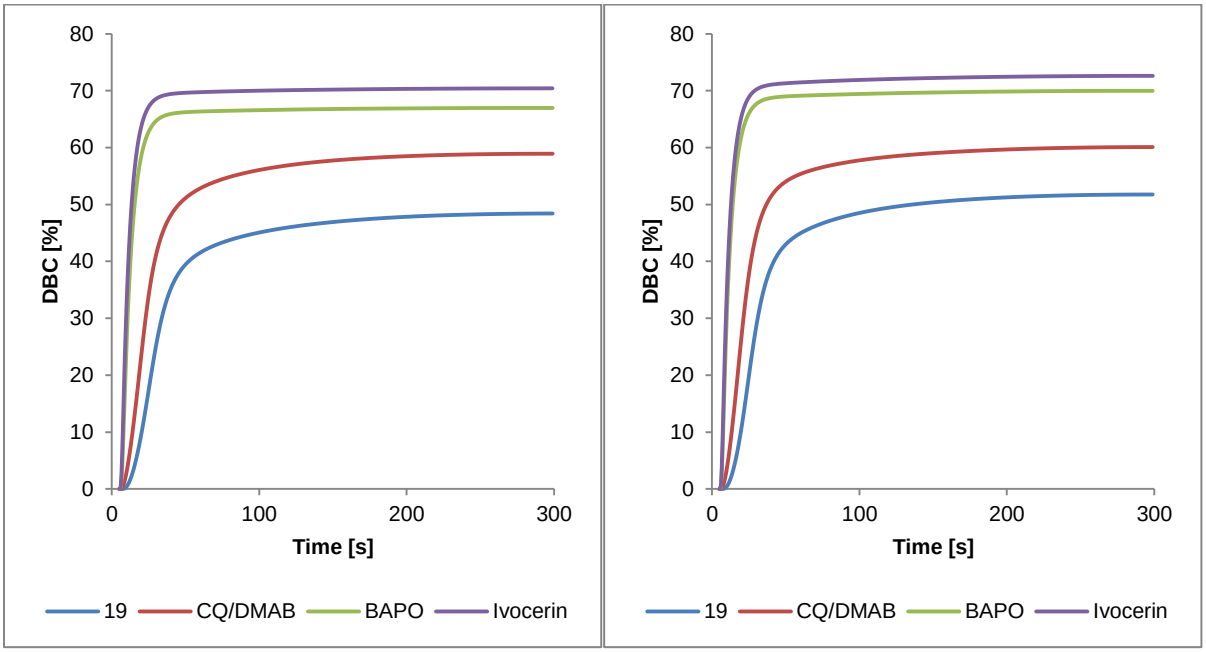

Figure 32: Compared Conversion-time curves for all four photoinitiators (19 blue, CQ/DMAB red, BAPO green, Ivocerin purple) at a molar concentration related to 0,4 wt% and 0,8 wt% tetramesitoylsilane (19)

Compared to BAPO and Ivocerin, tetramesitoylsilane (**19**) showed low reactivity. For all four concentrations, the t_{max} and the t_{95} value of **19** was significantly higher than those of BAPO and Ivocerin, which indicates much slower polymerization. Further, the reached DBC values with **19** are much lower than those reached with BAPO and Ivocerin. Obviously, irradiation of tetramesitoylsilane (**19**) does not lead to such a fast formation of benzoyl radicals (α-cleavage) as it is the case for BAPO and Ivocerin, although 1 mol of **19** could theoretically create 4 mols of benzoyl radicals, compared to only 2 mols each for BAPO and Ivocerin. However, compared to the CQ/DMAB system, tetramesitoylsilane (**19**) showed good photochemical properties. At low initiator concentrations **19** could reach the same DBC and its t_{max} and t_{95} values were even lower (faster polymerization) than those of CQ/DMAB. With higher concentrations, the reactivity of CQ/DMAB exceeds those of tetramesitoylsilane (**19**), but still stays comparable. The figures below (Figure 33) show the obtained photo-DSC curves for the lowest and the highest initiator concentration.

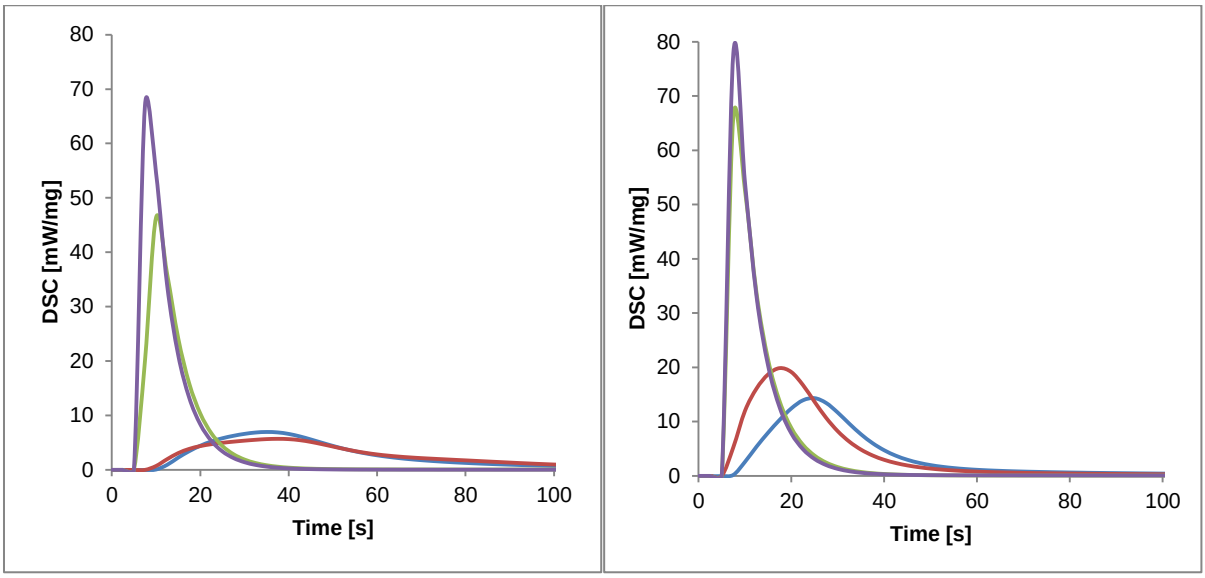

Figure 33: Achieved photo-DSC curves for all four photoinitiators (19 blue, CQ/DMAB red, BAPO green, Ivocerin purple) at molar concentration related to 0,1 wt%(left) and 0,8 wt% (right) tetramesitoylsilane (19)

Tetramesitoylsilane (**19**) could definitely be used as an alternative to the CQ/DMAB system for the photopolymerization of acrylates. Due to solubility issues, it could be difficult to use tetramesitoylsilane (**19**) also for the polymerization of methacrylates as well.

Experimental section

1. Synthesis

All reactions, if not mentioned otherwise explicitly were carried out in argon-atmosphere, applying common Schlenk techniques and excluding light with wavelengths below 520 nm (orange- light lab).

1.1 Oxygen- substituted acyl silanes

1.1.1 Mesityl-1,3-dithiane (10)

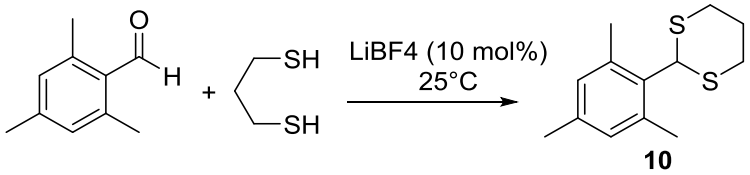

10

Compound	Equivalents	n [mmol]	m [g]	V [mL]
Mesitaldehyde	1,3	19,08	2,83	2,81
1,3-Propanedithiol	1	14,68	1,59	1,47
Lithium tetrafluoroborate	0,1	1,47	0,14	

For the preparation of **10**, 1,3 eq. of mesitaldehyde and 0,1 eq. of lithium tetrafluoroborate were weighed into a schlenk tube and 1 eq. of dithiane was added over 10min at RT using a syringe. The reaction mixture was then stirred for 3h at that temperature. The formation of the product (white solid) occurred spontaneously. Afterwards the reaction mixture was distilled using a Kugelrohr apparatus (200°C; 0,006 mbar), giving the pure product **10** as a white solid in almost quantitative yield (99%). $LiBF_4$ remained in the distillation flask and could be reused.

Yield: 3,450 g white solid
99% of theory
99% of literature[51]

mp.: 129-131°C (128-130°C in literature[63])

^{1}H-NMR: δ_H (400 MHz, $CDCl_3$): 6,83 (2H, s, Ar-**H**); 5,62 (1H, s, Mes-C**H**); 3,19 – 2,80 (4H, m, S-C**H**$_2$); 2,74 (3H, s, Ar-C**H**$_3$); 2,41 (3H, s, Ar-C**H**$_3$); 2,24 (3H, s, Ar-C**H**$_3$); 2,18 - 1,75 (2H, m, S-CH$_2$-C**H**$_2$)

GC-MS (DCM): m/z (relative intensity): 238 (M, 9%), 163 (100%), 149 (22%), 91 (3%)

1.2 Acyl silanes

1.2.1 Mesitoylsilanes

1.2.1.1 Tris(trimethylsilyl)mesitoylsilane (25)

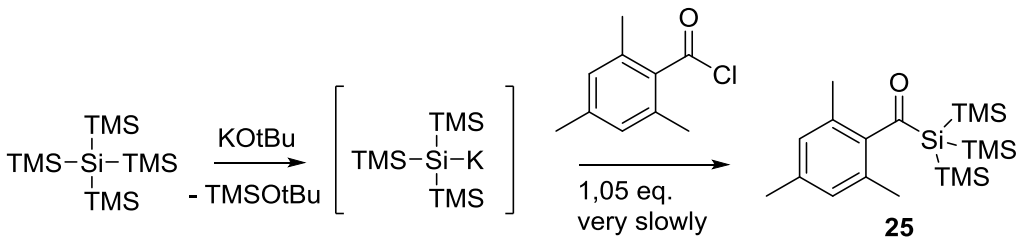

Compound	Equivalents	n [mmol]	m [g]	V [mL]
Tetrakis(trimethylsilyl)silane	1	3,12	1,00	
Potassium tert.- butoxide	1,05	3,27	0,37	
2,4,6-Trimethylbenzoylchloride	1,05	3,27	0,60	0,55

For the synthesis of **25**, 1 g of tetrakis(trimethylsilyl)silane (1 eq., 3,12 mmol) and 0,37 g of potassium tert- butoxide (1,05 eq., 3,27 mmol) were weighed into a Schlenk tube and 12 mL of dry 1,2-dimethoxyethane were added as a solvent. The mixture was stirred for 2h at RT and the solution containing the silanide was then taken using a syringe and a septum. 0,55 mL of 2,4,6-trimethylbenzoylchloride (1,05 eq., 3,27 mmol) were weighed into the now empty Schlenk tube together with 20 mL of dry diethylether. The mixture was then cooled down to -40°C (acetonitrile/liquid nitrogen). When this temperature was reached, the silanide solution was added very slowly (over 90 min) to the acid chloride solution. After finishing the addition, the cooling bath was removed and the mixture was allowed to reach RT in 1h. After that, the reaction mixture was stirred for another hour at RT before being quenched with 50 mL of a mixture of 3% H_2SO_4 (pH 5) and ice. Afterwards the layers were separated

and the aqueous layer was extracted 3 times with diethylether (each 30 mL). The combined organic layers were dried over Na_2SO_4 and then filtrated. After the evaporation of the solvent, the crude product was dried applying high vacuum. After recrystallization from acetone, the product could be obtained as a bright yellow solid with little amounts of tetrakis(trimethylsilyl)silane contaminations, which were then removed using a silicagel column and PE:Et_2O 15:1 giving 130 mg of the pure product.

Yield: 0,130 g bright yellow solid
11% of theory
No yield given in literature[64]

mp.: 89-91°C (86-88°C in literature[64])

^{1}H-NMR: δ_H (400 MHz, $CDCl_3$): 6,58 (2H, m, Ar-**H**); 2,08 (3H, s, Ar-C**H$_3$**); 1,96 (6H, s, Ar-(C**H$_3$**)$_2$); 0,00 (27H, s, Si(C**H$_3$**)$_3$)

^{13}C-NMR: δ_C (100 MHz, $CDCl_3$): 237,20 (C=O); 141,77 ; 139,42 ; 133,71 ; 128,60 (C_{arom}) ; 21,13 (p-methyl); 19,27 (o-methyl); 2,66 ($SiMe_3$)

^{29}Si-NMR: δ_{Si} (79 MHz, $CDCl_3$): -11,45 (3Si, **Si**$(CH_3)_3$), -74,29 (1Si, **Si**$(TMS)_3$)

1.2.1.2 Tetramesitoylsilane (19)

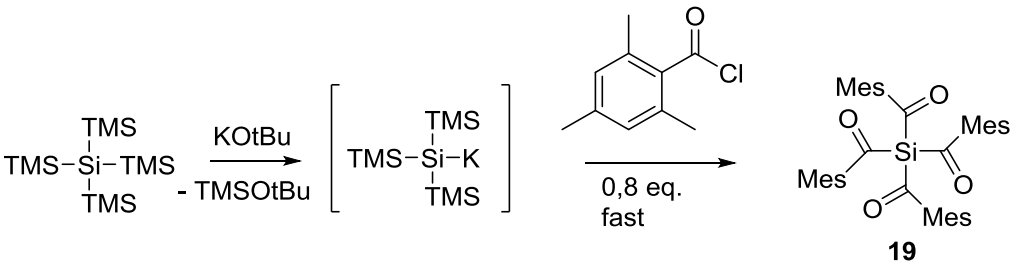

19

Compound	Equivalents	n [mmol]	m [g]	V [mL]
Tetrakis(trimethylsilyl)silane	1	3,12	1,00	
Potassium tert.- butoxide	1,05	3,27	0,37	
2,4,6-Trimethylbenzoylchloride	0,8	2,49	0,46	0,42

For the synthesis of **19**, 1 g of tetrakis(trimethylsilyl)silane (1 eq., 3,12 mmol) and 0,37 g of potassium tert- butoxide (1,05 eq., 3,27 mmol) were weighed into a Schlenk tube and 10 mL of dry 1,2-dimethoxyethane were added as a solvent. The mixture was stirred for 2h at RT and the solution containing the silanide was then taken using

a syringe and a septum. 0,42 mL of 2,4,6-trimethylbenzoylchloride (0,8 eq., 2,49 mmol) were weighed into the now empty Schlenk tube together with 5 mL of dry diethylether. The mixture was then cooled down to -40°C (acetonitrile/liquid nitrogen). When this temperature was reached, the silanide solution was added quite fast to the acid chloride solution. After finishing the addition, the cooling bath was removed and the mixture was allowed to reach RT in 1h. After that, the reaction mixture was stirred for another hour at RT before being quenched with 50 mL of a mixture of 3% H_2SO_4 and ice. Afterwards the layers were separated and the aqueous layer was extracted 3 times with diethylether (each 30 mL). The combined organic layers were dried over Na_2SO_4 and then filtrated. After the evaporation of the solvent, the crude product was dried applying high vacuum. After recrystallization from acetone, the product could be obtained as an intense yellow solid after filtration. Little amounts of tetrakis(trimethylsilyl)silane were removed using small amounts of diethylether to dissolve the contaminants giving the pure product.

Yield: 0,149 g deep yellow solid
8% of theory
33% of literature[45] with different method

mp.: >230°C

^{1}H-NMR: δ_H (400 MHz, $CDCl_3$): 6,61 (8H, m, Ar-**H**), 2,25 (12H, s, Ar-C**H$_3$**), 2,05 (24H, s, Ar-(C**H$_3$**)$_2$)

^{13}C-NMR: δ_C (100 MHz, $CDCl_3$): 237,20 (C=O); 141,77 ; 139,42 ; 133,71 ; 128,60 (C_{arom}) ; 21,13 (p-methyl); 19,27 (o-methyl)

^{29}Si-NMR: δ_{Si} (79 MHz, $CDCl_3$): -95,55

Anal. Calcd. for $C_{40}H_{44}O_4Si$: C, 77,88 ; H, 7,19. Found: C, 77,56 ; H, 7,47.

1.2.2 Toluoylsilanes

1.2.2.1 Tris(trimethylsilyl)-o-toluoylsilane (26)

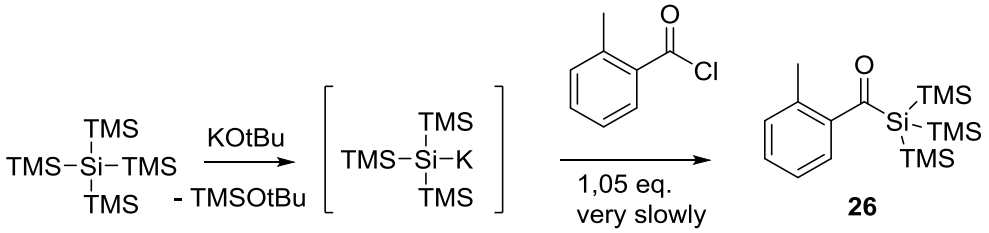

Compound	Equivalents	n [mmol]	m [g]	V [mL]
Tetrakis(trimethylsilyl)silane	1	31,17	10,00	
Potassium tert.- butoxide	1,05	32,73	3,67	
o-Toluoylchloride	1,05	32,73	5,06	4,27

For the synthesis of **26**, 10 g of tetrakis(trimethylsilyl)silane (1 eq., 31,17 mmol) and 3,67 g of potassium tert- butoxide (1,05 eq., 32,73 mmol) were weighed into a Schlenk tube and 60 mL of dry 1,2-dimethoxyethane were added as a solvent. The mixture was stirred for 2h at RT and the solution containing the silanide was then taken using a syringe and a septum. 4,27 mL of o-toluoylchloride (1,05 eq., 32,73 mmol) were weighed into the now empty Schlenk tube together with 100 mL of dry diethylether. The mixture was then cooled down to -70°C (ethanol/liquid nitrogen) When this temperature was reached, the silanide solution was added very slowly (over 90 min) to the acid chloride solution. After finishing the addition, the cooling bath was removed and the mixture was allowed to reach RT in 1h. After that, the reaction mixture was stirred for another hour at RT before being quenched with 200 mL of a mixture of 3% H_2SO_4 and ice. Afterwards the layers were separated and the aqueous layer was extracted 3 times with diethylether (each 50 mL). The combined organic layers were dried over Na_2SO_4 and then filtrated. After the evaporation of the solvent, the crude product was dried applying high vacuum. After recrystallization from n-pentane, the product could be obtained as a deep yellow liquid (1,974 g).

Yield: 1,974 g deep yellow liquid
20% of theory
No yield given in literature[65]

^{1}H-NMR: δ_H (400 MHz, $CDCl_3$): 7,48 - 6,80 (4H, m, Ar-**H**);
2,31 (3H, s, Ar-C**H$_3$**);
0,21 (27H, s, Si(C**H$_3$**)$_3$)

^{13}C-NMR: δ_C (100 MHz, $CDCl_3$): 240,55 (C=O); 146,14 ; 133,50 ; 131,43 ; 129,73 ; 128,61 ; 124,89 (C_{arom}) ; 19,83 (o-methyl); 2,54 ($SiMe_3$)

^{29}Si-NMR: δ_{Si} (79 MHz, $CDCl_3$): -14,19 (3Si, **Si**$(CH_3)_3$), -74,10 (1Si, **Si**$(TMS)_3$)

2. Characterization

All characterization experiments were carried out under light protection (exclusion of light with wavelengths below 520 nm) in an orange-light lab. Additionally, if possible, darkly tinted glassware was used.

2.1 UV-Vis spectroscopy

For UV-Vis spectroscopy, tetramesitoylsilane (**19**) and the reference photoinitiators camphorquinone, BAPO and Ivocerin were dissolved in dry dichloromethane ($c_{tetrames}$ = 1 x 10^{-3} mol L^{-1} ; c_{CQ} = 1 x 10^{-2} mol L^{-1} ; c_{BAPO} = 1 x 10^{-3} mol L^{-1} ; $c_{Ivocerin}$ = 1 x 10^{-3} mol L^{-1}, 3 ml solutions each) under light protection (orange-light lab). Directly afterwards, the samples were placed into quarz cuvettes and the spectra were recorded.

For the investigation of the influence of a Si-Si bond next to the benzoyl chromophore on the nπ* transition band, a solution of tris(trimethylsilyl)mesitoylsilane (**25**) in acetonitrile was prepared (c = 5 x 10^{-3} mol L^{-1} ; 3 mL solution) under light protection (orange-light lab). Directly afterwards, the sample was placed into a quarz cuvette and the spectrum could be obtained. This spectrum was then compared to a spectrum of benzoyltrimethylsilane (**30**) from literature[59].

2.2 Steady state photolysis (SSP)

A two-necked photoreactor was equipped with a quickfit, which had been closed with a quarz window. One end of an optical waveguide was then placed on this quarz window inside the quickfit, the other end was connected to a LED (Omnicure 400 nm) and an Omnicure unit (Omnicure LX400+). The intensity of the LED was adjusted to be 1 W/cm^2 right after the quarz window (corresponds to 70% intensity on the display of the Omnicure unit). Tetramesitoylsilane (**19**) as well as the reference initiators BAPO and Ivocerin were dissolved in dichloromethane (40 mL solution, c_0 = 1x10^{-3} mol L^{-1}). Each solution was then transferred to the photoreactor and degassed using an argon flow (20 min). At the beginning of the experiment, the distance between the quickfit and the solution was 16 mm. The reaction solution was then irradiated while stirring at 500 rpm and samples (each 1 mL) were taken in a certain interval. For each sample an UV-Vis spectrum was acquired. The experiments were stopped,

when the absorption peak had disappeared. With each sample (1 mL) the height of the solution in the photoreactor was decreased by 1,5 mm. Therefore, the height at the end of the experiment was 56,5 mm (31 mL) for **19**, 64,0 mm (36 mL) for BAPO and 65,5 mm (37 mL) for Ivocerin.

2.3 Storage stability

To investigate the stability of the synthesized compounds in aqueous media, tris(trimethylsilyl)mesitoylsilane (**25**) and tetramesitoylsilane (**19**) were dissolved in acetone:water, ratio 9:1 (c_0 = 1x10^{-3} mol L^{-1}). The absorption of those solutions was then measured via UV-Vis spectroscopy after defined time intervals (0 min, 30 min, 120 min, 300 min) using quarz cuvettes. Between these measurements the solutions were stored at RT in the dark.

The storage stability of tetramesitoylsilane (**19**) was also tested concerning the pH. For this reason three solutions of **19** were prepared in acetone:water, ratio 9:1. Then one of the solutions was acidified with conc. H_3PO_4 (pH 2). To another one, sat. NaOH solution was added (pH 11) and the third solution was kept neutral. UV-Vis spectra were recorded directly after the preparation of these solutions, which were then stored at 40°C and in the dark for 25 days. After this time, another spectrum was acquired.

2.4 Photo-DSC

For the first reactivity investigation of the synthesized compounds tetramesitoylsilane (**19**), tris(trimethylsilyl)mesitoylsilane (**25**) and tris(trimethylsilyl)-o-toluoylsilane (**26**), solutions of 0,25 mol% initiator in 1,6-hexanediol diacrylate (**32**, HDDA) were prepared (600 mg). As a light source, a medium pressure mercury lamp (Omnicure) and a 400- 500 nm filter was used. The lamp was calibrated and an irradiation intensity of 1 W/cm^2 at the tip of the light guide was chosen.

For the further investigations on tetramesitoylsilane (**19**), solutions of 0,1 wt%, 0,2 wt%, 0,4 wt% and 0,8 wt% of **19** in HDDA (600 mg) were prepared. Then the equimolar amounts of the reference initiators (CQ/DMAB, BAPO and Ivocerin) were calculated and weighed in to prepare solutions of those in HDDA (600 mg) as well.

As a light source, a medium pressure mercury lamp (Omnicure) with a 400-500 nm filter was used. The lamp was calibrated and an irradiation intensity of 1 W/cm^2 at the tip of the light guide was chosen.

For each experiment, two DSC pans were prepared from the same solution (double test). The photo-DSC software was fed with the exact weights of the samples. As a reference, an empty DSC pan was placed into the device.

The photopolymerization of 1,6-hexanediol diacrylate (HDDA) using tetramesitoylsilane (**19**) as initiator resulted in a slightly yellow polymer after polymerizing, which bleaches afterwards within several weeks in normal daylight.

Summary

The bimolecular photoinitiating system camphorquinone / dimethylaminobenzoic acid ethyl ester (CQ/DMAB), currently used for visible light photopolymerizaton of methacrylates in dental formulations shows quite low reactivity. Other highly efficient cleavable photoinitiators like BAPO show an absorption band, which does not overlap very well with the emission band of the applied dental LEDs. Diacylgermane-based structures like Ivocerin show a significant shift to longer wavelengths, but suffer from their high production costs.

From literature, silicon- based initiators might be an alternative, but suffer from limited stability so far. Therefore, during this work, two different strategies were taken to synthesize a novel high reactive long- wavelength photoinitiator based on silicon. Both of these strategies should target the repression of the Brook-rearrangement and therefore make the photoinduced α-cleavage possible.

The first strategy was the synthesis of substituted siloxanes, which should show low urge to undergo the Brook-rearrangement, because there is already one oxygen attached to the silicon atom (Scheme 60). Several syntheses (compounds **7**, **8**, **9**) were tried to achieve such a compound, but not a single one did lead to success. The fact that this type of compounds is extremely sensitive to multiple outer influences makes their syntheses quite sophisticated.

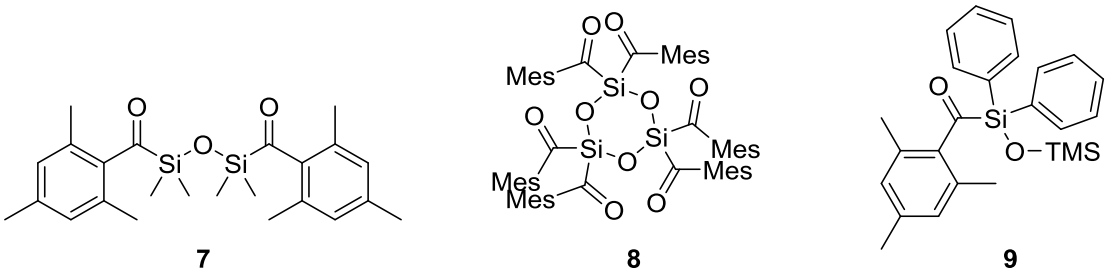

7 **8** **9**

Scheme 60: Oxygen- substituted acyl silanes, which should be synthesized

On the other hand, the strategy of multiple substitution at the silicon atom with aromatic acyl groups resulted in a successful synthesis of tetramesitoylsilane (**19**), a compound containing four mesitoyl groups attached to the silicon atom (Scheme 61). Also tris(trimethylsilyl)mesitoylsilane (**25**) and tris(trimethylsilyl)-o-toluoylsilane (**26**)

could be synthesized over a similar route using potassium tert. butoxide, tetrakis(trimethylsilyl)silane and the corresponding acid chlorides. Other than described in literature,[45] tetramesitoylsilane (**19**) could be achieved directly, starting from tetrakis(trimethylsilyl)silane.

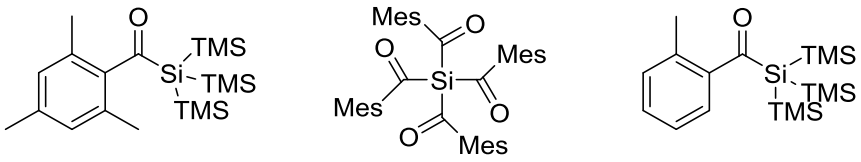

25 **19** **26**

Scheme 61: Synthesized compounds

To improve stability, solubility and reactivity, several analogue tetrasubstituted silanes (compounds **20**-**24**) were tried to be synthesized. Unfortunately, by applying the described synthesis pathway (Scheme 62) no products could be prepared. Either the acid chlorides were too unreactive or the products were simply not stable enough to survive the workup.

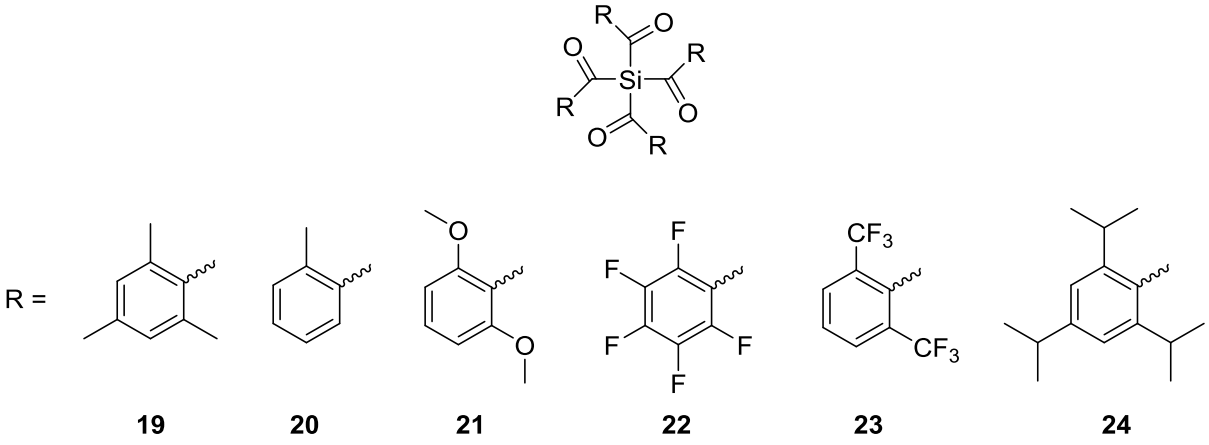

19 **20** **21** **22** **23** **24**

Scheme 62: Tetrasubstituted acylsilanes, which should be synthesized

For the synthesized compounds **25**, **19** and **26**, photochemical characterization could be carried out. Since tetramesitoylsilane (**19**) showed promising results from the beginning, this compound was investigated further on its applicability as long-wavelength photoinitiator. Photo-DSC experiments showed, that tetramesitoylsilane (**19**) could be used as visible light initiator for photopolymerization of acrylates. It could not reach the high reactivity of BAPO and Ivocerin, but its reactivity lies in the

range of the commercially applied camphorquinone/amine system. Due to its poor solubility in methacrylates, photopolymerization of dental formulations could not be carried out with **19**. The absorption band, caused by the nπ* transition reaches into the area of above 450 nm, showing high molar absorption coefficients. Steady state photolysis experiments provided information about the photobleaching behavior of tetramesitoylsilane (**19**) (entire photobleaching with 400 nm LED possible) and also its stability in aqueous media could be tested.

Materials and equipment

All chemicals used in this work have been ordered from Sigma-Aldrich, TCI Chemicals, abcr GmbH or Alfa Aesar. The monomer 1,6-hexanediol diacrylate was ordered from Alfa Aesar.

The solvents have been dried using the following standard procedures (internal TU distillation facility):

Tetrahydrofuran – sodium metal
Diethyl ether – sodium metal
Dichloromethane – CaH_2
Acetonitrile - CaH_2 and P_2O_5
n-Pentane – $MgSO_4$ and P_2O_5

All reactions were carried out in argon- atmosphere, applying Schlenk techniques and excluding light with wavelengths below 520 nm (orange- light lab).

The ^{1}H-NMR, ^{13}C-NMR and ^{29}Si-NMR signals were measured either on a BRUKER DPX-200 or an Avance DRX-400 FT-NMR spectrometer. For all ^{29}Si signals the INEPT pulse sequence (insensitive nuclei enhanced by polarization transfer) was applied. Deuterated chloroform with a degree of deuteration of 99,80% was used as solvent for all samples.

Photo-DSC analysis was done on a NETZSCH DSC 204 F1 using a radiation source distributed by OmniCure (Lumen Dynamics Series 2000) and a 400-500 nm filter from the same company.

UV-VIS measurements were carried out using a Shimadzu UV-1800 Spectrophotometer and quartz cuvettes. Peak deconvolution was carried out with PeakFit software, provided by AISN Software Inc.

GC-MS measurements were carried out on a Thermo Fisher Scientific ITQ 1100 employing a Fused Silica capillary column (30m x 0.25mm).

All IR-spectra were measured on a Perkin Elmer Spectrum 65 FT-IR Spectrometer with a Specac MKII Golden Gate ATR system.

TLC (thin layer chromatography) was carried out using silica gel 60 F_{254} aluminum plates by Merck.

Elemental analysis was carried out at the microanalysis laboratory at the University of Vienna.

Abbreviations

BAPO	Bisacylphosphine oxide (bismesitoylphenylphosphine oxide)
CQ	Camphorquinone
DCM	Dichloromethane
DMAB	N,N-Dimethylaminobenzoic acid
HDDA	1,6-Hexanediol diacrylate
HOMO	Highest occupied molecular orbital
Ivocerin	Di(4-methoxybenzoyl)diethylgermane
KOtBu	Potassium tert. butoxide
LUMO	Lowest unoccupied molecular orbital
TERP	Telluride-mediated polymerization
THF	Tetrahydrofurane

Literature

1. Younis, O.; Asgar, K.; Powers, J. M. *J. Dent. Res.* **1975,** 54, (6), 1133-7.
2. Greener, E. H. *J. Dent. Res.* **1976,** 55, (6), 1142.
3. Blaus, B. *Wikiversity Journal of Medicine* **2014**.
4. Albert, P.; Dermann, K.; Rentsch, H. *Chem. Unserer Zeit* **2000,** 34, (5), 300-305.
5. Wolter, H.; Storch, W.; Ott, H. *Mater. Res. Soc. Symp. Proc.* **1994,** 346, (Better Ceramics through Chemistry VI), 143-9.
6. Moszner, N.; Salz, U. *Prog. Polym. Sci.* **2001,** 26, (4), 535-576.
7. Salz, U.; Burtscher, P.; Vogel, K.; Moszner, N.; Rheinberger, V. *Polym. Prepr. (Am. Chem. Soc., Div. Polym. Chem.)* **1997,** 38, (2), 143-144.
8. Van Landuyt, K. L.; Yoshida, Y.; Hirata, I.; Snauwaert, J.; De Munck, J.; Okazaki, M.; Suzuki, K.; Lambrechts, P.; Van Meerbeek, B. *J. Dent. Res.* **2008,** 87, (8), 757-761.
9. Dietliker, K. K., *Chemistry & Technology of UV & EB Formulation for Coatings, Inks & Paints*. SITA Technology Ltd: 1991; Vol. 3: Photoinitiators for Free Radical and Cationic Polymerisation.
10. Gruber, H. F. *Prog. Polym. Sci.* **1992,** 17, (6), 953-1044.
11. Randy, Jablonski Diagram. For Diagrams: 2015.
12. Berner, G.; Rembold, M.; Sitek, F.; Rutsch, W. Latent catalysts for the crosslinking of polyurethane coatings by heat or light. EP250364A2, 1987.
13. Schlesinger, S. I. *Photogr. Sci. Eng.* **1974,** 18, (4), 387-93.
14. Berlin, K. D.; Burpo, D. H. *J. Org. Chem.* **1966,** 31, (4), 1304-6.
15. Terauchi, K.; Sakurai, H. *Bull. Chem. Soc. Jap.* **1969,** 42, (3), 821-3.
16. Ganster, B.; Fischer, U. K.; Moszner, N.; Liska, R. *Macromolecules (Washington, DC, U. S.)* **2008,** 41, (7), 2394-2400.
17. Peddle, G. J. D. *J. Organometal. Chem.* **1968,** 14, (1), 139-47.
18. Kosugi, M.; Naka, H.; Sano, H.; Migita, T. *Bull. Chem. Soc. Jpn.* **1987,** 60, (9), 3462-4.
19. Villazana, R.; Sharma, H.; Cervantes-Lee, F.; Pannell, K. H. *Organometallics* **1993,** 12, (11), 4278-9.
20. Singh, A. K.; Roy, M. *J. Photochem. Photobiol., A* **1992,** 69, (1), 49-52.
21. Benedikt, S.; Moszner, N.; Liska, R. *Macromolecules (Washington, DC, U. S.)* **2014,** 47, (16), 5526-5531.

22. Brook, A. G.; Peddle, G. J. D. *Can. J. Chem.* **1963,** 41, (9), 2351-6.

23. Ganster, B. Bathochrom verschobene Photoinitiatoren für Dentalformulierungen. University of Technology Vienna, 2007.

24. West, R. *J. Organomet. Chem.* **1965,** 3, (4), 314-20.

25. Brook, A. G.; Quigley, M. A.; Peddle, G. J. D.; Schwartz, N. V.; Warner, C. M. *J. Am. Chem. Soc.* **1960,** 82, 5102-6.

26. Brook, A. G.; Harris, J. W.; Lennon, J.; El Sheikh, M. *J. Am. Chem. Soc.* **1979,** 101, (1), 83-95.

27. Dalton, J. C. *Org. Photochem.* **1985,** 7, 149-230.

28. Duff, J. M.; Brook, A. G. *Can. J. Chem.* **1973,** 51, (17), 2869-83.

29. Brook, A. G.; Duff, J. M. *J. Am. Chem. Soc.* **1967,** 89, (2), 454-5.

30. Brook, A. G.; Pearce, R.; Pierce, J. B. *Can. J. Chem.* **1971,** 49, (10), 1622-8.

31. Page, P. C. B.; Klair, S. S.; Rosenthal, S. *Chem. Soc. Rev.* **1990,** 19, (2), 147-95.

32. Watanabe, H.; Kogure, T.; Nagai, Y. *J. Organometal. Chem.* **1972,** 43, (2), 285-91.

33. Watanabe, H.; Ohsawa, N.; Sawai, M.; Fukasawa, Y.; Matsumoto, H.; Nagai, Y. *J. Organomet. Chem.* **1975,** 93, (2), 173-9.

34. Brook, A. G.; Pierce, J. B.; Duff, J. M. *Can. J. Chem.* **1975,** 53, (19), 2874-9.

35. Trommer, M.; Sander, W. *Organometallics* **1996,** 15, (1), 189-93.

36. Brook, A. G.; Duff, J. M. *Can. J. Chem.* **1973,** 51, (3), 352-60.

37. Brook, A. G.; Krishna, R.; Kallury, M. R.; Poon, Y. C. *Organometallics* **1982,** 1, (7), 987-94.

38. Mochida, K.; Ichikawa, K.; Okui, S.; Sakaguchi, Y.; Hayashi, H. *Chem. Lett.* **1985**, (9), 1433-6.

39. Page, P. C. B.; McKenzie, M. J. *Sci. Synth.* **2002,** 4, 513-567.

40. Brook, A. G.; Duff, J. M.; Jones, P. F.; Davis, N. R. *J. Am. Chem. Soc.* **1967,** 89, (2), 431-4.

41. Corey, E. J.; Seebach, D.; Freedman, R. *J. Am. Chem. Soc.* **1967,** 89, (2), 434-6.

42. Baines, K. M.; Brook, A. G.; Ford, R. R.; Lickiss, P. D.; Saxena, A. K.; Chatterton, W. J.; Sawyer, J. F.; Behnam, B. A. *Organometallics* **1989,** 8, (3), 693-709.

43. Gutekunst, G.; Brook, A. G. *J. Organomet. Chem.* **1982,** 225, (1), 1-3.

44. Capperucci, A.; Degl'Innocenti, A.; Faggi, C.; Ricci, A.; Dembech, P.; Seconi, G. *J. Org. Chem.* **1988,** 53, (15), 3612-14.

45. Ohshita, J.; Tokunaga, Y.; Sakurai, H.; Kunai, A. *J. Am. Chem. Soc.* **1999,** 121, (25), 6080-6081.

46. Harloff, J.; Popowski, E.; Fuhrmann, H. *J. Organomet. Chem.* **1999,** 592, (1), 136-146.

47. Marschner, C. *Eur. J. Inorg. Chem.* **1998**, (2), 221-226.

48. Fischer, R.; Konopa, T.; Baumgartner, J.; Marschner, C. *Organometallics* **2004,** 23, (8), 1899-1907.

49. Yamamoto, K.; Hayashi, A.; Suzuki, S.; Tsuji, J. *Organometallics* **1987,** 6, (5), 974-9.

50. Wu, X.-F.; Neumann, H.; Beller, M. *Tetrahedron Lett.* **2012,** 53, (5), 582-584.

51. Kazahaya, K.; Tsuji, S.; Sato, T. *Synlett* **2004**, (9), 1640-1642.

52. Bouillon, J.-P.; Huguenot, F.; Portella, C. *Synthesis* **2002**, (4), 552-556.

53. MacPhee, J. A.; Dubois, J. E. *Tetrahedron* **1980,** 36, (6), 775-7.

54. Schlosser, M.; Geneste, H. *Chem. - Eur. J.* **1998,** 4, (10), 1969-1973.

55. Brook, A. G.; Nyburg, S. C.; Abdesaken, F.; Gutekunst, B.; Gutekunst, G.; Krishna, R.; Kallury, M. R.; Poon, Y. C.; Chang, Y. M.; Winnie, W. N. *J. Am. Chem. Soc.* **1982,** 104, (21), 5667-72.

56. Herzog, U.; Roewer, G. *J. Organomet. Chem.* **1997,** 544, (2), 217-223.

57. Pae, D. H.; Xiao, M.; Chiang, M. Y.; Gaspar, P. P. *J. Am. Chem. Soc.* **1991,** 113, (4), 1281-8.

58. Berry, M. B.; Griffiths, R. J.; Sanganee, M. J.; Steel, P. G.; Whelligan, D. K. *Org. Biomol. Chem.* **2004,** 2, (16), 2381-2392.

59. Beate, G., Dissertation. In *Technische Universität Wien*.

60. Allen, N. S.; Hardy, S. J.; Jacobine, A. F.; Glaser, D. M.; Catalina, F.; Navaratnam, S.; Parsons, B. J. *J. Photochem. Photobiol., A* **1991,** 62, (1), 125-39.

61. Wolf, T. J. A.; Voll, D.; Barner-Kowollik, C.; Unterreiner, A.-N. *Macromolecules (Washington, DC, U. S.)* **2012,** 45, (5), 2257-2266.

62. Berdzinski, S.; Strehmel, N.; Lindauer, H.; Strehmel, V.; Strehmel, B. *Photochem. Photobiol. Sci.* **2014,** 13, (5), 789-798.

63. Firouzabadi, H.; Iranpoor, N.; Hazarkhani, H. *J. Org. Chem.* **2001,** 66, (22), 7527-7529.

64. Brook, A. G.; Wessely, H. J. *Organometallics* **1985,** 4, (8), 1487-8.

65. Ohshita, J.; Masaoka, S.; Masaoka, Y.; Hasebe, H.; Ishikawa, M.; Tachibana, A.; Yano, T.; Yamabe, T. *Organometallics* **1996,** 15, (14), 3136-3146.